NASA TECHNICAL MEMORANDUM

NASA TM X-72700

NASA TM X-7270

(NASA-TM-X-72700) PRELIMINARY STUDY OF THE MINIMUM TEMPERATURES FOR VALID TESTING IN A CRYOGENIC WIND TUNNEL (NASA) 125 p HC $5.25 CSCL 14B

N75-2807

Unclas

G3/09 29867

PRELIMINARY STUDY OF THE MINIMUM TEMPERATURES FOR VALID TESTING IN A CRYOGENIC WIND TUNNEL

by Robert M. Hall

This informal documentation medium is used to provide accelerated or special release of technical information to selected users. The contents may not meet NASA formal editing and publication standards, may be revised, or may be incorporated in another publication.

NATIONAL AERONAUTICS AND SPACE ADMINISTRATION
LANGLEY RESEARCH CENTER, HAMPTON, VIRGINIA 23665

1. Report No.	2. Government Accession No.	3. Recipient's Catalog No.
NASA TM X-72700		

4. Title and Subtitle	5. Report Date
Preliminary Study of the Minimum Temperatures for Valid Testing in a Cryogenic Wind Tunnel	AUGUST 1975
	6. Performing Organization Code
7. Author(s) Robert M. Hall	8. Performing Organization Report No.
	10. Work Unit No.
9. Performing Organization Name and Address NASA Langley Research Center Hampton, VA 23665	11. Contract or Grant No.
	13. Type of Report and Period Covered Technical Memorandum
12. Sponsoring Agency Name and Address National Aeronautics & Space Administration Washington, DC 20546	14. Sponsoring Agency Code

15. Supplementary Notes

16. Abstract

The minimum operating temperature which avoids real-gas effects, such as condensation, has been determined for $M_{\infty} = 0.85$ flow over a 0.137-meter NACA 0012-64 airfoil mounted in the Langley 1/3-meter transonic cryogenic tunnel. For temperatures within 5 K of reservoir saturation and total pressures from 1.2 to 4.5 atmospheres, the pressure distributions over the airfoil are not altered by real-gas effects. This ability to test at total temperatures below those which avoid saturation over the airfoil allows an increase in Reynolds number capability of at least 17 percent for a constant tunnel total pressure. Similarly, 17 percent less total pressure is required to obtain a given Reynolds number.

17. Key Words (Suggested by Author(s))	18. Distribution Statement
Facilities, research and support Wind tunnel, cryogenic, condensation	Unclassified - Unlimited

19. Security Classif. (of this report)	20. Security Classif. (of this page)	21. No. of Pages	22. Price
Unclassified	Unclassified	[illegible]	[illegible]

NATIONAL AERONAUTICS AND SPACE ADMINISTRATION

PRELIMINARY STUDY OF THE MINIMUM TEMPERATURES FOR VALID TESTING IN A CRYOGENIC WIND TUNNEL

By

Robert M. Hall
Langley Research Center
Hampton, Virginia

SUMMARY

The minimum operating temperature which avoids real-gas effects, such as condensation, has been determined for $M_\infty = 0.85$ flow over a 0.137-meter NACA 0012-64 airfoil mounted in the Langley 1/3-meter transonic cryogenic tunnel. For temperatures within 5 K of reservoir saturation and total pressures from 1.2 to 4.5 atmospheres, the pressure distributions over the airfoil are not altered by real-gas effects. This ability to test at total temperatures below those which avoid saturation over the airfoil allows an increase in Reynolds number capability of at least 17 percent for a constant tunnel total pressure. Similarly, 17 percent less total pressure is required to obtain a given Reynolds number.

INTRODUCTION

Cryogenic Wind Tunnels

Cryogenic wind tunnels are a new development in the field of experimental aerodynamics. Cryogenic tunnels will, indeed, form a new generation of wind tunnels capable of large Reynolds number increases over their conventional, ambient temperature counterparts. As explained in reference 1, at a constant Mach number the increase in Reynolds number at cryogenic temperatures is a result of the decrease in the viscous force term in the equation for Reynolds number. The cryogenic test gas is nitrogen since the method developed for cooling the tunnels consists of spraying liquid nitrogen directly into the tunnel circuit and utilizing the latent heat of vaporization of the liquid nitrogen and the sensible heat of the gaseous nitrogen to cool the tunnel structure and test gas.

Significantly, in a cryogenic wind tunnel the increase in Reynolds number accelerates as the temperature drops as shown in figure 1. Consequently, it is beneficial to operate the tunnel at as low a temperature as possible. However, real-gas effects eventually place a lower limit on the operating temperature.

The real-gas effects can be separated into two types. The first type of effects occurs because low temperature gaseous nitrogen does not have an ideal equation of state: The molecules in the gaseous state are influenced by their neighbors, which violates the assumptions of an ideal gas. The second type of effects occurs when condensate is formed in the flow. Hence the stream evolves into a complex two-phase flow system with liquid droplets suspended in the gas.

For condensation to occur in a tunnel, the flow must be saturated. When a model is mounted in the tunnel, three stages of saturation can occur. The first stage occurs when the region of high local Mach number over the model is saturated but the test section is not. The second stage occurs when both the region of high local Mach number over the model and the test section are saturated. The third, and final, stage occurs when the tunnel reservoir conditions are saturated. Under these conditions the injected liquid nitrogen does not evaporate and the tunnel begins to fill with liquid nitrogen.

Previous Studies

Since the completion in 1973 of the Langley 1/3-meter transonic cryogenic tunnel (previously designated the pilot cryogenic transonic pressure tunnel), studies have been made at Langley to determine how cold the tunnel can be operated before either condensation or other real-gas effects perturb the test results. As reported by Ray in reference 1, tests using a 0.137-meter NACA 0012-64 airfoil found no effects of condensation for a pressure of 2.5 atmospheres with a temperature which produced free-stream saturation. However, no conclusions could be made about the minimum temperature which could be used without real-gas effects because no effects were observed.

Studying the real-gas behavior of gaseous nitrogen, Adcock in reference 2 has analytically examined the behavior of gaseous nitrogen at low temperatures by using the data and equation of state from reference 3 to compare low-temperature nitrogen to an ideal gas. The results of Adcock's investigation show that for pressures up to 5 atmospheres with temperatures down to those which produce free-stream saturation, the various nondimensional ratios used to describe isentropic expansions and normal-shock flow in cryogenic nitrogen differ from their ideal values by less than one half of one percent.

Present Studies

Because of the potential increase in Reynolds number capability for operating below local saturation conditions, an experimental program has been undertaken to extend the scope of Ray's work with the NACA 0012-64 airfoil. Studies have been made at a constant test-section Mach number of 0.85 with total pressures from 1.2 to 5.0 atmospheres with temperatures within 2 K of reservoir saturation. The temperature at which condensation, or other real-gas effects, perturbs the flow is determined at a constant Reynolds number by reducing total temperature and pressure until the pressure distribution over the airfoil deviates from the pressure distribution obtained with unsaturated conditions. The results of these studies are presented herein.

SYMBOLS

c	airfoil chord, 0.137 meter
C_p	pressure coefficient, $\frac{p - p_\infty}{q_\infty}$
M	Mach number
p	pressure
q	dynamic pressure
R	Reynolds number based on a chord of 0.137 meter
T	temperature
x	linear dimension along airfoil chord line

Subscripts:

L	local conditions
t	total conditions
∞	free-stream conditions

APPARATUS

Tunnel

The Langley 1/3-meter transonic cryogenic tunnel was used for these tests. A sketch of the tunnel is presented as figure 2. This continuous flow, fan-driven tunnel uses nitrogen as the test gas and is cooled by injecting liquid nitrogen directly into the stream. Injection of liquid nitrogen provides a total temperature range from slightly greater than 77 K to 350 K. Since the tunnel may also be pressurized to 5 atmospheres, the combined low temperature and high pressure can produce a Reynolds number of over 328 million per meter (100 million per foot). Some of the design features and operational characteristics of the tunnel are given in reference 4.

Airfoil

A sketch of the 0.137 meter NACA 0012-64 airfoil used for these tests is presented as figure 3. As shown in figure 3, there are twenty pressure orifices over both the top and the bottom of the airfoil. The airfoil was installed between flats in the octagonal test section with the leading edge 0.62 meter from the beginning of the test section.

Data Acquisition and Error Discussion

The pressures over the airfoil were measured by using a single 1.7 atmoshperes (25 psi) differential pressure transducer and a scanning valve system. After the transducer output for all of the airfoil orifices was recorded, the tunnel parameters were recorded. The total time to acquire all the information for complete pressure distribution was 50 seconds.

The accuracy of the pressure transducer was 0.5 percent of full scale or 0.0085 atmosphere. There was no significant error introduced by either the signal conditioning or the data acquisition systems. However, during the 50-second acquisition period the tunnel conditions were observed to fluctuate by the following amounts: Mach number, ± 0.003; total temperature, ± 0.5 K; and total pressure, ± 0.02 atmosphere.

TESTS

Total temperatures at which condensation or other real-gas effects perturb the pressure distribution over the 0.137-meter NACA 0012-64 airfoil at zero incidence were determined for pressures from 1 to 5 atmospheres. The free-stream Mach number was 0.85 and the maximum local Mach number over the airfoil was 1.2. The three stages of saturation -- local, free-stream, and reservoir -- are shown as a function of total pressure in figure 4.

To experimentally determine the total temperature at which condensation effects begin as a function of total pressure, paths at six different Reynolds numbers were investigated. The Reynolds numbers used were chosen so that the total pressures required spanned the pressure envelope of the tunnel. A reference pressure distribution was taken above the upper saturation line, M_L=1.2, if it was possible to do so within the pressure envelope of the tunnel. The six constant Reynolds number paths and the total conditions sampled are shown in figure 5.

RESULTS AND DISCUSSION

Computer plots of the pressure coefficients as a function of x/c were made for each data point taken. A note of caution is appropriate when interpreting the pressure coefficients for this NACA 0012-64 airfoil. The airfoil chord is 0.137 meter, and the tunnel test-section is 0.343 meter between flats. Consequently, the chord to height ratio is 0.4, which is considerable larger than normally used for airfoil testing. Therefore the pressure distributions over the airfoil are not expected to be free of wall effects. However, since wall effects would be expected to be independent of temperature for a given Reynolds number, the possible effects are of no consequence for the purpose of this study.

To determine if condensation or other real-gas effects perturb the flow over the airfoil, pressure distributions at different total temperatures along a constant Reynolds number line are compared graphically to the reference pressure distribution. Even though the agreement between the reference distribution and those distributions considered to be affected by condensation may in many cases appear to be within experimental accuracy, there is always a systematic positive shift in the pressure coefficient from the 20 percent chord position of the airfoil back to the recompression shock.

Results

The results for the pressure distributions taken along each of the six constant Reynolds number lines are summarized respectively in Tables I through VI. Each table is divided into two sections. The top section contains the pressure distributions which are used as unaffected reference distributions while the bottom section contains the lower temperature pressure distributions. The free-stream Mach number, total temperature, total pressure, and chord Reynolds number are presented in the leftmost columns. The next column lists the reference distribution which has the closest Mach number and hence should be used for the graphic comparison. The column labelled "Low T Effects" states whether the lower temperature distributions show no effect, possible effect, or definite effect when compared to its reference distribution. For each Reynolds number line the following sequence of pressure distributions are compared with the listed reference distribution and presented as comparison figures: The lowest temperature distribution which showed no effect, the highest temperature distribution which showed the first possible signs of low-temperature effects, the highest temperature distribution which showed definite effects, and the lowest temperature distribution taken. Individual plots of all the pressure distributions are shown in figures given in the appendix and are numbered to correspond with the numbers given in the tables.

Not all of the orifice pressure values are shown in each of the pressure distribution plots. At various times during the test program pressure leaks occurred in the tubing from the airfoil to the pressure gauge. The values for the leaking orifices have not been plotted.

DISCUSSION

For path 3 two reference distributions are presented. Although point 30 is listed as having a Mach number of 0.862 and point 29 as 0.858, one may observe in appendix figures A29 and A30 that the pressure distribution from point 29 actually corresponds to the higher Mach number. This error in Mach numbers is a result of the uncertainty in Mach number of ± 0.003.

The reference distribution for path 5 is taken at T_t=106.3 K and p_t=4.96 atmospheres. This temperature is just 1.7 K below the local saturation line and since no effects are observed for the first four paths until 10 K below the local saturation line, the T_t=106.3 K was assumed to be an unaffected distribution.

Path 5 does not display an increasing degradation in the pressure distributions as the temperature is lowered. For example, in Table V point 63 shows less effect than points 61 or 62 which are taken at higher temperatures. Similarly, point 66 at a total temperature of 93.0 K showed only a slight deviation while point 65 at 93.6 K showed a larger deviation. Although all of these irregularities could be due to the uncertainty in temperature of 0.5 K, in this sequence of pressure distributions there are no large low-temperature effects for tunnel operations within 2 K of saturated total conditions.

For path 6, point 68 with a total temperature of 101.1 K is used as a reference distribution. Another reference distribution was taken at 102.5 K, but a computer tape problem would not allow analysis of this point. Even though T_t=101.1 K is 3 K above the corresponding temperature at which the lower pressure paths experience effects, it was thought that some substantiation was necessary to show that T_t=101.1 K is an unaffected distribution.

Consequently, since paths 5 and 6 both have high Reynolds numbers of 41.8 and 43.9 million, good agreement between T_t=101.1 K and the reference of path 5, point 54, should serve as verification that T_t=101.1 K is unaffected by condensation. As figure 29 shows, good agreement does exist and T_t=101.1 K is considered an unaffected pressure distribution.

A conservative experimental lower limit to tunnel operation can be given in figure 30 by plotting the total conditions where the first "possible" pressure distribution deviations occurred. This line is considered conservative because at the first visual sign of deviation the pressure distribution is labelled as possibly deviating when, in fact, the difference in pressure distribution may be insignificant to the aircraft designer. Additional work to quantify the differences in pressure distribution should be done in order to more systematically compare the reference distribution to the data condition in question.

The implications of figure 30 are far-reaching. First of all, there appears to be no serious condensation problems in testing far below locally saturated conditions for the airfoil tested. In fact, there is no low temperature effect until the total conditions are at least 2 K below those which give a saturated test section, or equivalently, within 5 K of reservoir saturation. For this experiment the ability to run below the local saturation boundary allowed an increase in Reynolds number of 17 percent for a constant total pressure. This increase is present over the entire pressure range from 1.2 to 4.5 atmospheres. If, instead of holding total pressure constant, Reynolds number is held constant, the ability to operate with saturated flow allows a reduction in total pressure of more than 17 percent over the total pressure range.

SUMMARY OF RESULTS

The minimum operating temperature which avoids real-gas effects, such as condensation, has been determined for $M_\infty = 0.85$ flow over a 0.137-meter NACA 0012-64 airfoil mounted in the Langley 1/3-meter transonic cryogenic tunnel. For temperatures within 5 K of reservoir saturation and total pressures from 1.2 to 4.5 atmospheres, the pressure distributions over the airfoil are not altered by real-gas effects. This ability to test at total temperatures below those which avoid saturation over the airfoil allows an increase in Reynolds number capability of at least 17 percent for a constant tunnel total pressure. Similarly, 17 percent less total pressure is required to obtain a given Reynolds number.

REFERENCES

1. Ray, Edward J.; Kilgore, Robert A.; Adcock, Jerry B.; and Davenport, Edwin E.: Analysis of Validation Tests at the Langley Pilot Transonic Cryogenic Tunnel. NASA TN D-7828, 1975.

2. Adcock, Jerry B.; Kilgore, Robert A.; and Ray, Edward J.: Cryogenic Nitrogen as a Transonic Wind-Tunnel Test Gas. AIAA Paper No. 75-143, Jan. 1975.

3. Jacobsen, R. T.: The Thermodynamic Properties of Nitrogen from 65 to 2000 K with Pressures to 10,000 Atmospheres. Ph. D. Thesis, Washington State Univ., 1972.

4. Kilgore, Robert A.: Design Features and Operational Characteristics of the Langley Pilot Transonic Cryogenic Tunnel. NASA TM X-72012, 1974.

TABLE I. - Path 1

Pressure Distribution No.	M_∞	T_t, K	p_t, atm	R	Reference Distribution No.	Low T Effects	Comparison Figure
1	0.847	116.2	2.11	15.5×10^6			
2	.855	114.8	2.11	15.8	Unsaturated	reference	distributions
3	.858	114.3	2.09	15.8			
4	.855	105.4	1.84	15.7	2	No	-
5	.854	100.4	1.73	15.8	2	No	-
6	.857	95.0	1.58	15.7	2	No	-
7	.855	91.2	1.49	15.6	2	No	-
8	.852	87.3	1.39	15.5	2	No	-
9	.857	86.5	1.37	15.5	3	No	-
10	.858	85.2	1.34	15.6	3	No	Fig. 6
11	.856	84.2	1.31	15.4	2	Possible	Fig. 7
12	.857	83.7	1.30	15.4	2	Possible	-
13	.852	83.2	1.29	15.4	1	Possible	-
14	.855	82.6	1.27	15.3	2	Definite	Fig. 8
15	.854	81.3	1.20	14.8	2	Definite	Fig. 9

TABLE II. - Path 2

Pressure Distribution No.	M_∞	T_t, K	p_t, atm	R	Reference Distribution No.	Low T Effects	Comparison Figure
16	.854	107.3	3.16	26.2×10^6	Unsaturated	reference	distribution
17	.858	101.8	2.91	26.1	16	No	-
18	.858	98.8	2.79	26.1	16	No	-
19	.858	95.9	2.67	26.1	16	No	-
20	.854	94.2	2.56	25.7	16	No	-
21	.854	93.0	2.52	25.7	16	No	-
22	.854	91.9	2.48	25.8	16	No	-
23	.855	91.6	2.48	25.9	16	No	-
24	.855	91.3	2.44	25.7	16	No	-
25	.859	90.0	2.40	25.8	16	Possible	Fig. 10
26	.854	89.8	2.40	25.8	16	No	Fig. 11
27	.855	88.6	2.32	25.5	16	Definite	Fig. 12
28	.853	86.2	2.20	25.0	16	Definite	Fig. 13

TABLE III. - Path 3

Pressure Distribution No.	M_∞	T_t, K	p_t, atm	R	Reference Distribution No.	Low T Effects	Comparison Figure
29	.858	109.4	4.28	34.5×10^6	Unsaturated	reference	distributions
30	.862	109.1	4.28	34.7			
31	.856	106.5	4.11	34.4	30	No	-
32	.858	102.2	3.84	34.2	29	No	-
33	.861	100.4	3.75	34.4	29	No	-
34	.856	97.4	3.58	34.2	30	No	-
35	.858	94.9	3.41	33.9	30	No	-
36	.863	94.5	3.41	34.2	29	No	-
37	.854	93.7	3.36	34.0	30	No	Fig. 14
38	.861	93.0	3.29	33.8	29	Possible	Fig. 15
39	.855	92.7	3.30	33.9	30	Possible	-
40	.854	92.2	3.22	33.3	30	Definite	Fig. 16
41	.856	92.0	3.22	33.5	30	Possible	-
42	.857	91.4	3.21	33.7	30	Definite	-
43	.856	90.3	3.13	33.4	30	Possible	Fig. 17

TABLE IV. - Path 4

Pressure Distribution No.	M_∞	T_t, K	p_t, atm	R	Reference Distribution No.	Low T Effects	Comparison Figure
44	.854	112.5	5.00	38.5×10^6	Unsaturated	reference	distribution
45	.854	105.5	4.50	38.2	44	No	-
46	.856	103.4	4.40	38.5	44	No	-
47	.858	101.5	4.20	37.8	44	No	-
48	.857	99.6	4.10	38.0	44	No	-
49	.853	97.1	3.91	37.6	44	No	Fig. 18
50	.854	95.4	3.82	37.6	44	Possible	Fig. 19
51	.857	93.9	3.71	37.5	44	Definite	Fig. 20
52	.855	92.5	3.62	37.4	44	Definite	-
53	.855	90.8	3.50	37.1	44	Definite	Fig. 21

TABLE V. - Path 5

Pressure Distribution No.	M_∞	T_t, K	p_t, atm	R	Reference Distribution No.	Low T Effects	Comparison Figure
54	.861	106.3	4.96	41.8×10^6		Reference	distribution
55	.856	104.4	4.83	41.7	54	No	-
56	.859	102.3	4.71	42.0	54	No	-
57	.855	100.5	4.56	41.7	54	No	-
58	.853	98.5	4.41	41.5	54	No	-
59	.858	96.7	4.28	41.5	54	No	-
60	.856	96.2	4.28	41.7	54	No	-
61	.856	95.6	4.21	41.4	54	Possible	Fig. 22
62	.855	95.5	4.20	41.4	54	Possible	-
63	.856	95.2	4.14	41.1	54	No	Fig. 23
64	.857	93.8	4.08	41.3	54	Possible	-
65	.857	93.6	4.08	41.4	54	Definite	Fig. 24
66	.856	93.0	4.00	41.0	54	Possible	Fig. 25

TABLE VI. - Path 6

Pressure Distribution No.	M_∞	T_t, K	p_t, atm	R	Reference Distribution No.	Low T Effects	Comparison Figure
67*	.858	102.5	4.99			Reference	distributions
68	.858	101.1	4.83	43.9×10^6			
69	.858	100.1	4.79	44.0	68	No	-
70	.856	98.9	4.71	44.1	68	No	-
71	.857	98.1	4.63	43.9	68	No	-
72	.856	97.2	4.56	43.8	68	No	Fig. 26
73	.857	96.2	4.48	43.8	68	Possible	Fig. 27
74	.857	95.6	4.39	43.3	68	Possible	-
75	.856	93.5	4.29	43.7	68	Definite	Fig. 28

* Data acquisition problem prevented analysis of this point.

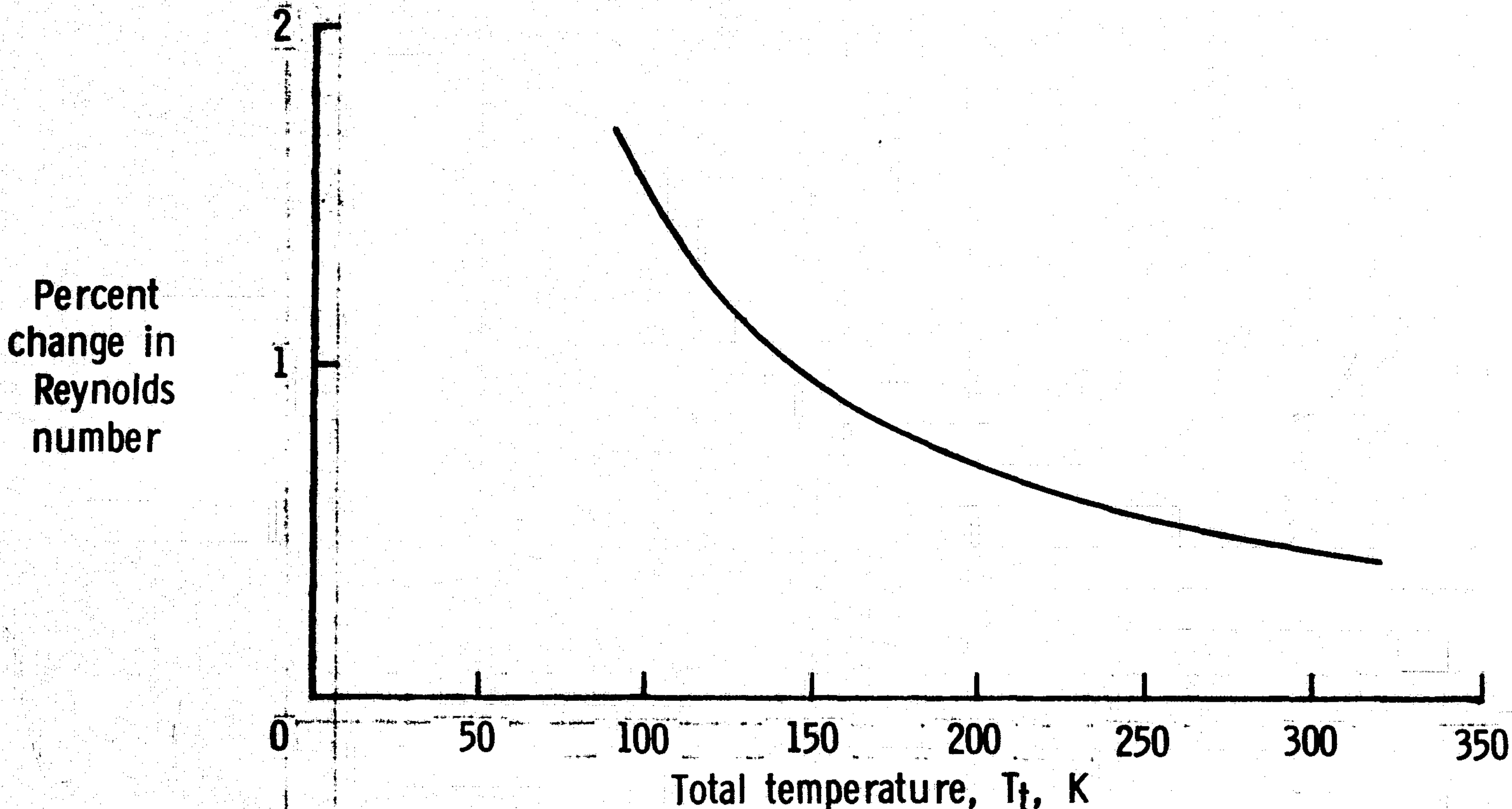

Figure 1.- Percent change in Reynolds number per one degree reduction in T_t as a function of T_t.

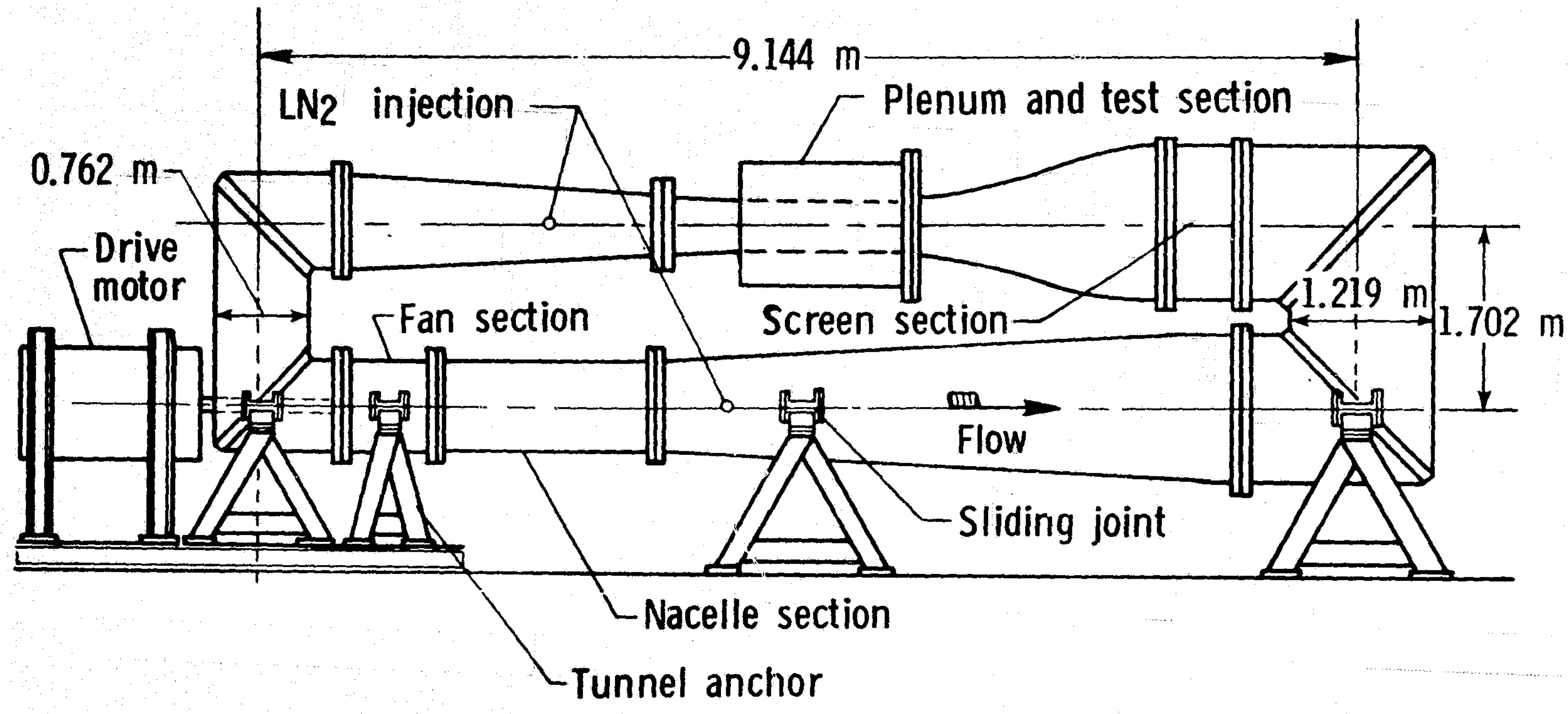

Figure 2.- Schematic of Langley 1/3-meter transonic cryogenic tunnel.

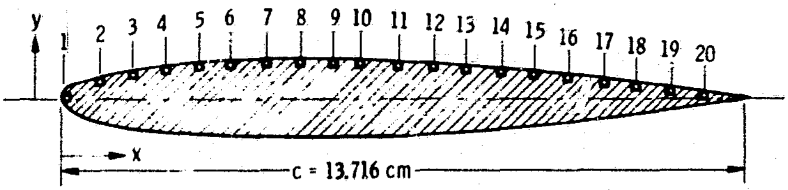

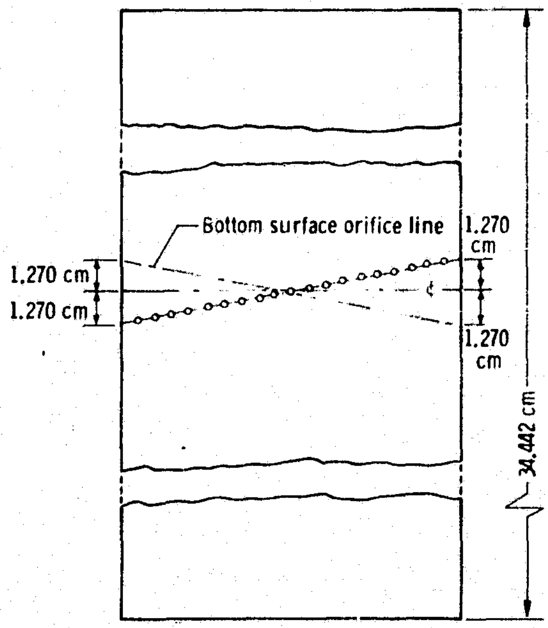

Airfoil coordinates	
x	y
0	0
0.175	± 0.249
.348	± 0.335
.699	± 0.447
1.046	± 0.523
1.372	± 0.582
2.062	± 0.668
2.743	± 0.726
4.115	± 0.800
5.486	± 0.823
6.858	± 0.800
8.230	± 0.729
9.601	± 0.615
10.973	± 0.455
12.344	± 0.257
13.030	± 0.140
13.716	± 0.015

Orifice locations		
Orifice number	Orifice station x, cm	$\frac{x}{c}$
1	0	0
2	0.698	0.0509
3	1.372	.1000
4	2.062	.1504
5	2.743	.2000
6	3.429	.2500
7	4.115	.3000
8	4.801	.3500
9	5.486	.4000
10	6.172	.4500
11	6.858	.5000
12	7.544	.5500
13	8.230	.6000
14	8.915	.6500
15	9.601	.7000
16	10.287	.7500
17	10.973	.8000
18	11.659	.8500
19	12.344	.9000
20	13.030	.9500

Figure 3.- Two dimensional NACA 0012-64 airfoil. Lower surface orifices are located at same x/c location as those on upper surface.

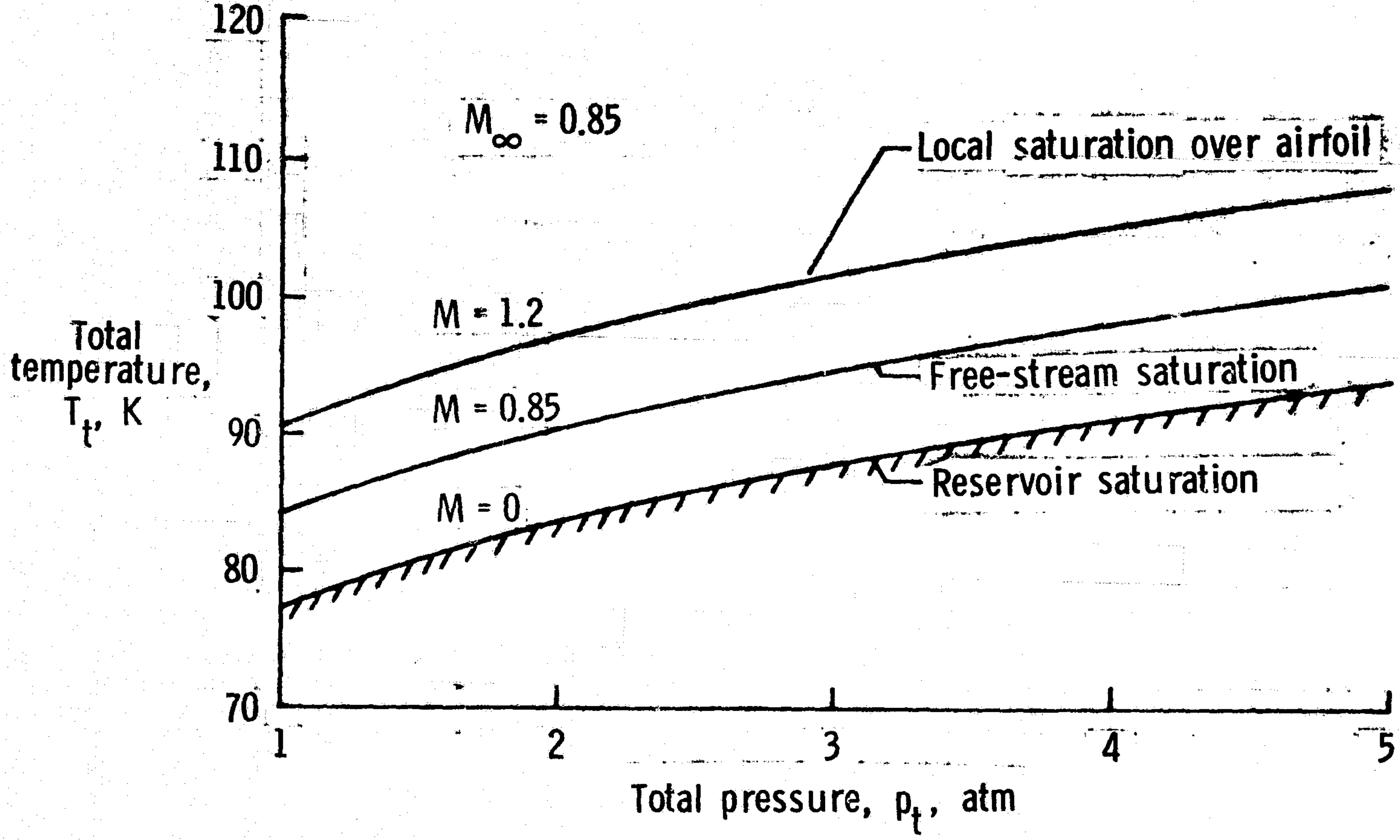

Figure 4.- The three stages of saturation as a function of total pressure.

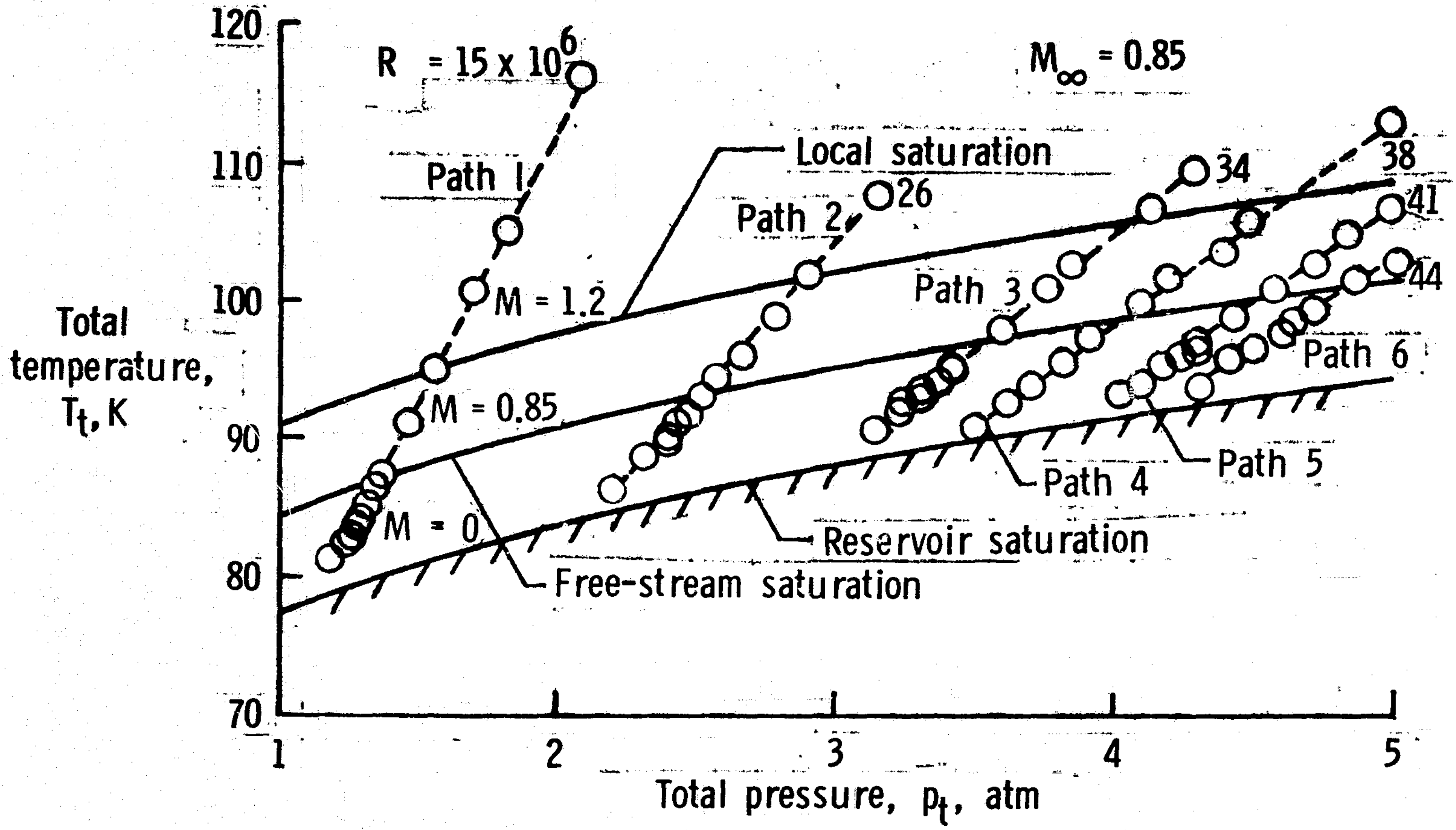

Figure 5.- Constant Reynolds number paths and total conditions sampled.

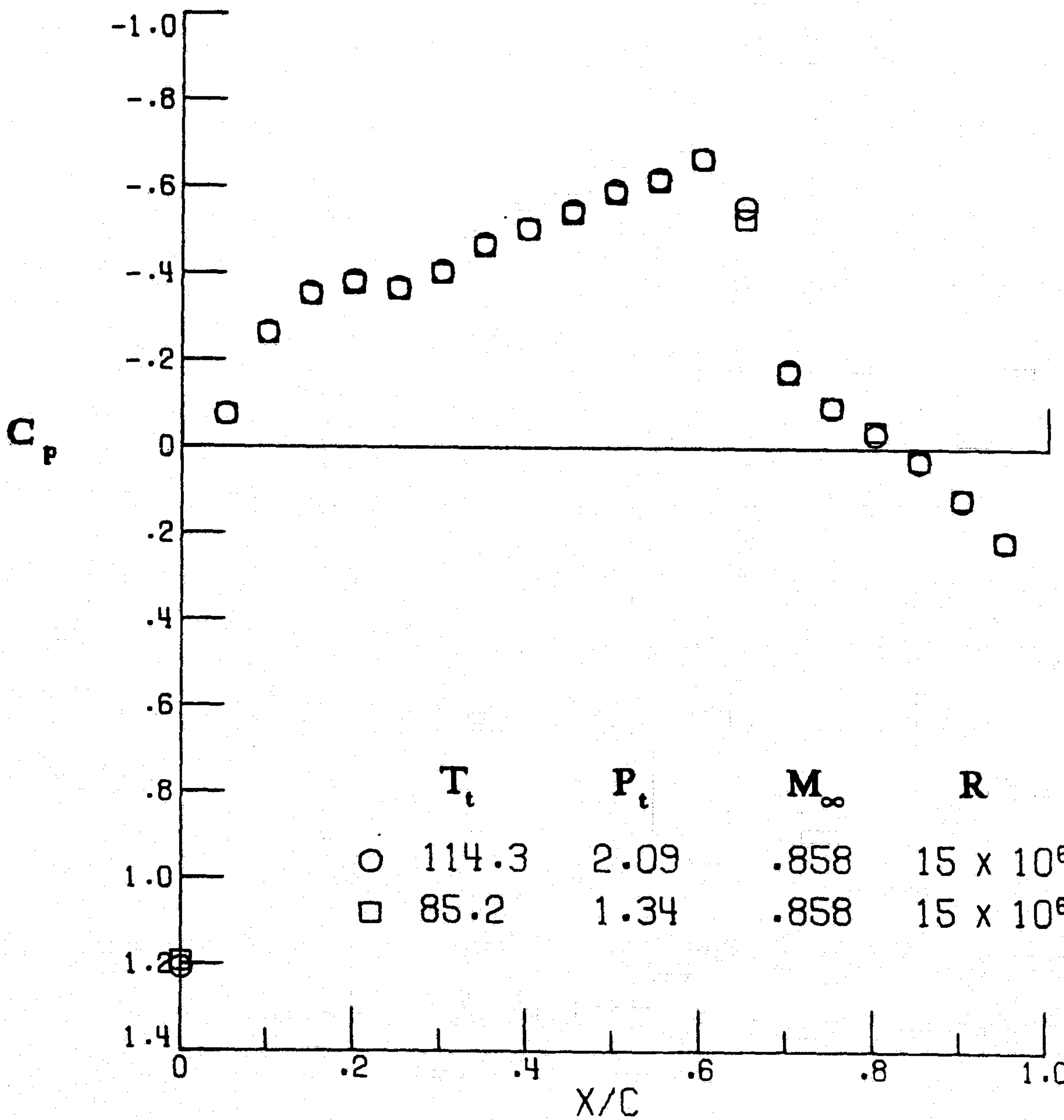

Figure 6. - Path 1, T_t = 85.2K is 1.5K below free-stream saturation line, no effect.

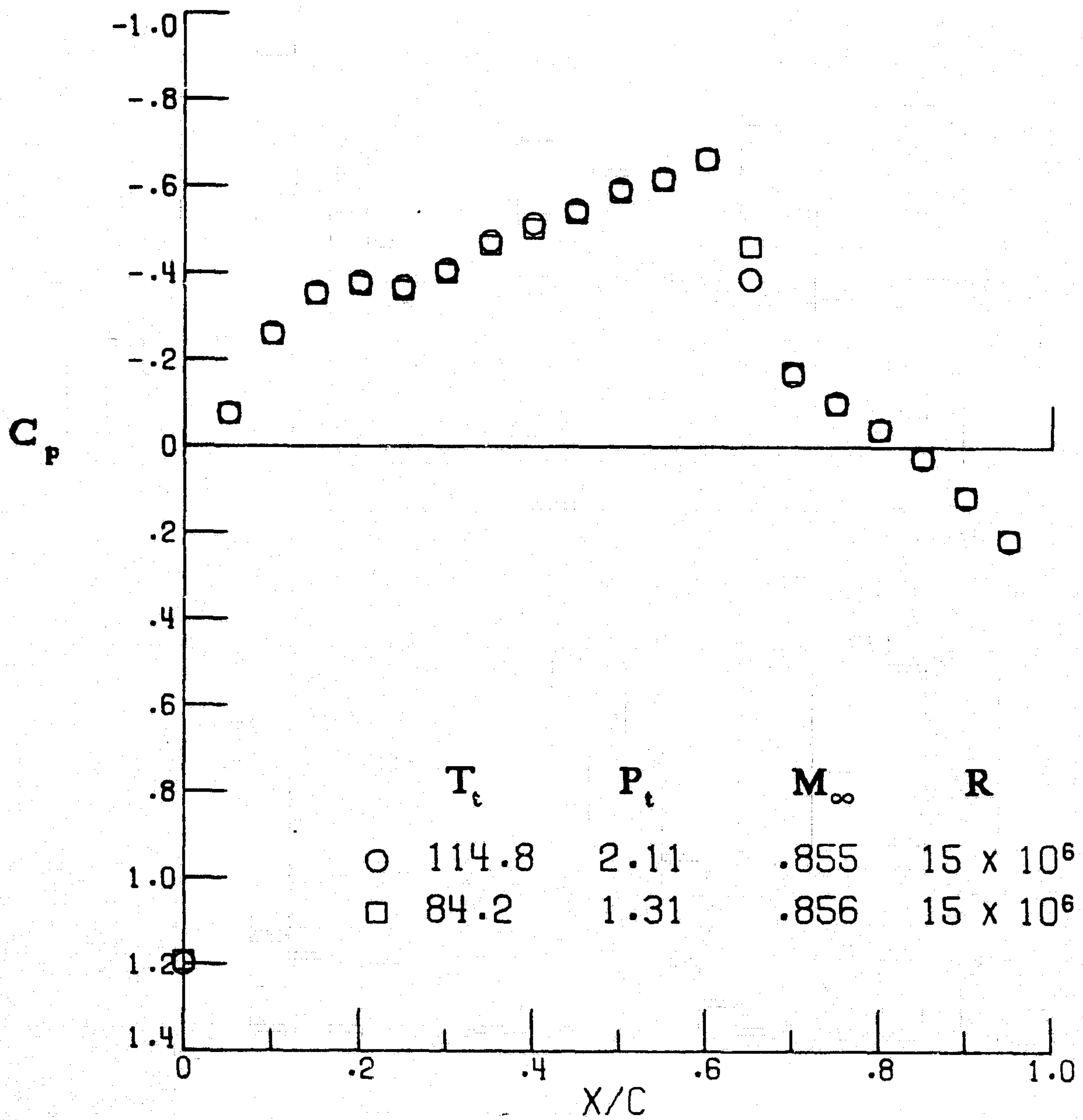

Figure 7. - Path 1, T_t = 84.2K is 2.5K below free-stream saturation line, possible effect.

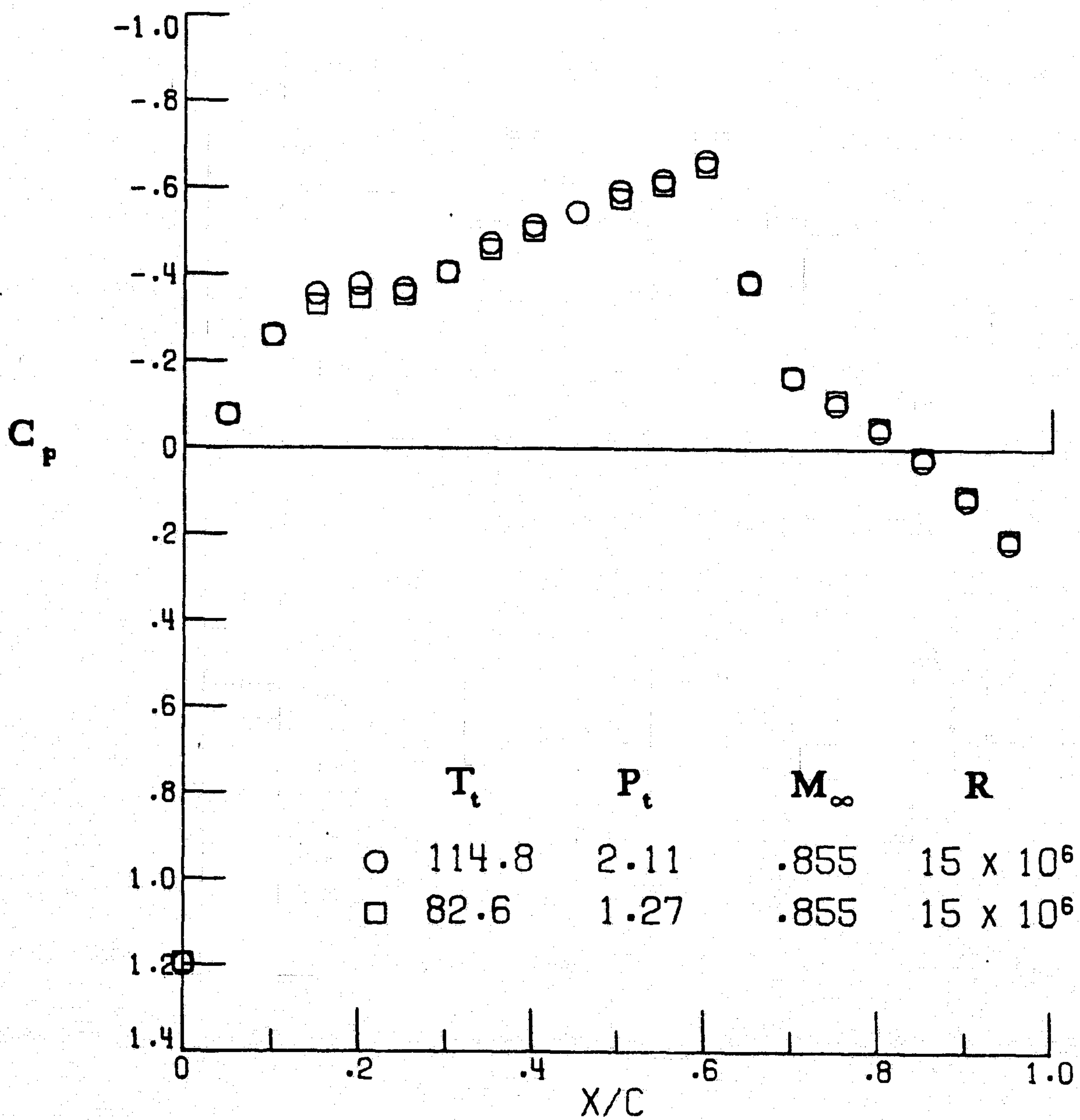

Figure 8. - Path 1, T_t = 82.6K is 3.5K below free-stream saturation line, definite effect.

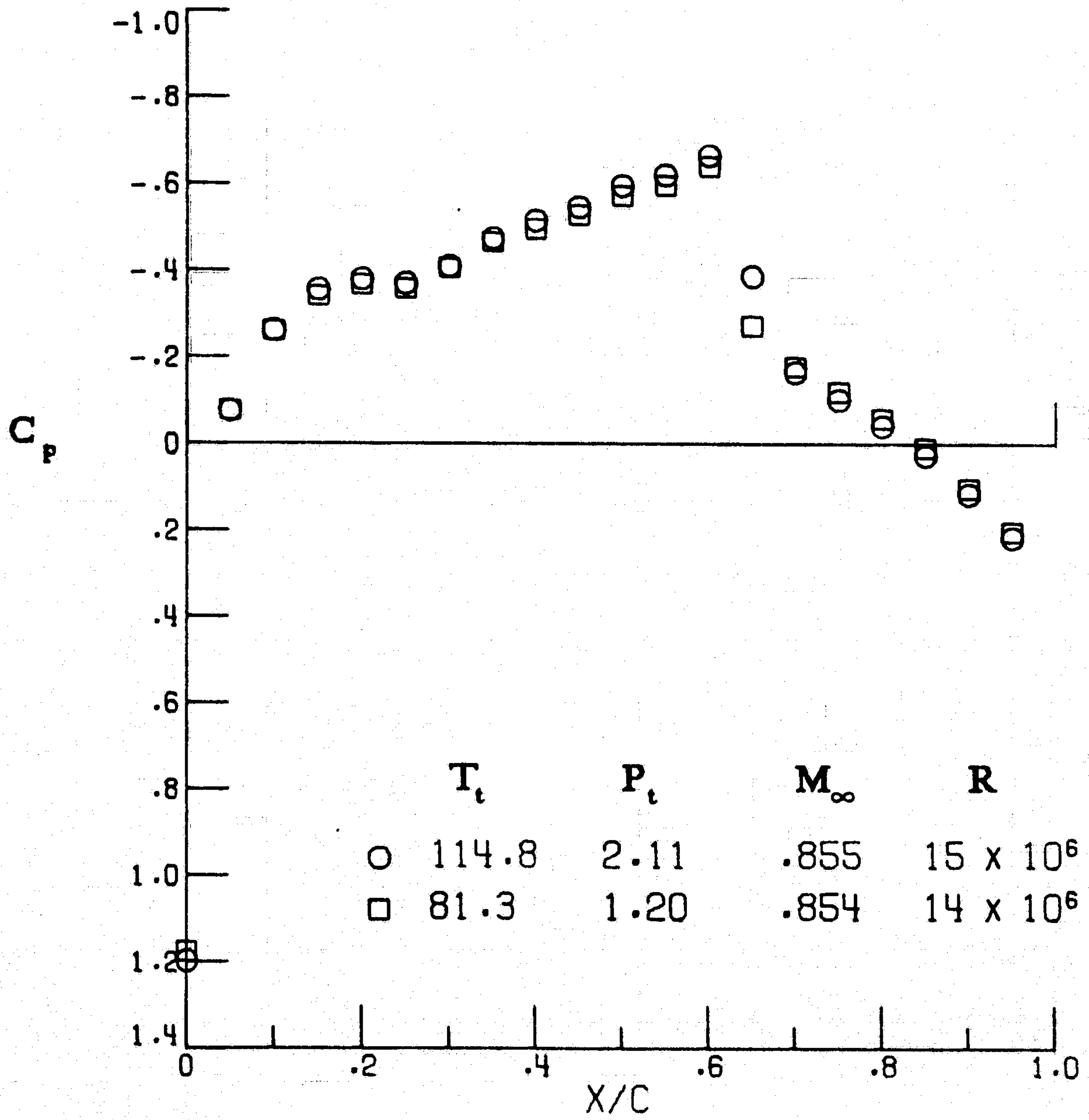

Figure 9. - Path 1, T_t = 81.3K is 4.5K below free-stream saturation line, definite effect.

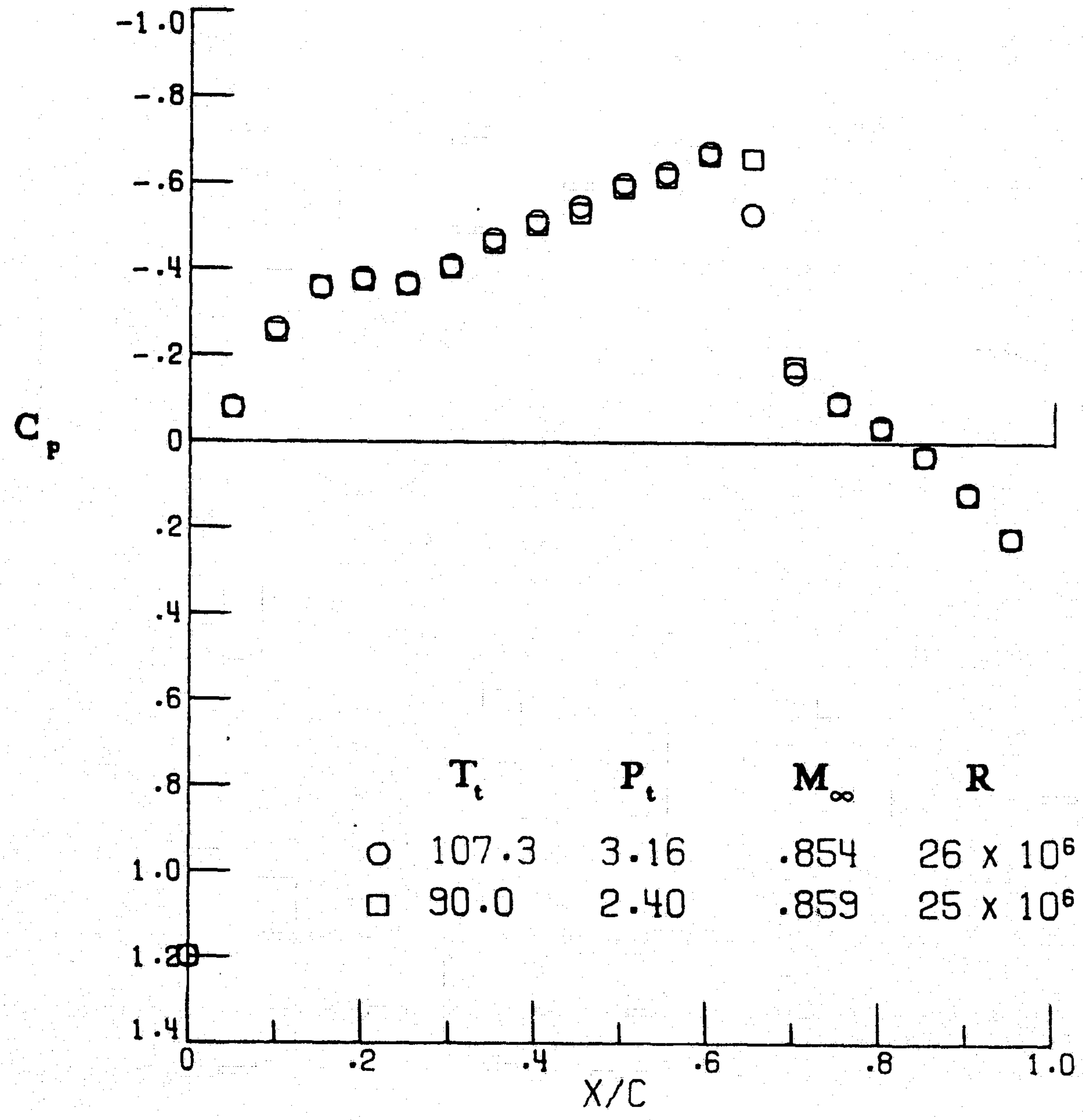

Figure 10. - Path 2, T_t = 90.0K is 2.5K below free-stream saturation line, possible effect.

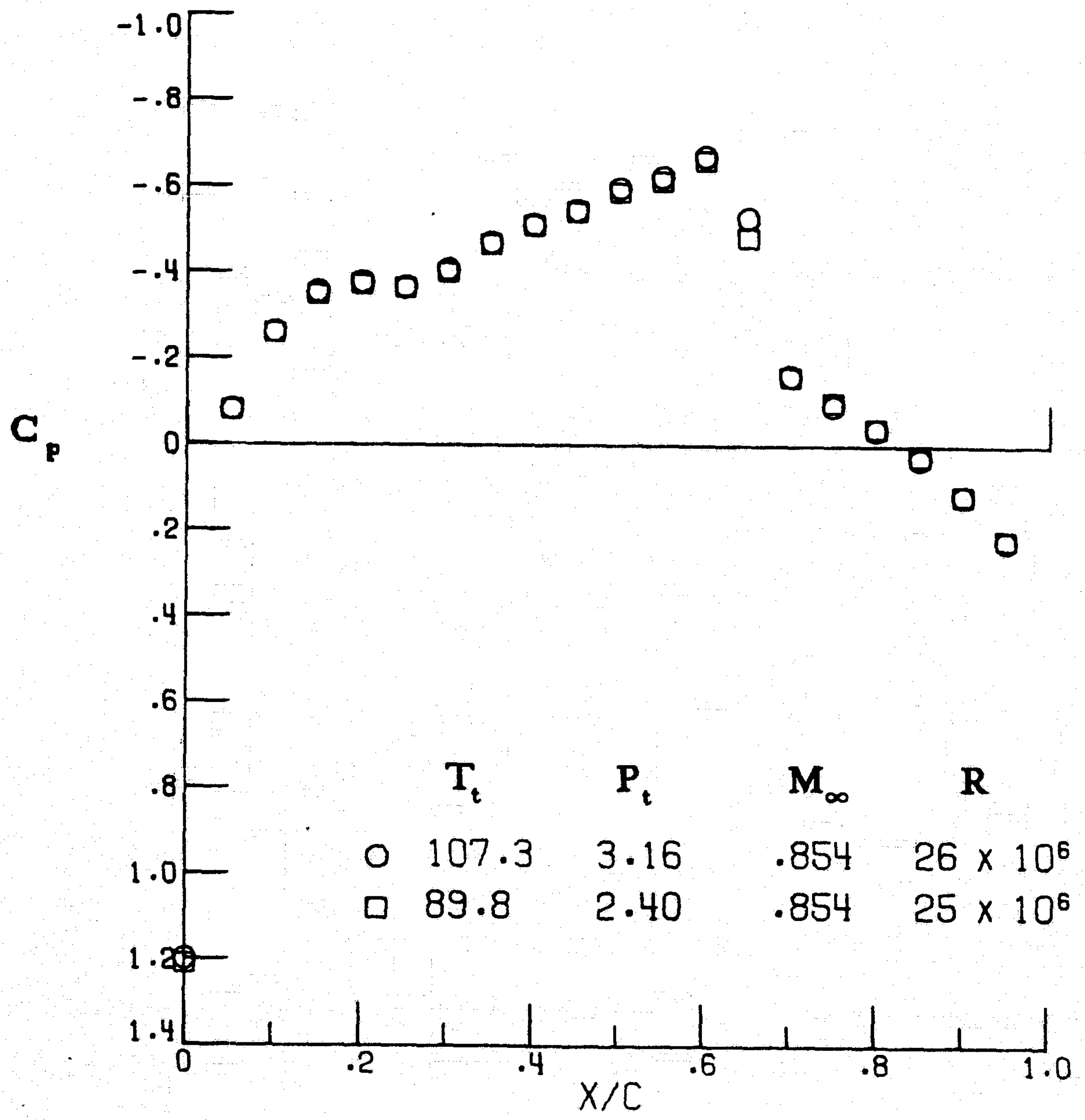

Figure 11. - Path 2, T_t = 89.8K is 2.7K below free-stream saturation line, no effect.

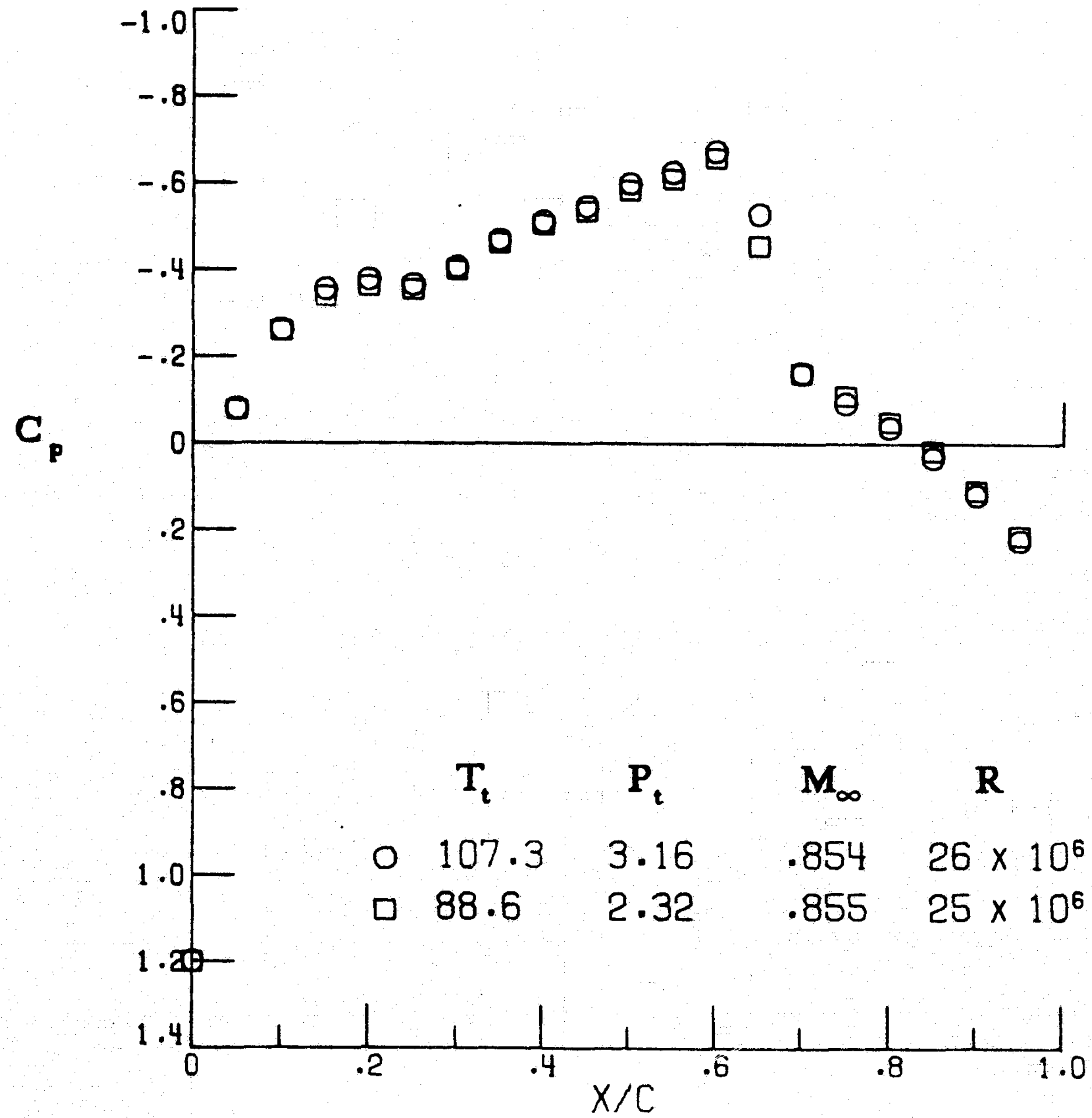

Figure 12. - Path 2, T_t = 88.6K is 3.5K below free-stream saturation line, definite effect.

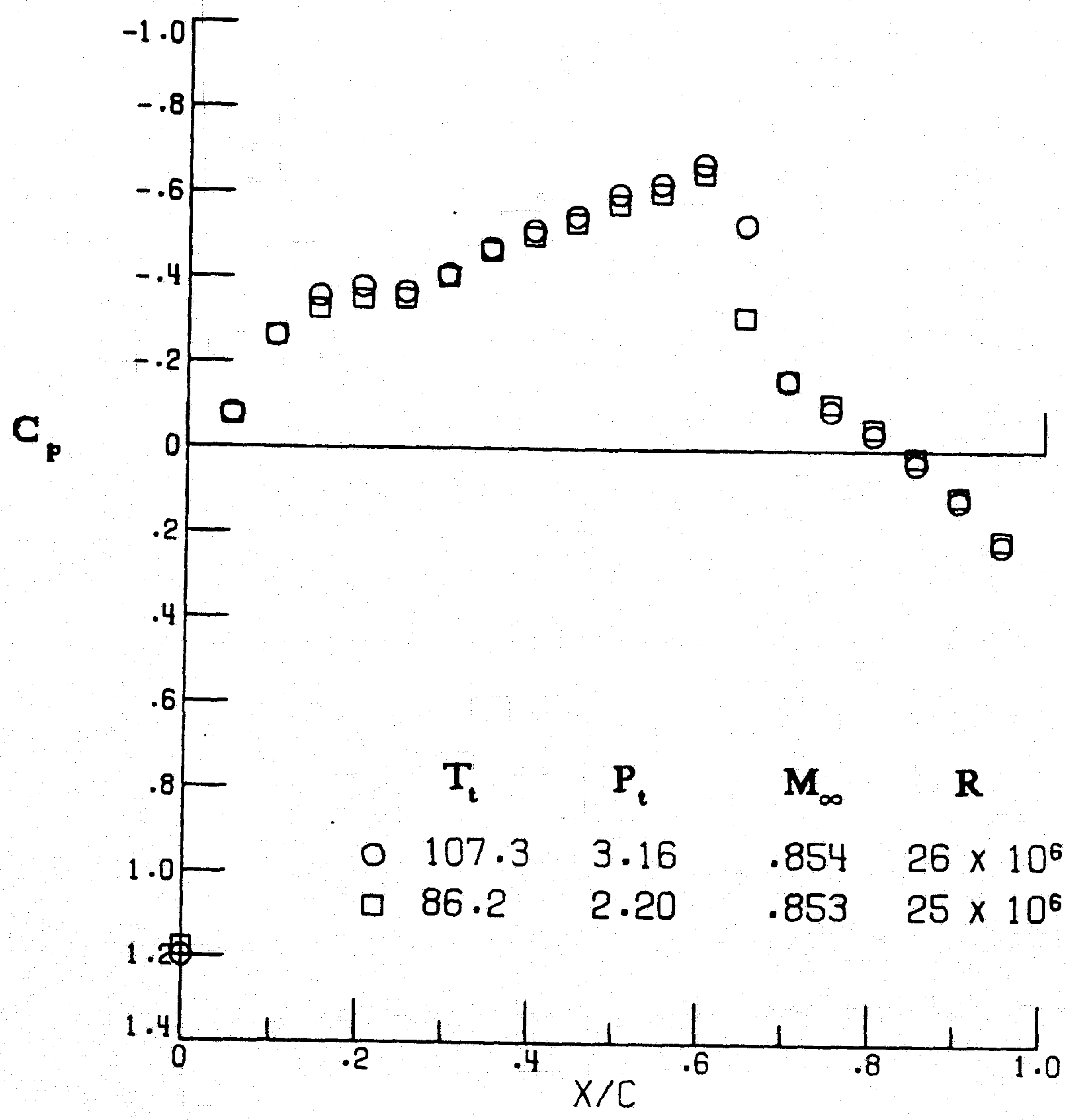

Figure 13. - Path 2, T_t = 86.2K is 5.5K below free-stream saturation line, definite effect.

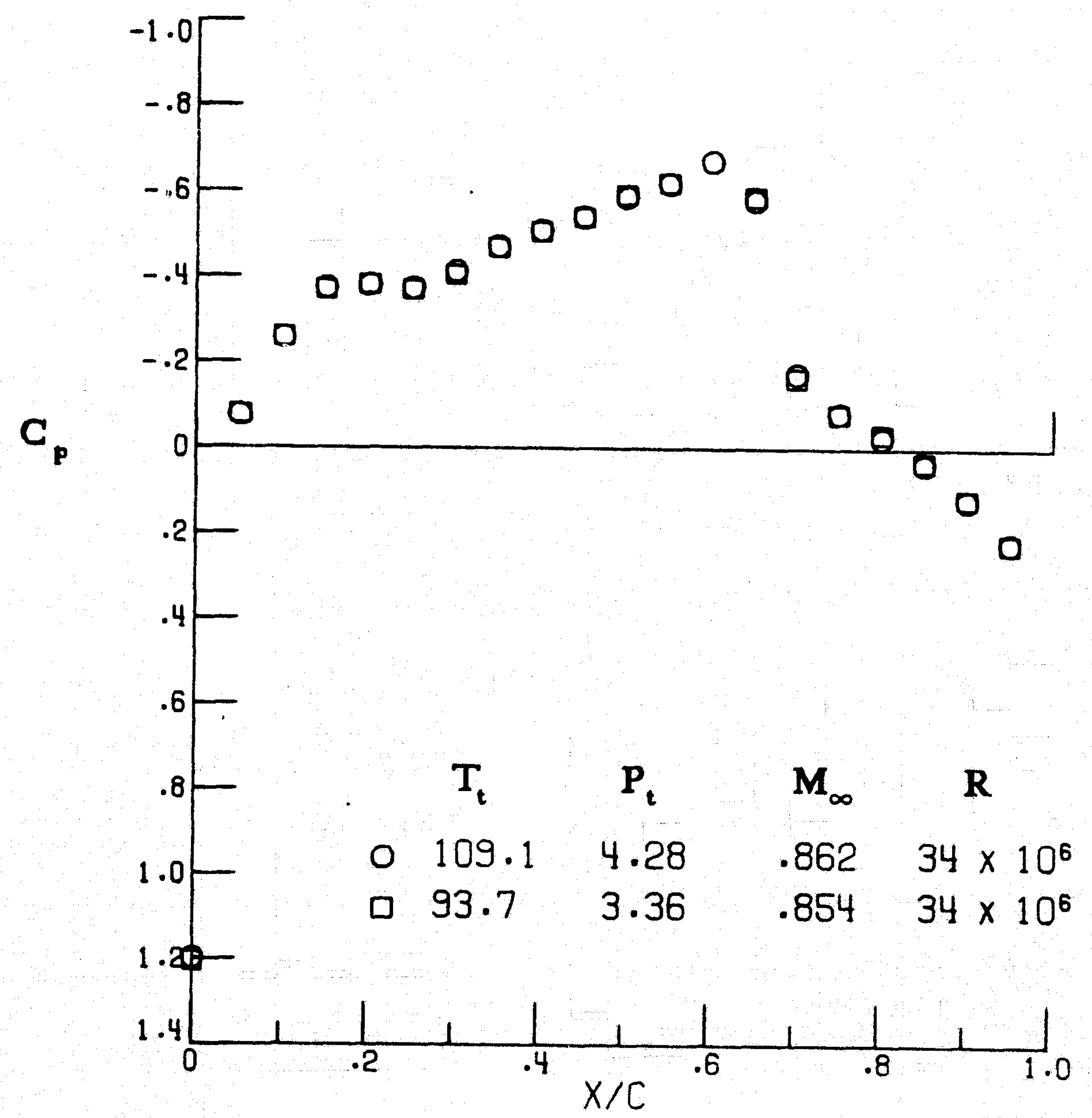

Figure 14. - Path 3, T_t = 93.7K is 2.5K below free-stream saturation line, no effect.

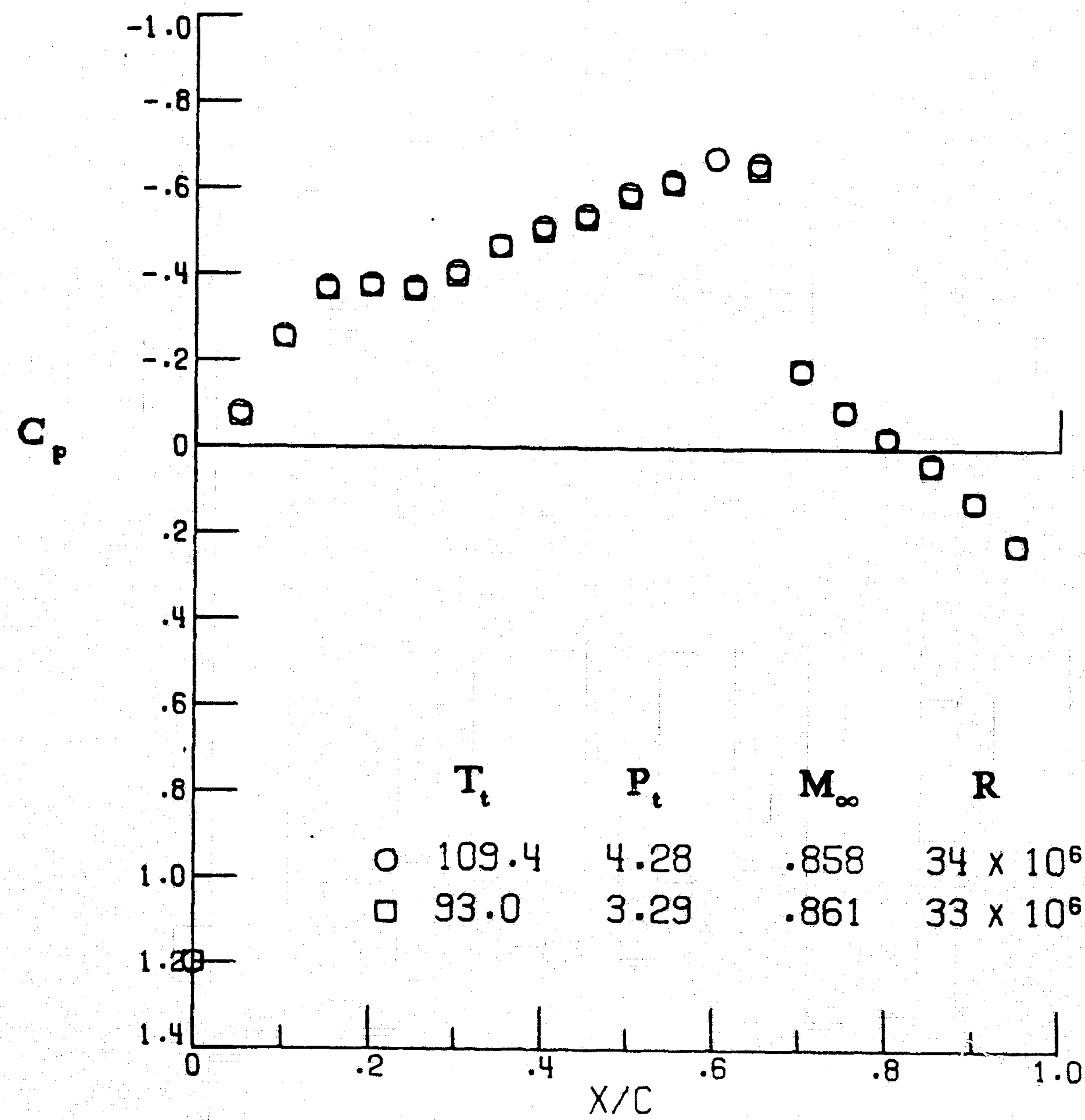

Figure 15. - Path 3, T_t = 93.0K is 3K below free-stream saturation line, possible effect.

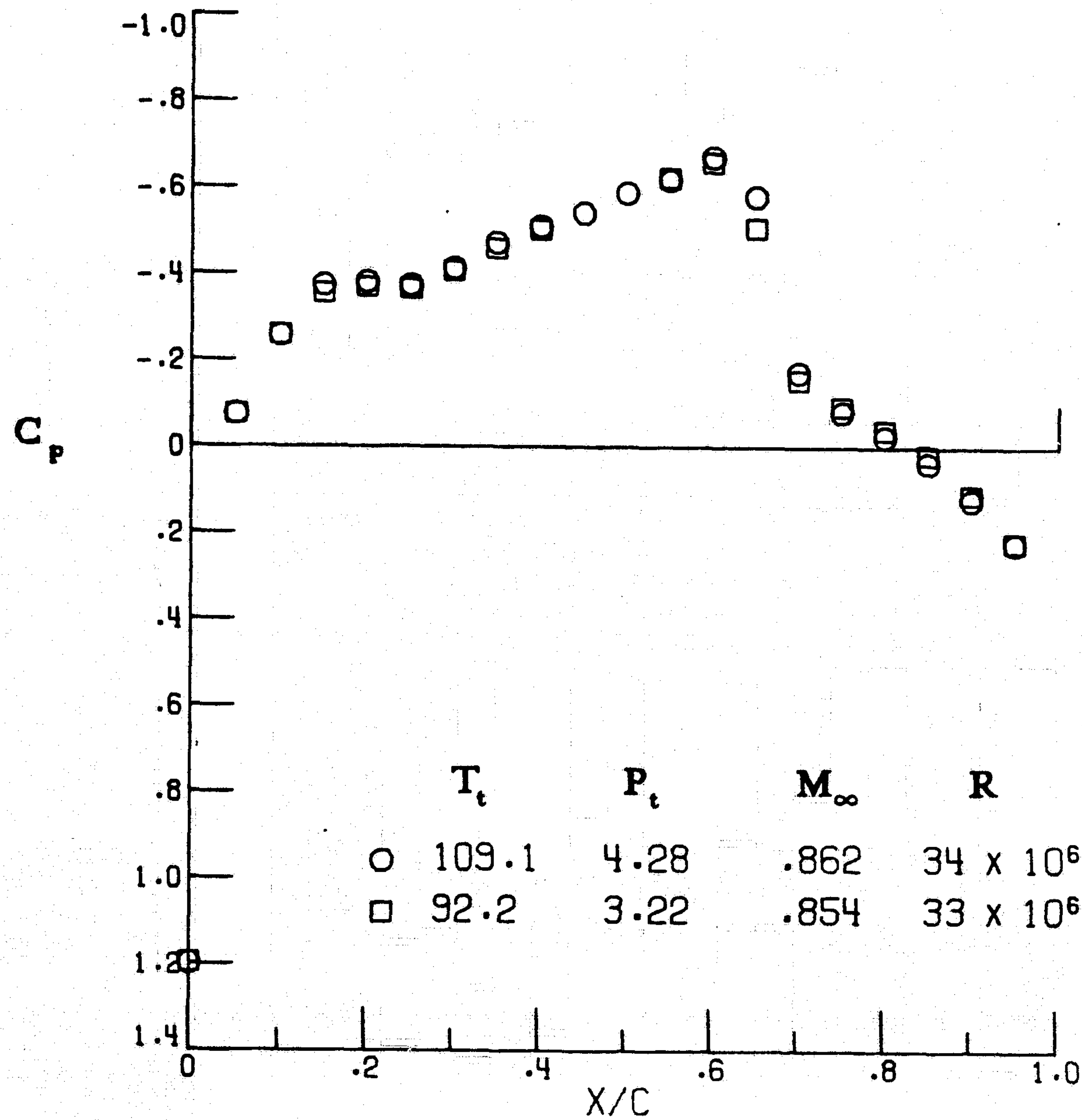

Figure 16. - Path 3, T_t = 92.2K is 3.5K below free-stream saturation line, definite effect.

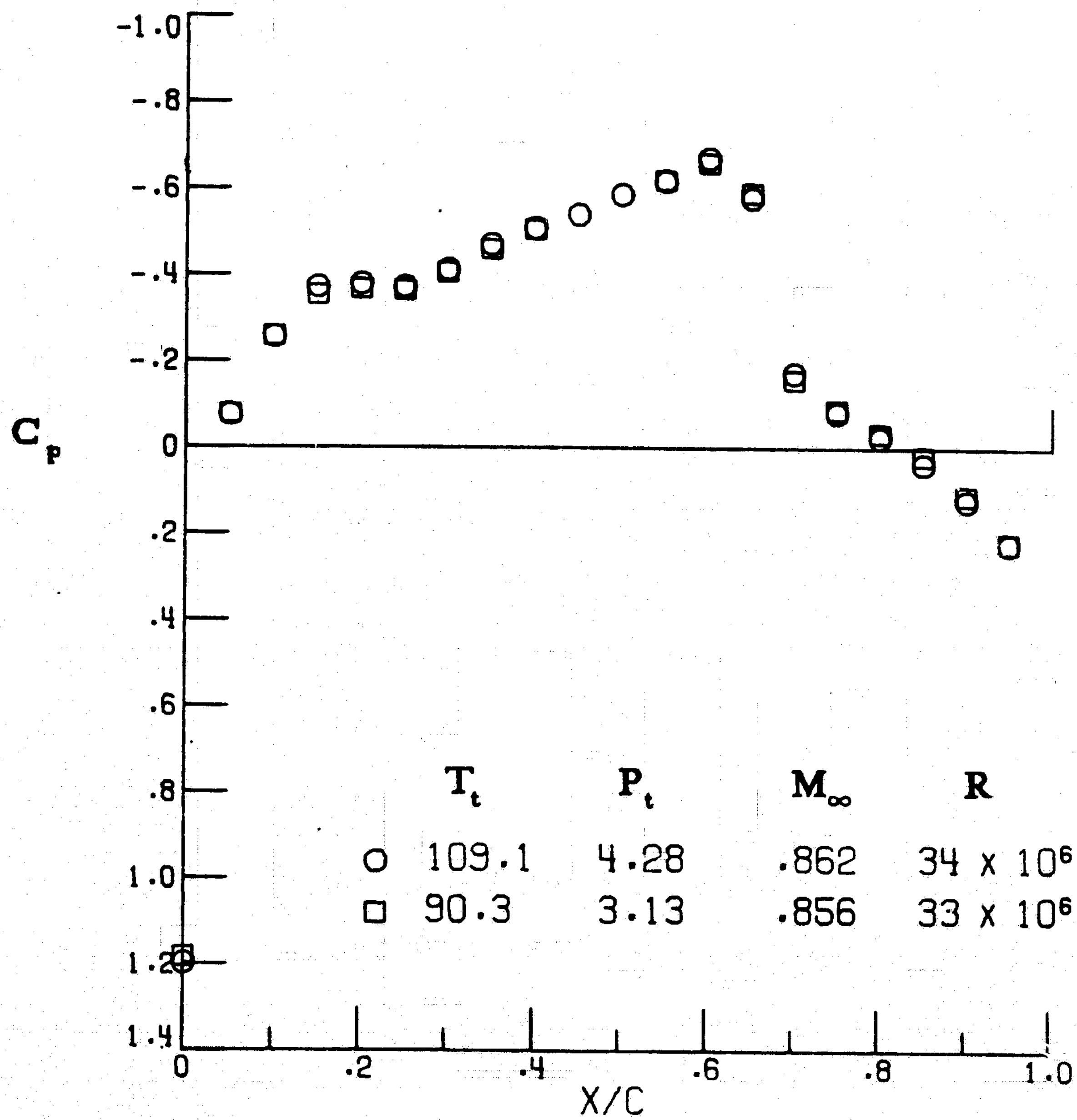

Figure 17. - Path 3, T_t = 90.3K is 5K below free-stream saturation line, possible effect.

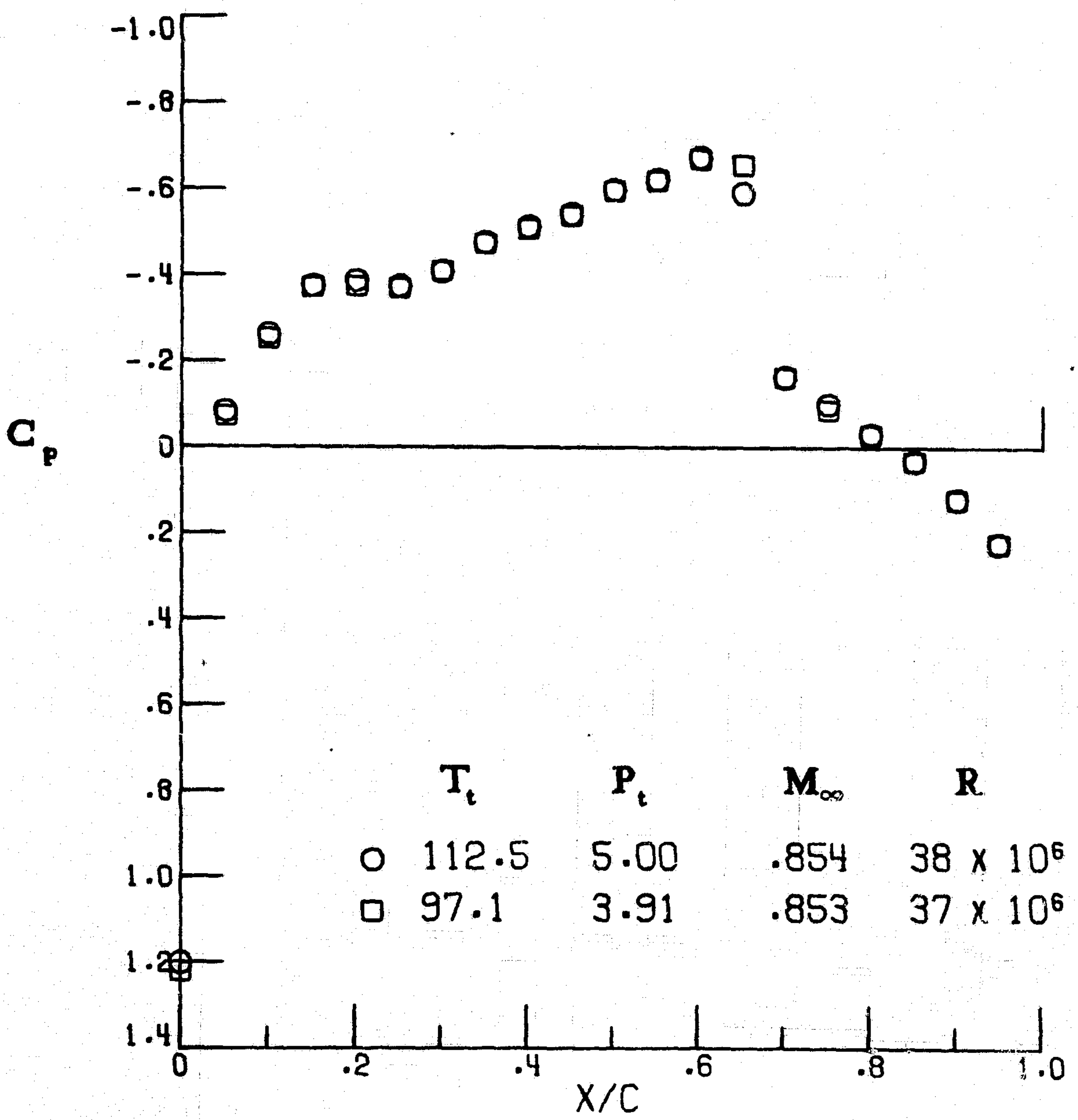

Figure 18. - Path 4, T_t = 97.1K is 1K below free-stream saturation line, no effect.

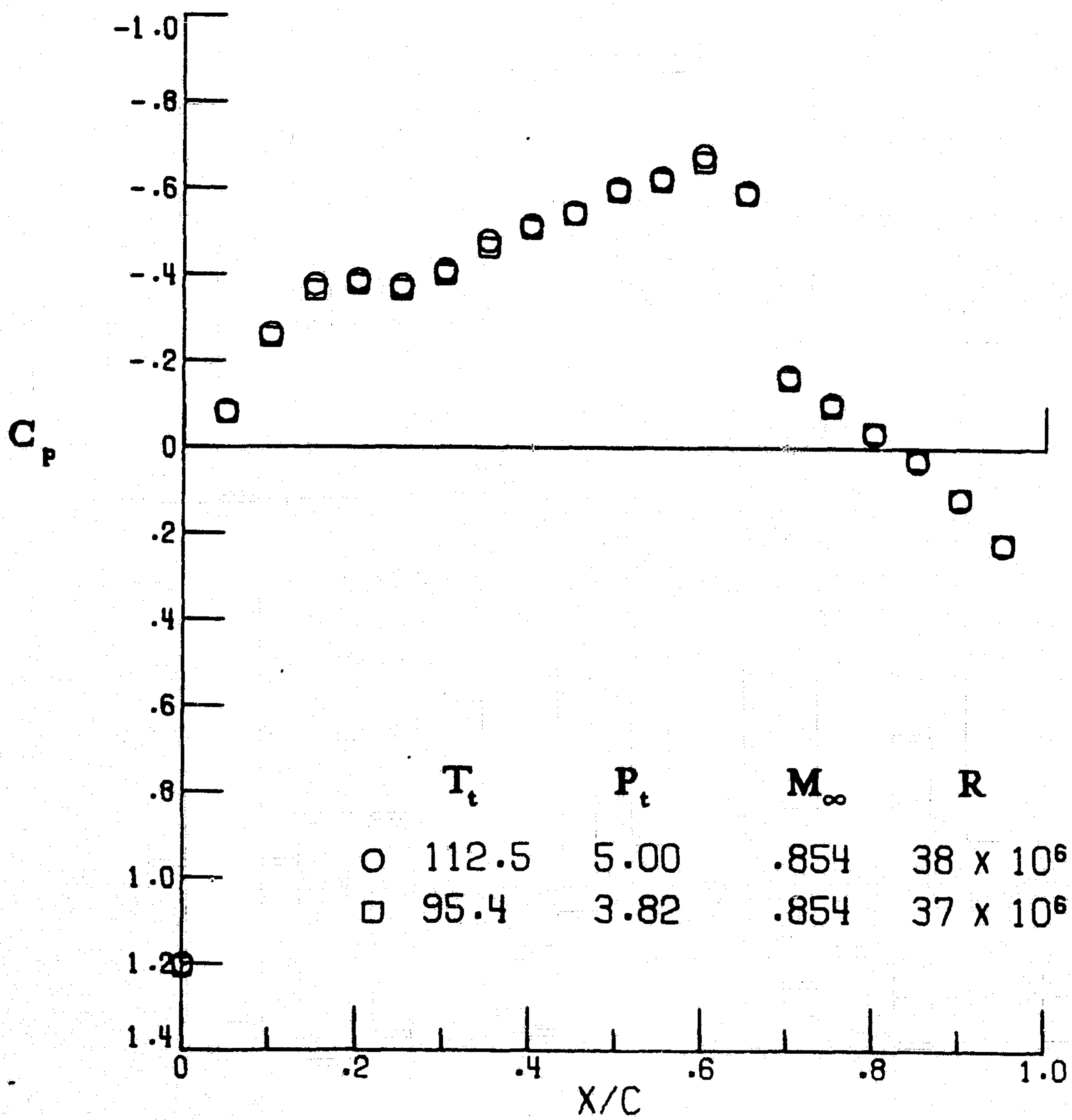

Figure 19. - Path 4, T_t = 95.4K is 2.5K below free-stream saturation line, possible effect.

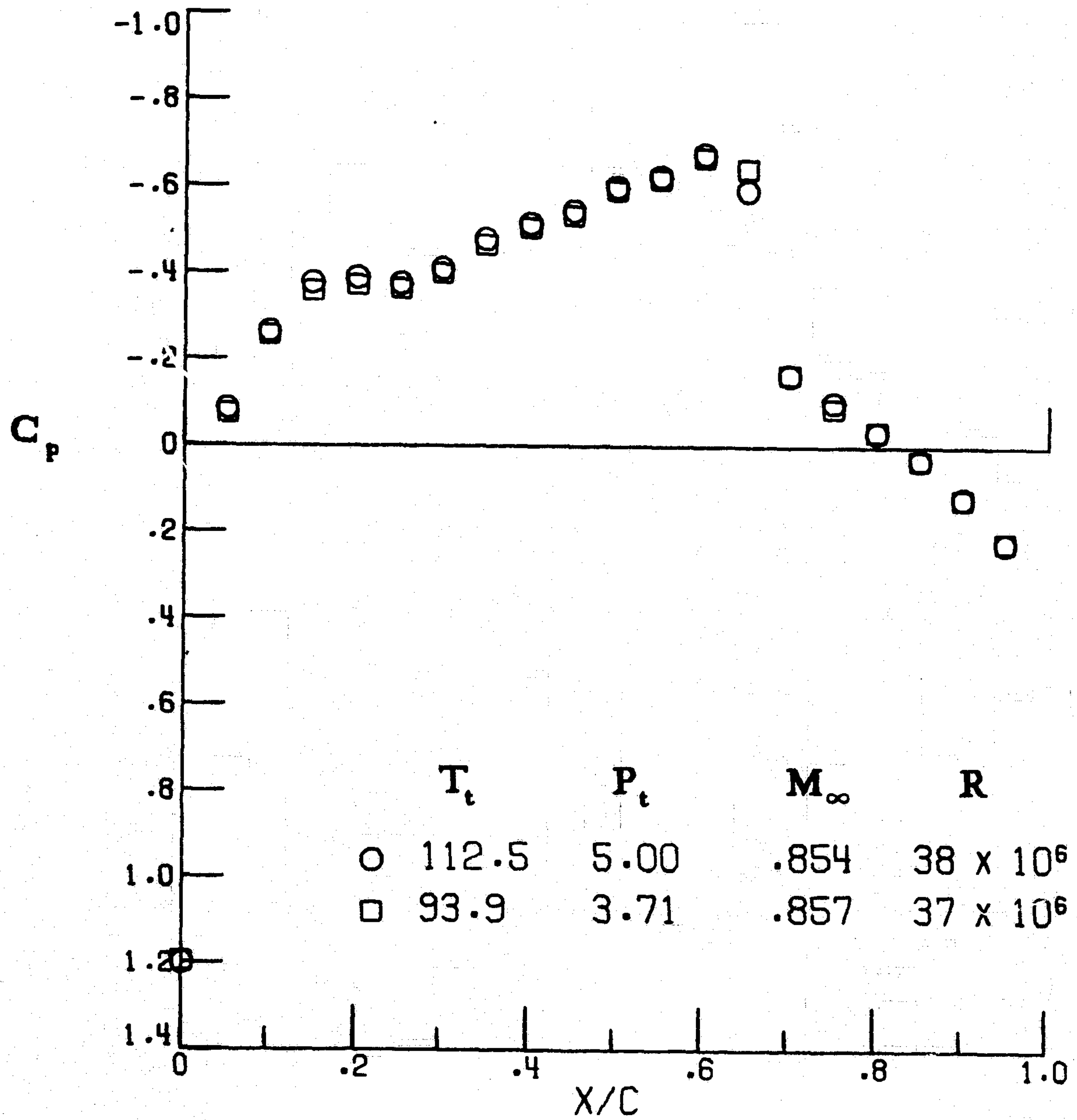

Figure 20. - Path 4, T_t = 93.9K is 3.5K below free-stream saturation line, definite effect.

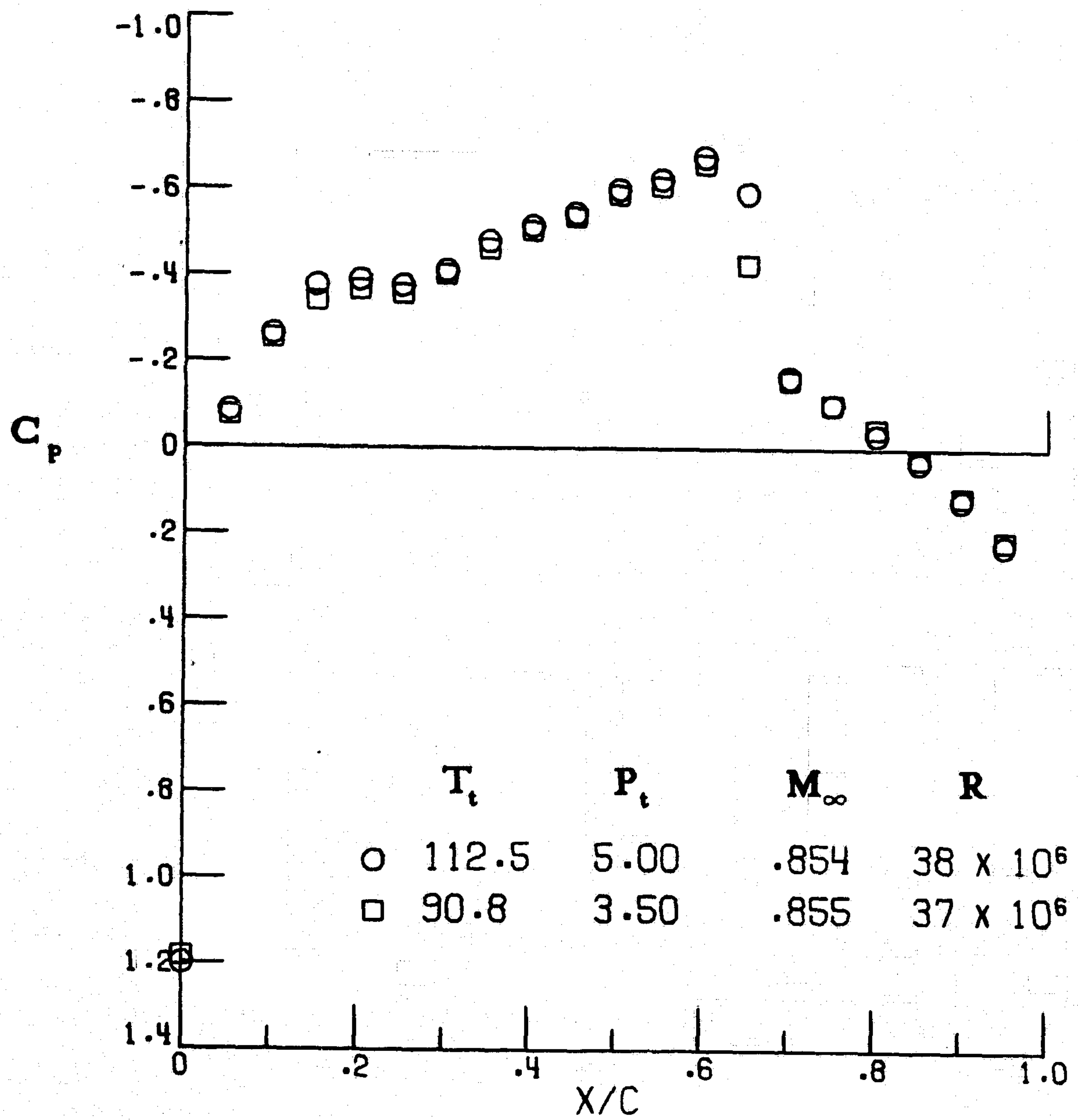

Figure 21. - Path 4, T_t = 90.8K is 6K below free-stream saturation line, definite effect.

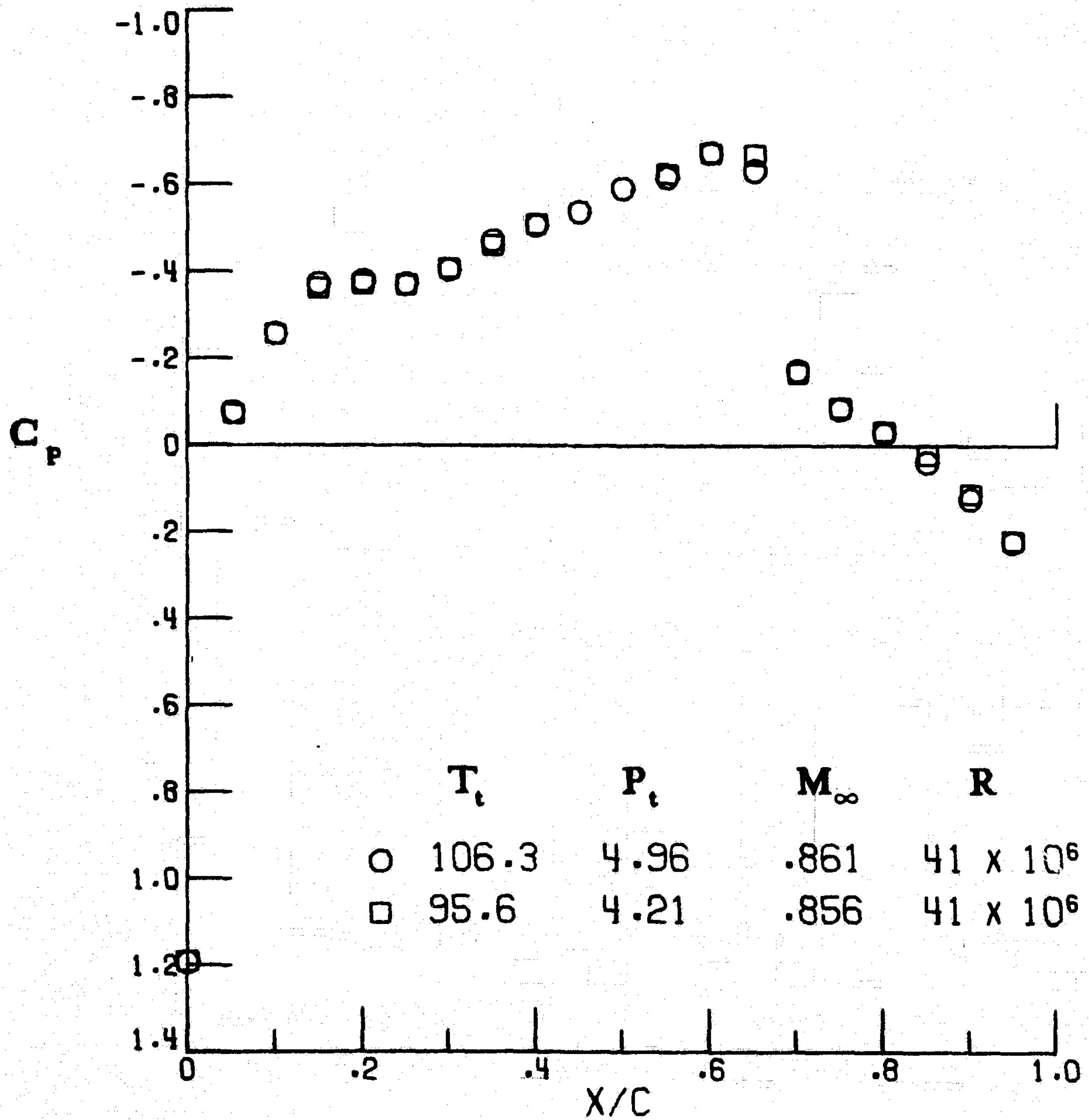

Figure 22. - Path 5, T_t = 95.6K is 3.6K below free-stream saturation line, possible effect.

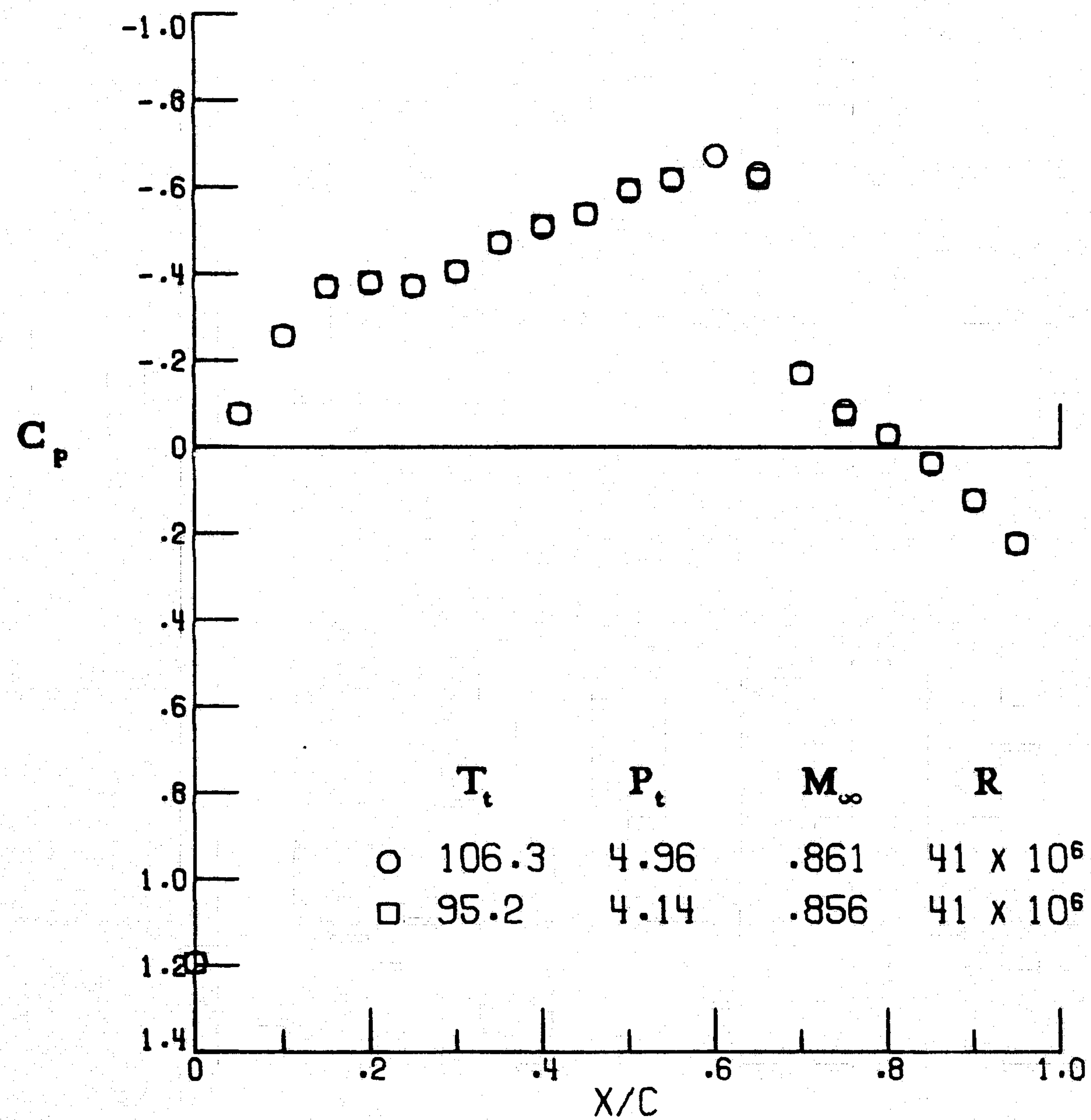

Figure 23. - Path 5, T_t = 95.2K is 3.8K below free-stream saturation line, no effect.

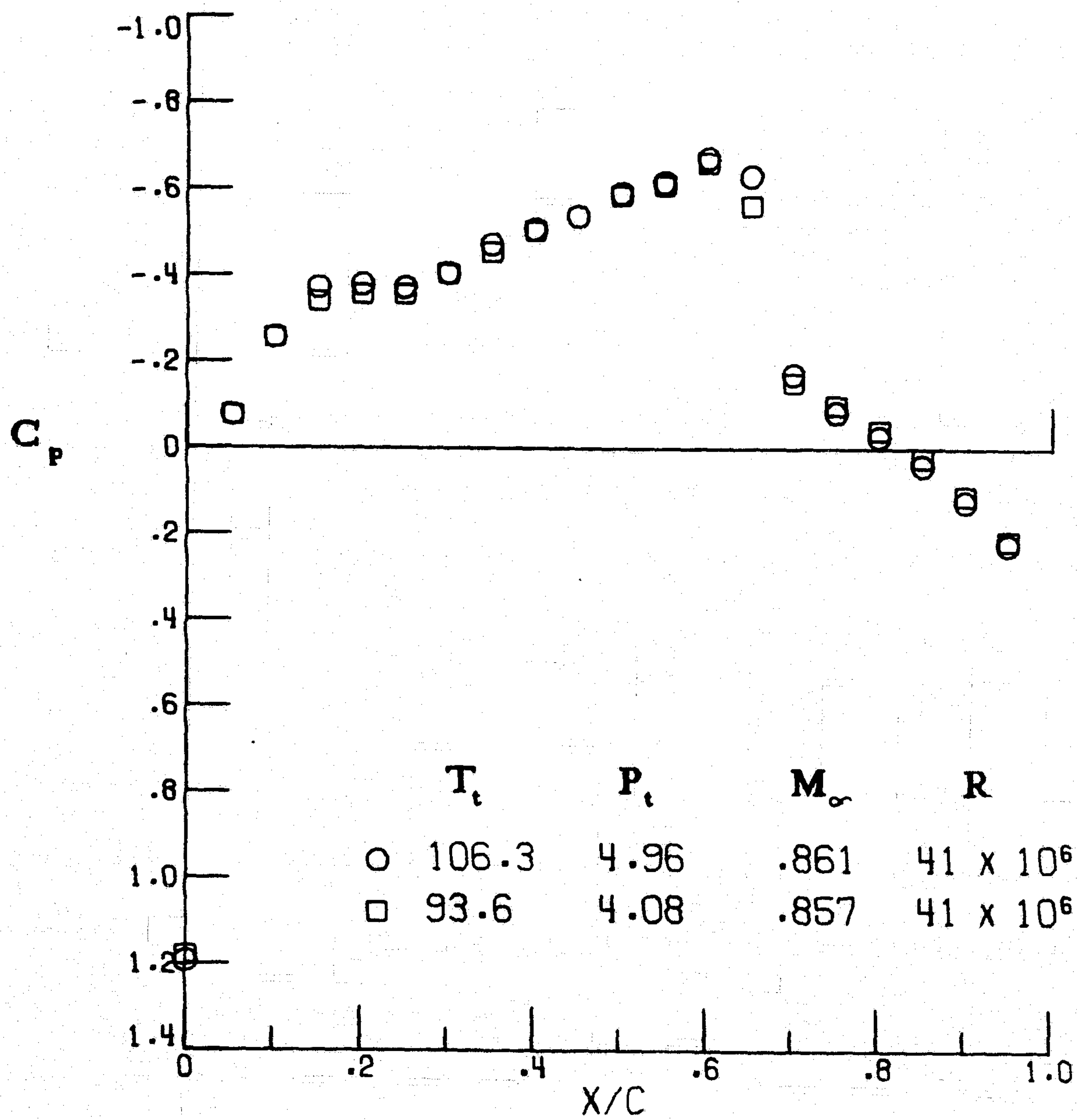

Figure 24. - Path 5, T_t = 93.6K is 5.0K below free-stream saturation line, definite effect.

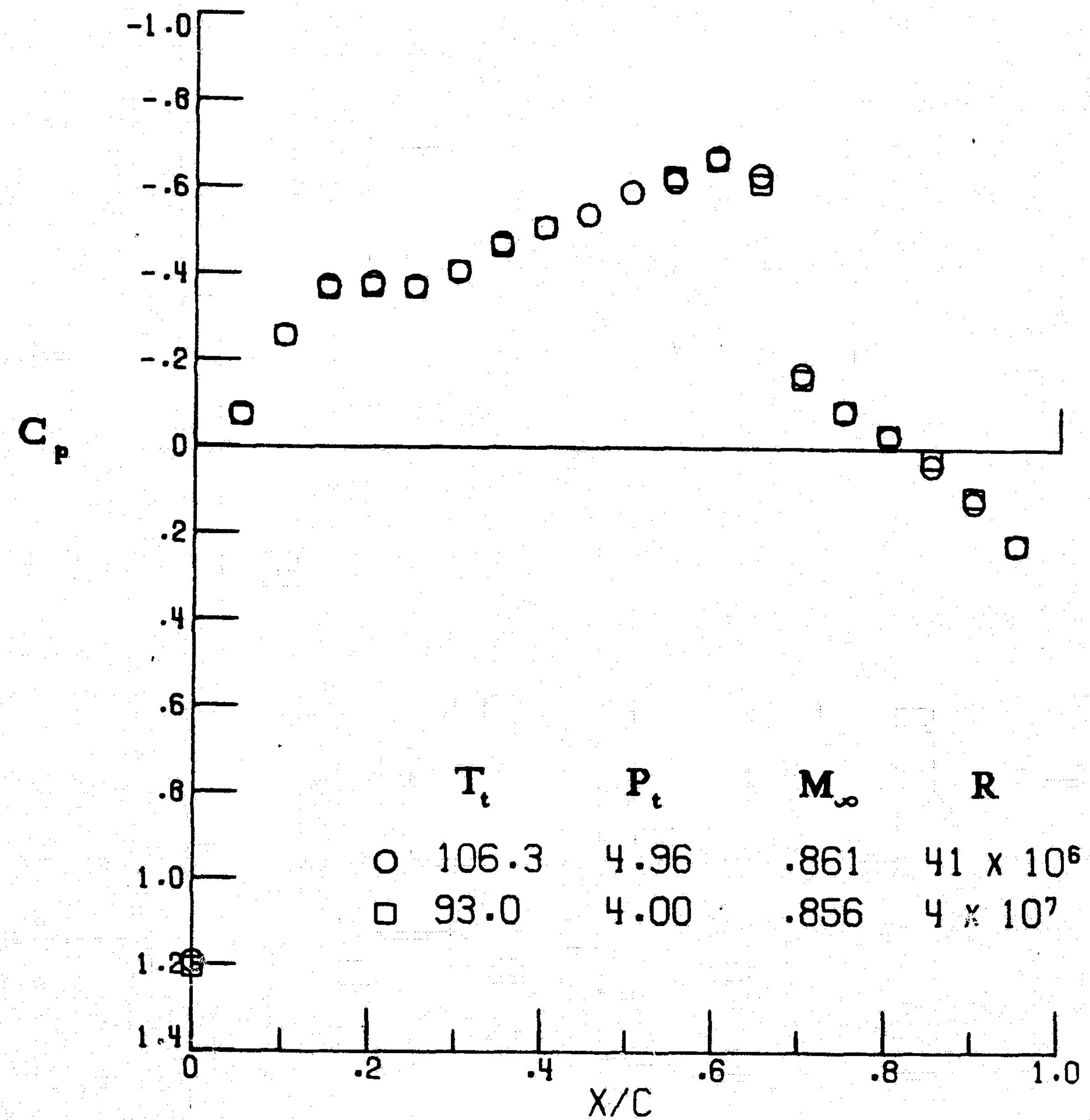

Figure 25. - Path 5, T_t = 93.0K is 5.2K below free-stream saturation line, possible effect.

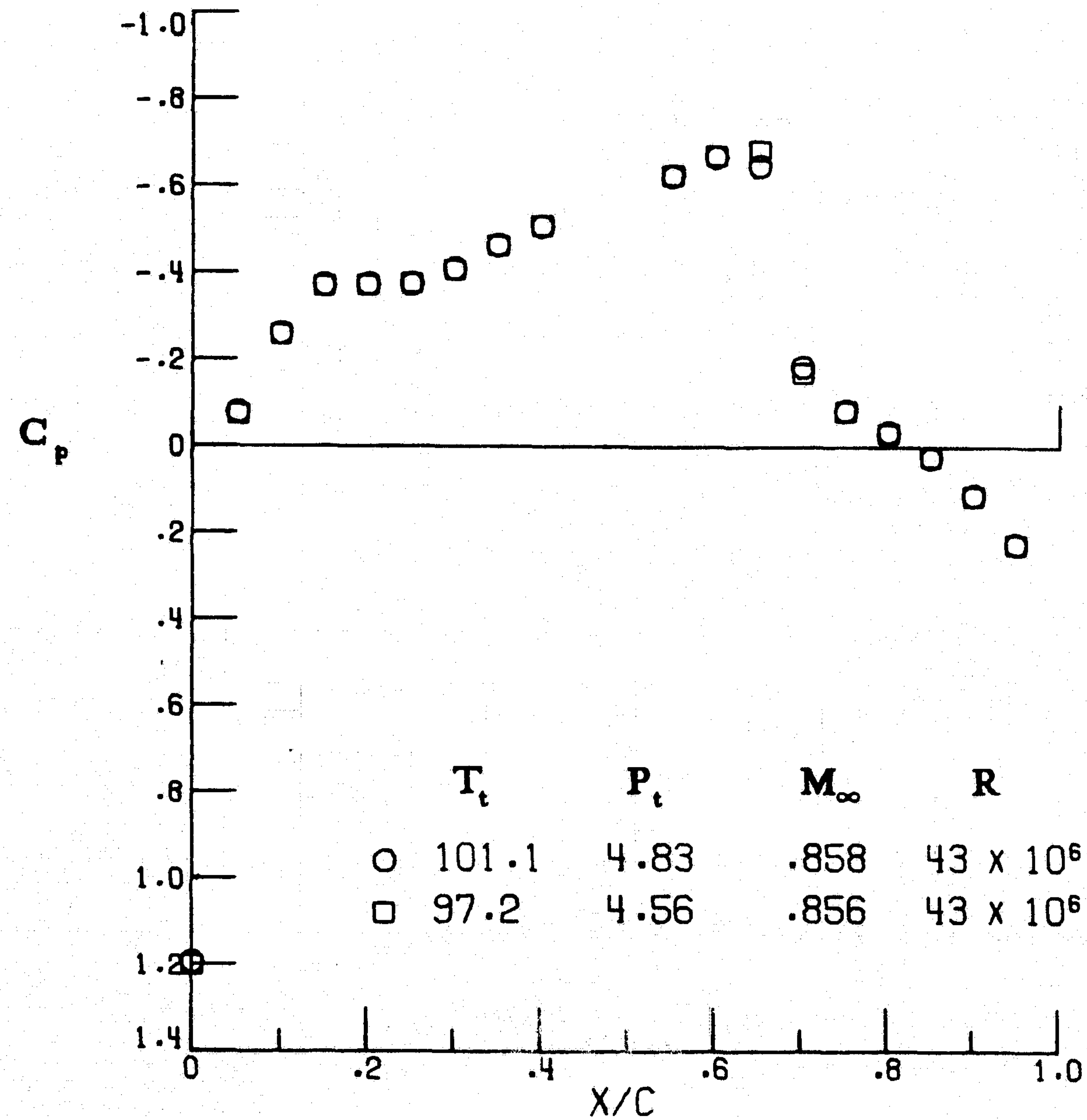

Figure 26. - Path 6, T_t = 97.2K is 3K below free-stream saturation line, no effect.

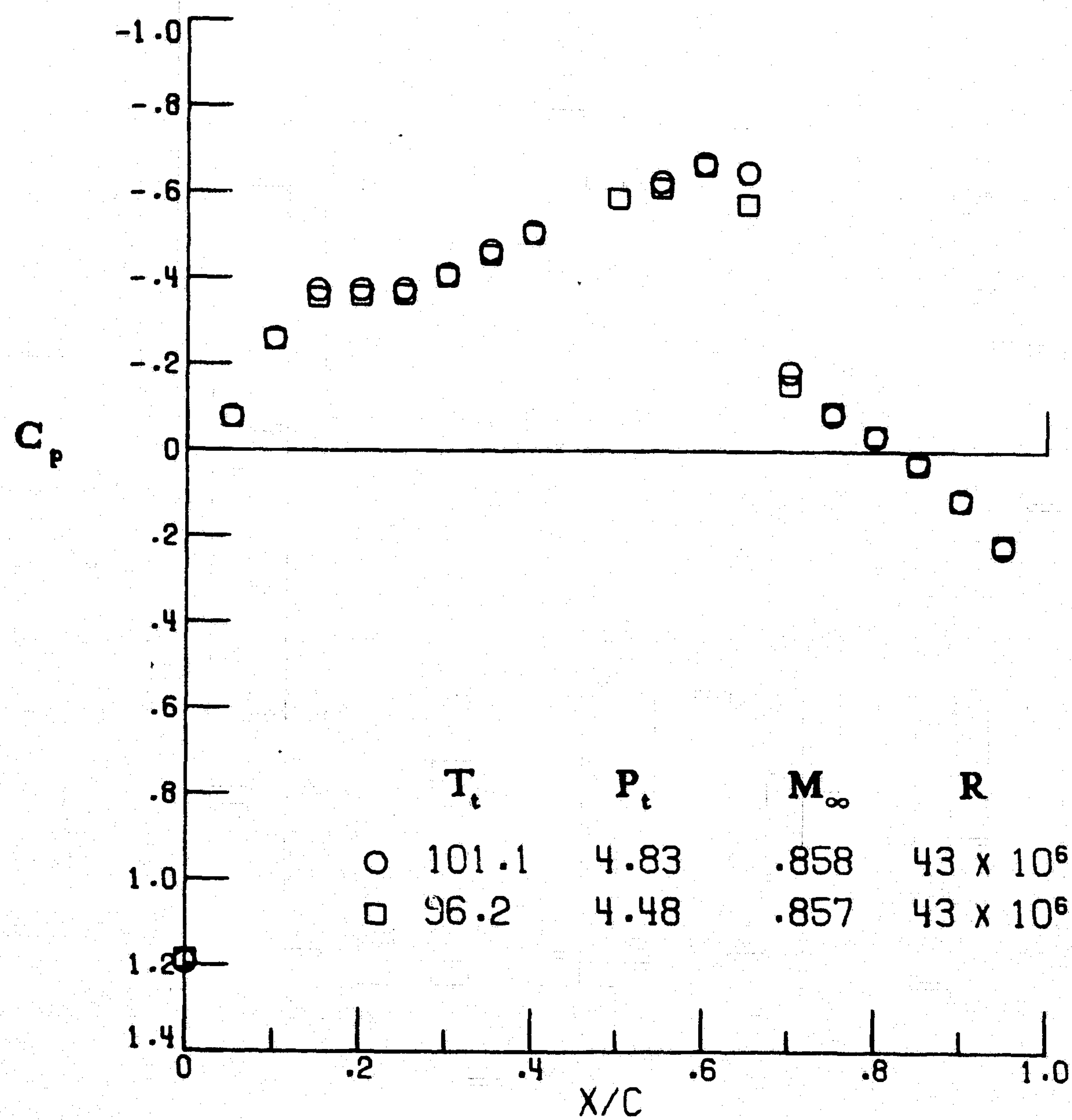

Figure 27. - Path 6, T_t = 96.2K is 3.5K below free-stream saturation line, possible effect.

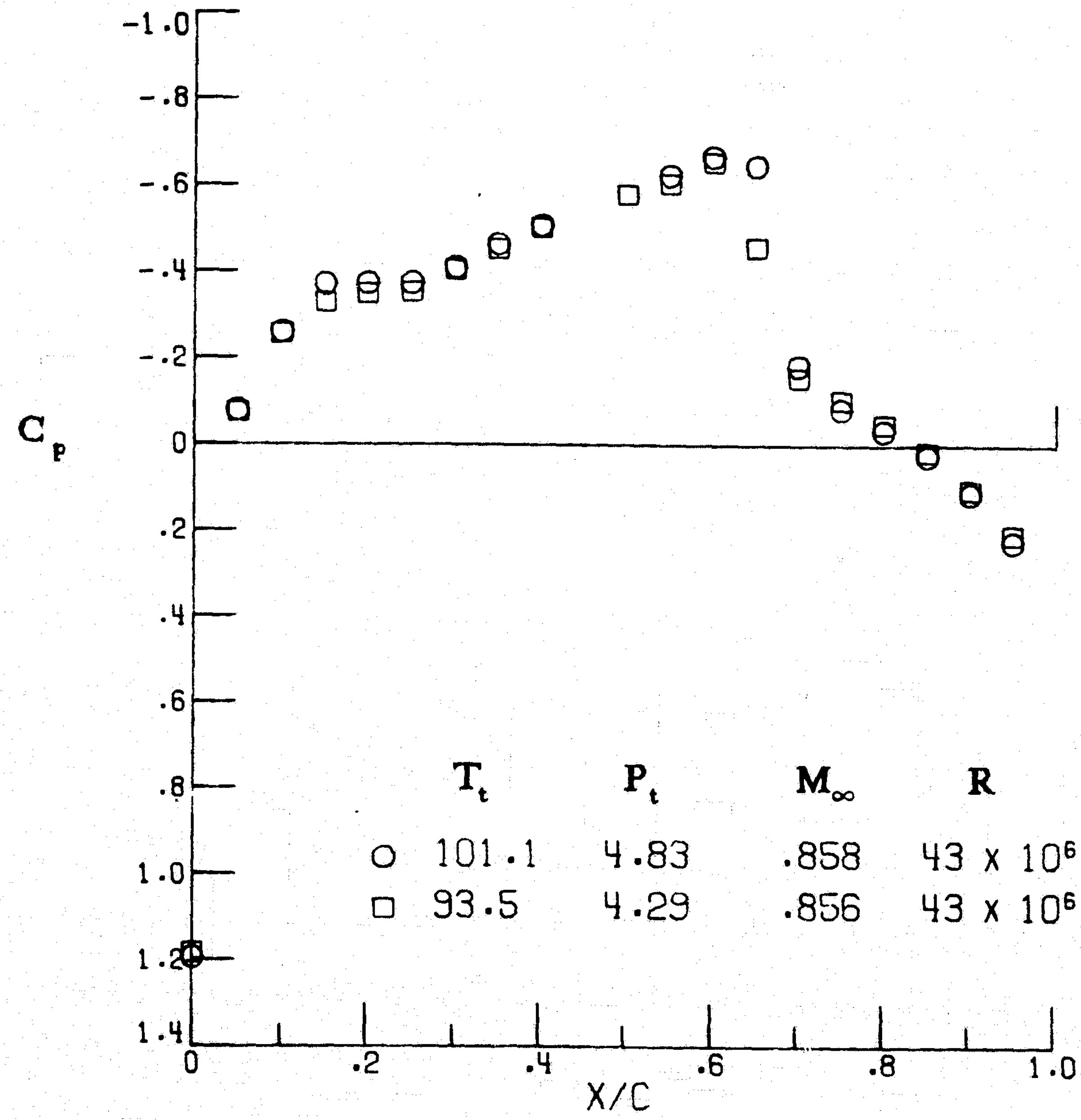

Figure 28. - Path 6, T_t = 93.5K is 5.5K below free-stream saturation line, definite effect.

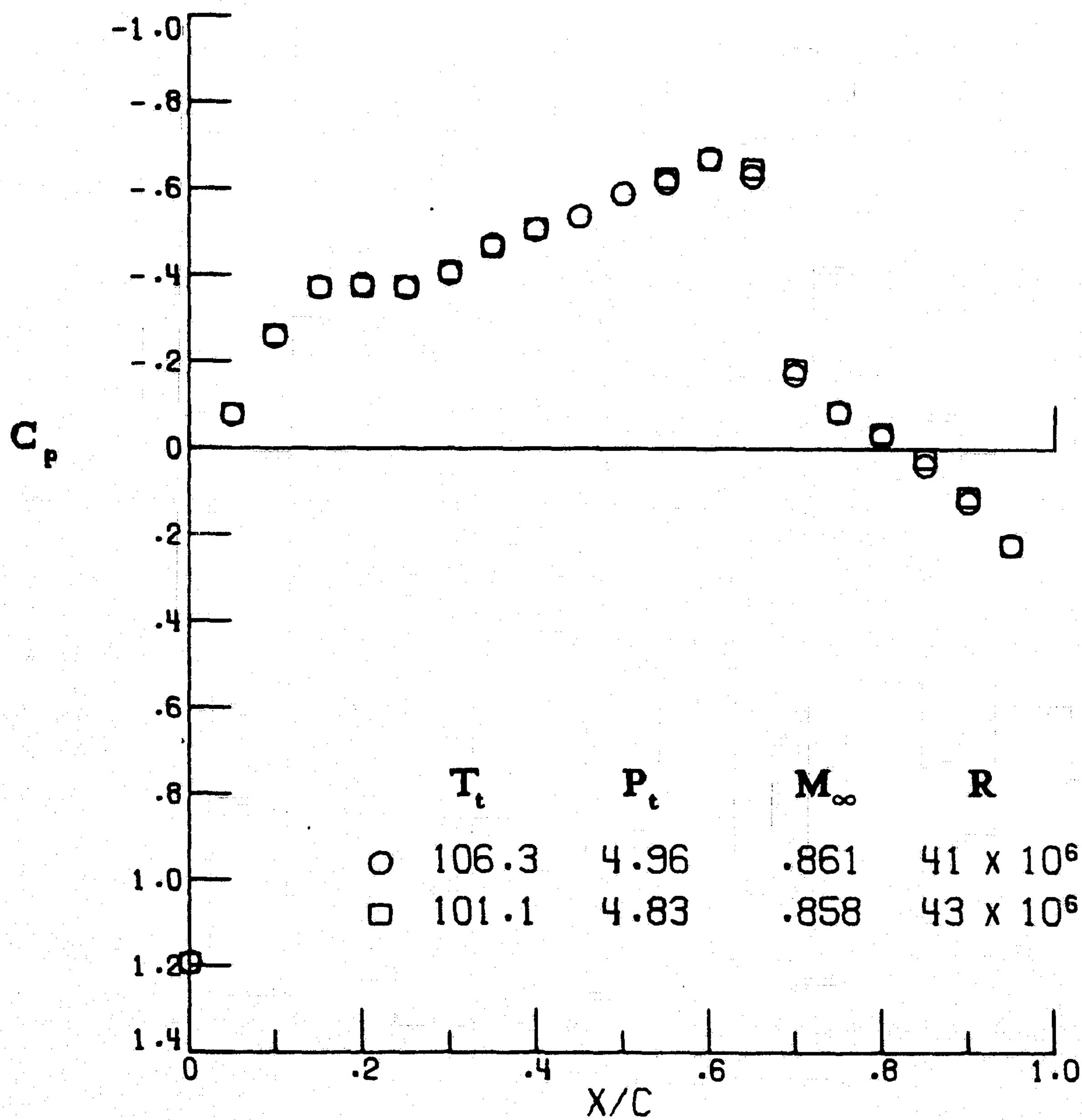

Figure 29. - Comparison of point 68 of path 6 to point 54 of path 5.

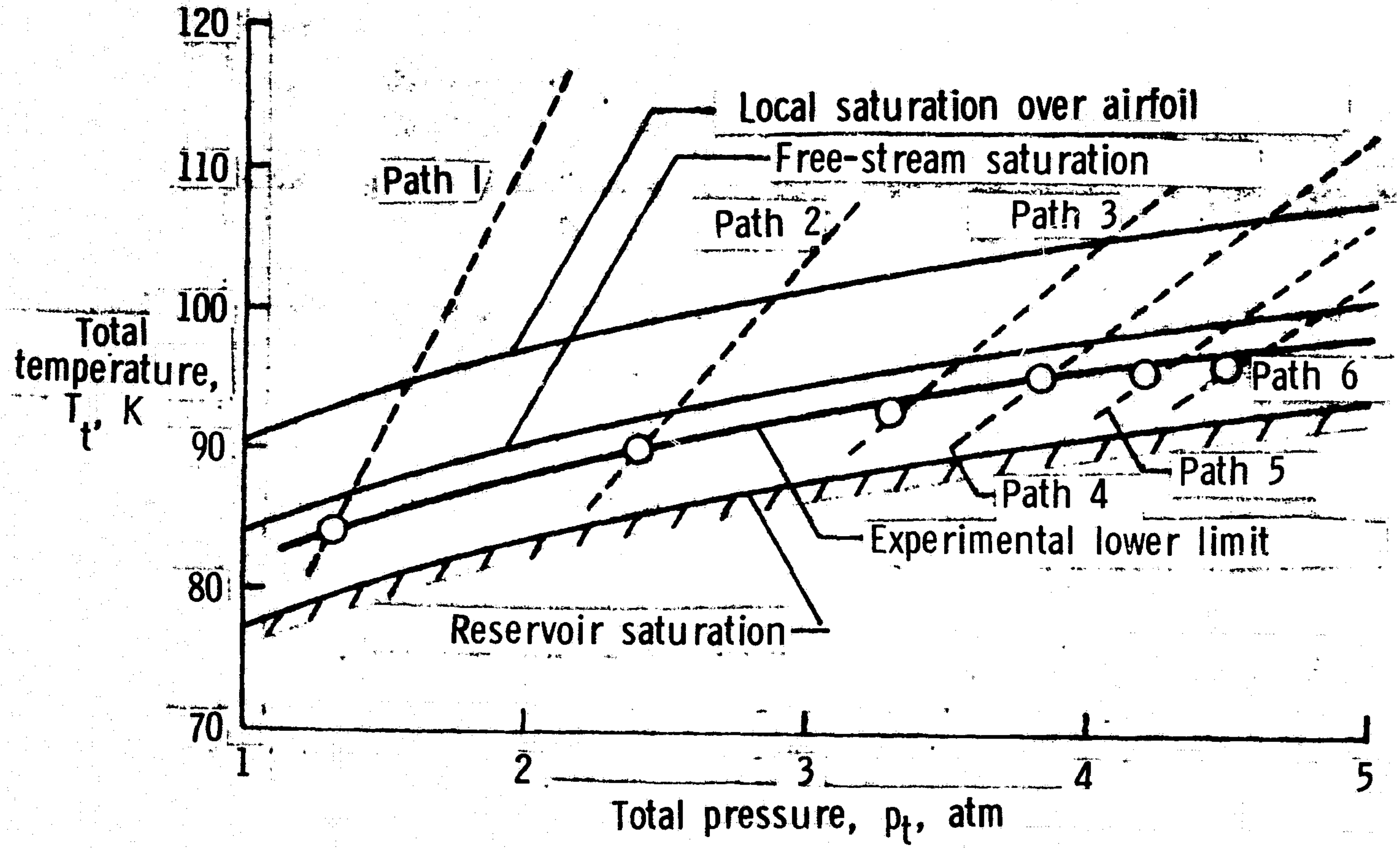

Figure 30.- Experimental lower limit at which pressure distributions begin to differ from their references.

APPENDIX

PRESSURE DISTRIBUTIONS FOR DATA POINTS LISTED IN TABLES

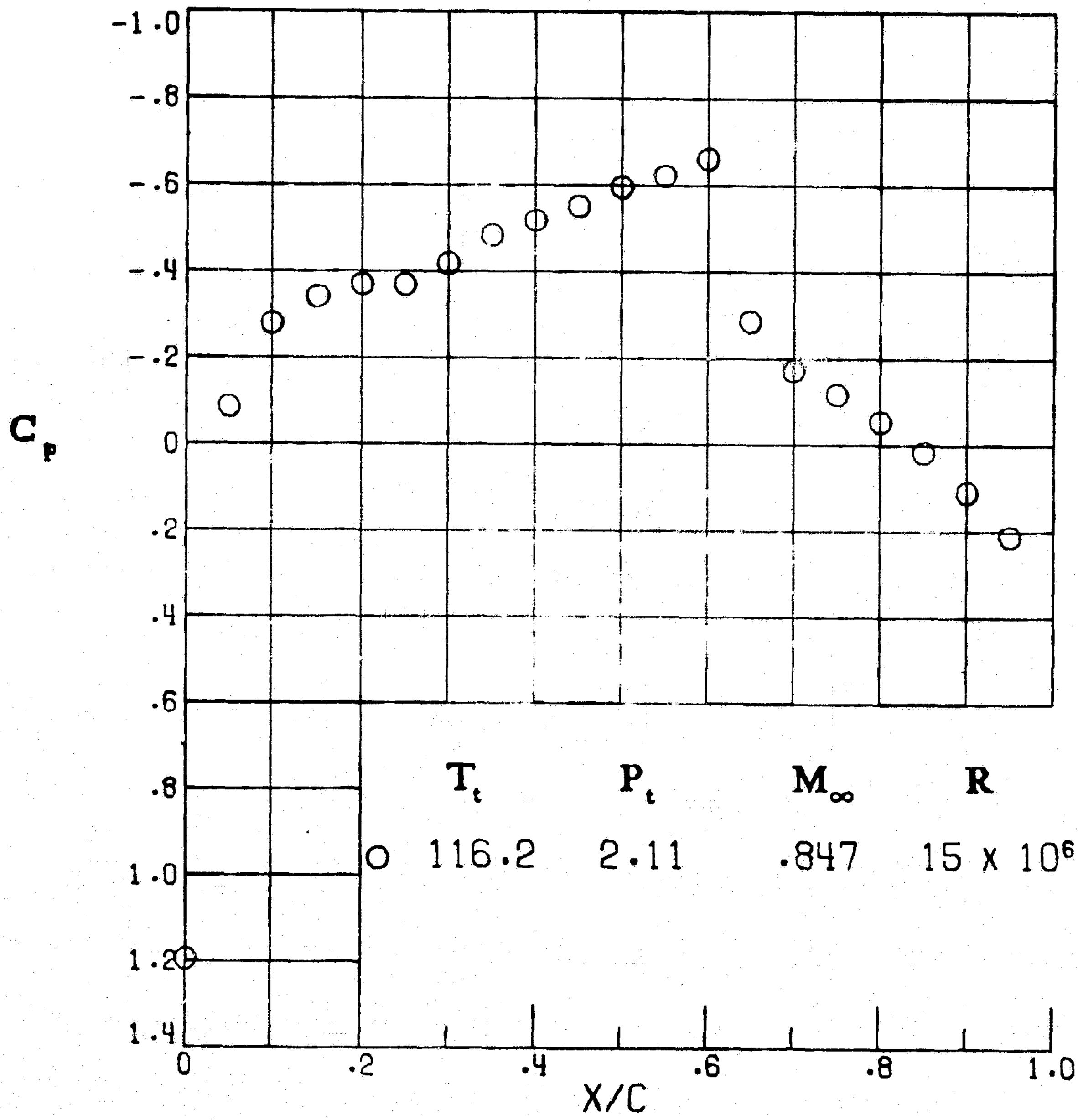

Figure A1.- Path I, reference, above local saturation.

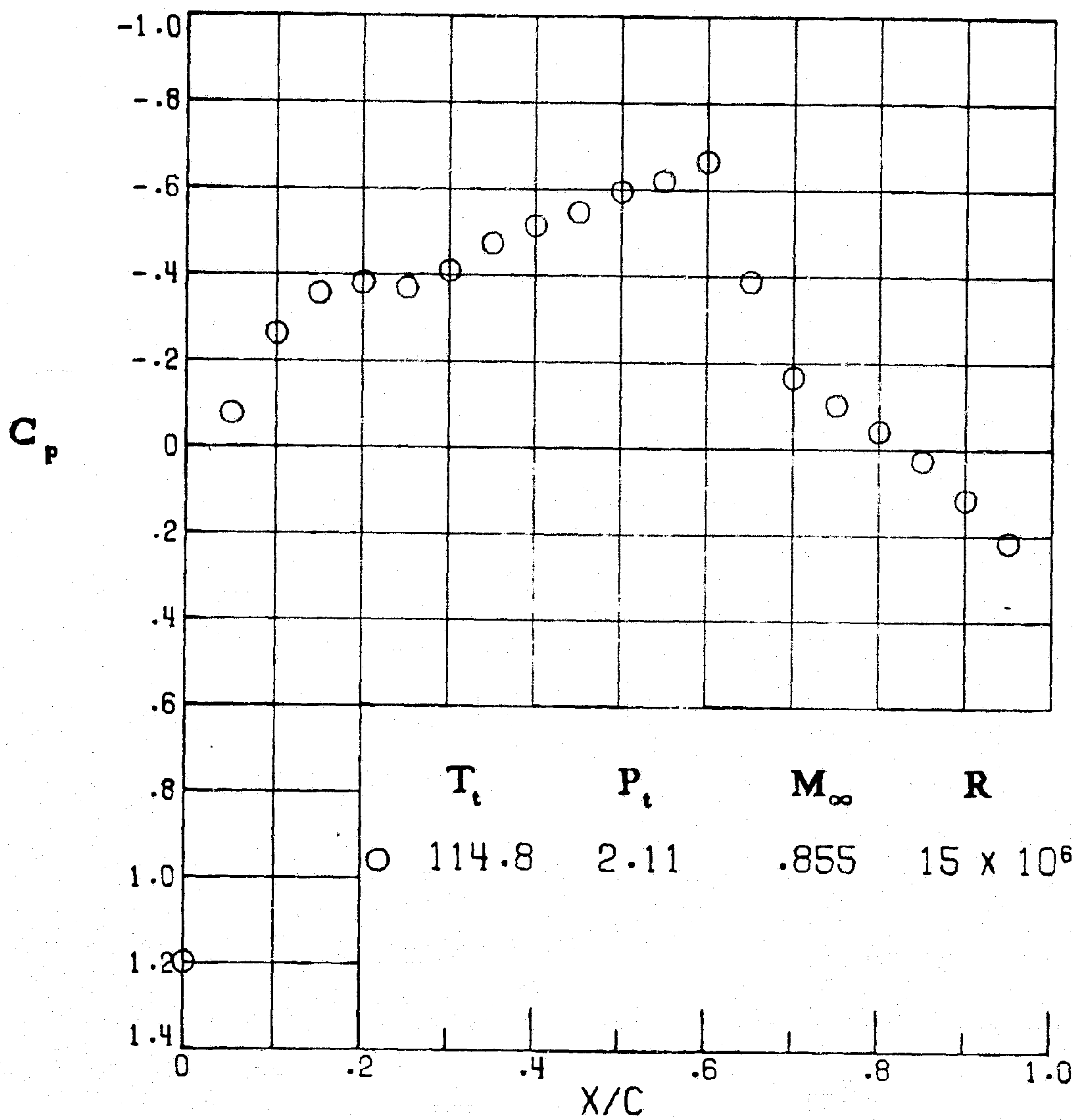

Figure A2.- Path I, reference, above local saturation.

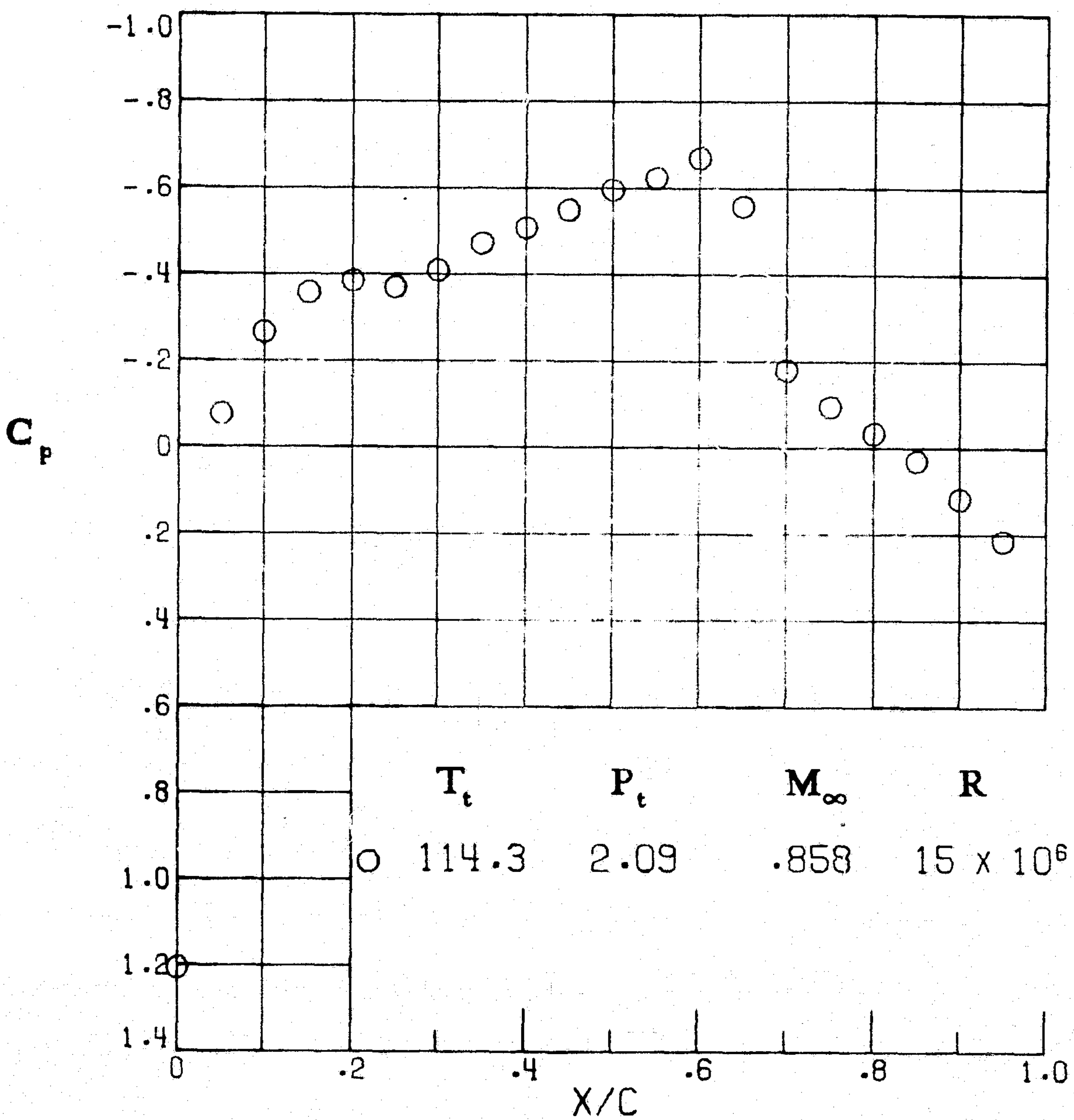

Figure A3.- Path I, reference, above local saturation.

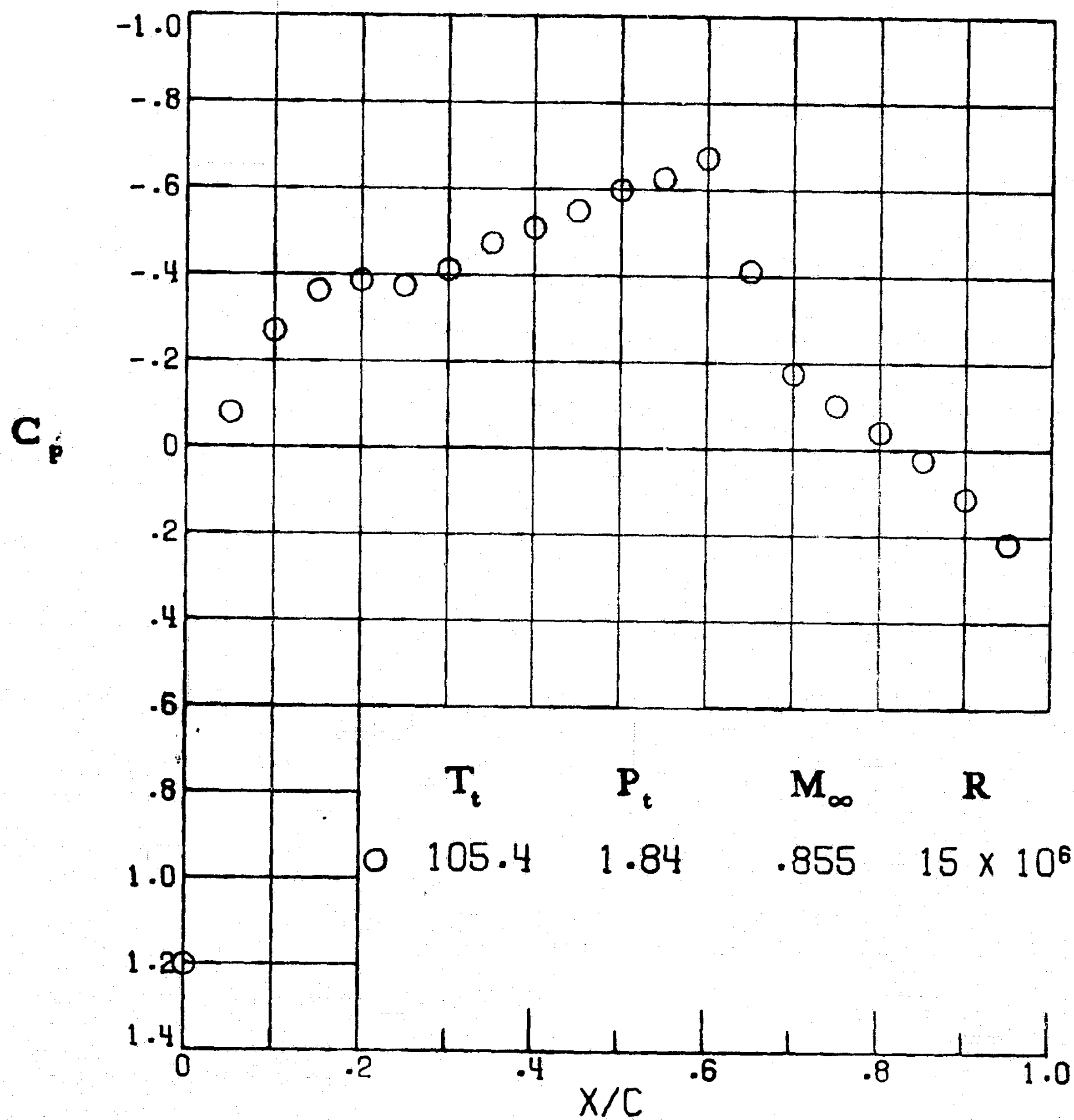

Figure A4.- Path 1, above local saturation.

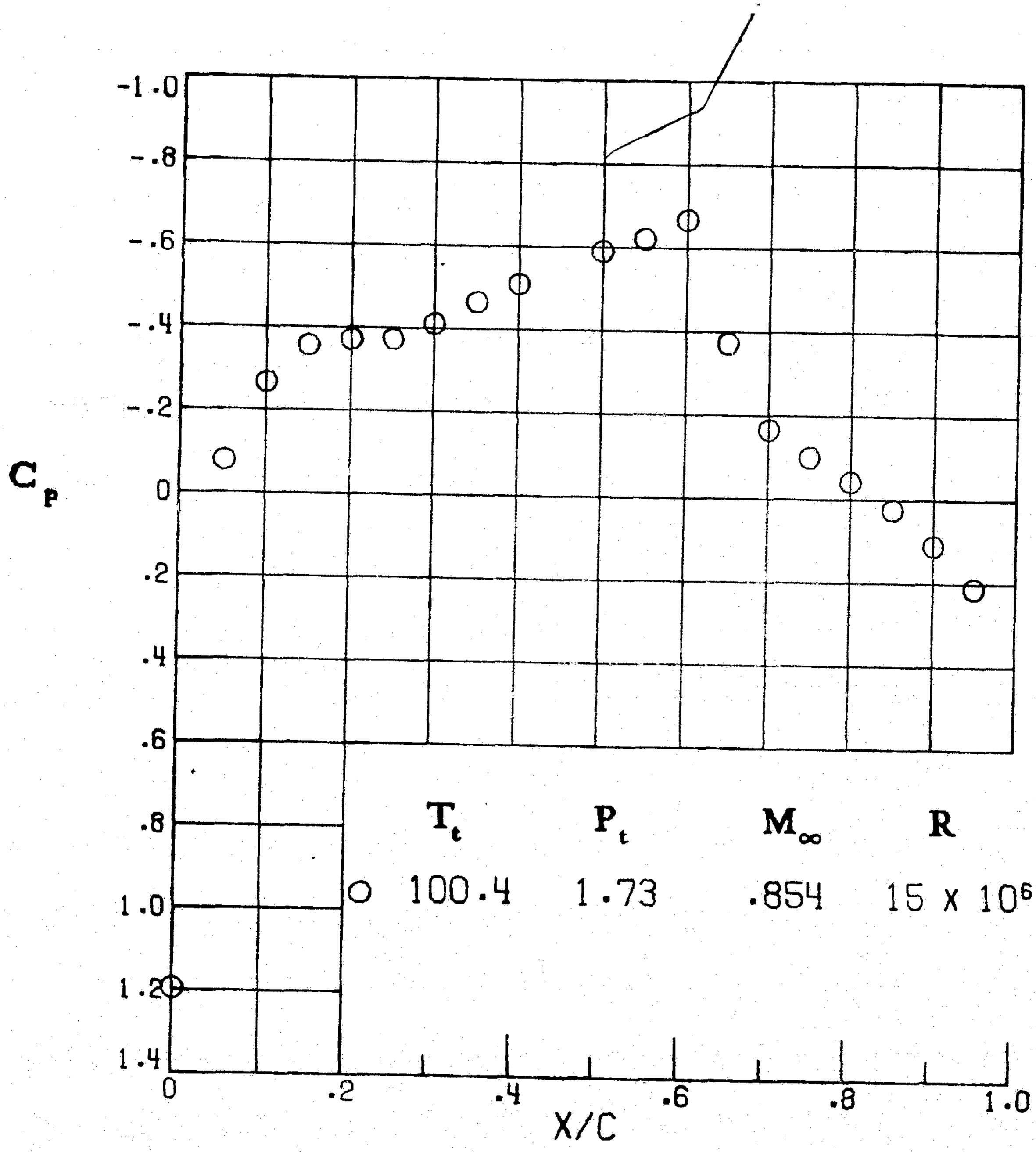

Figure A5.- Path 1, above local saturation.

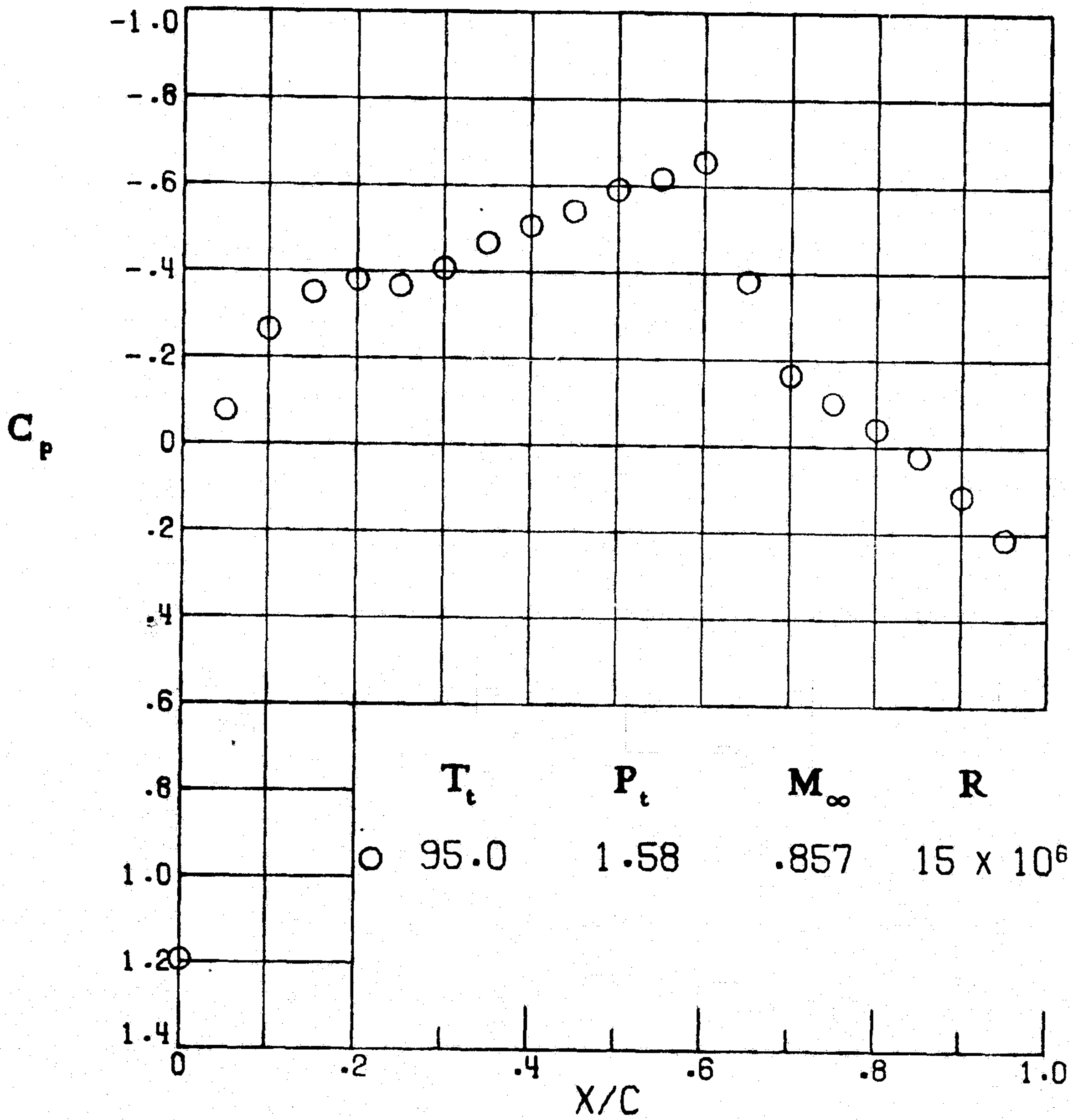

Figure A6.- Path 1, local saturation.

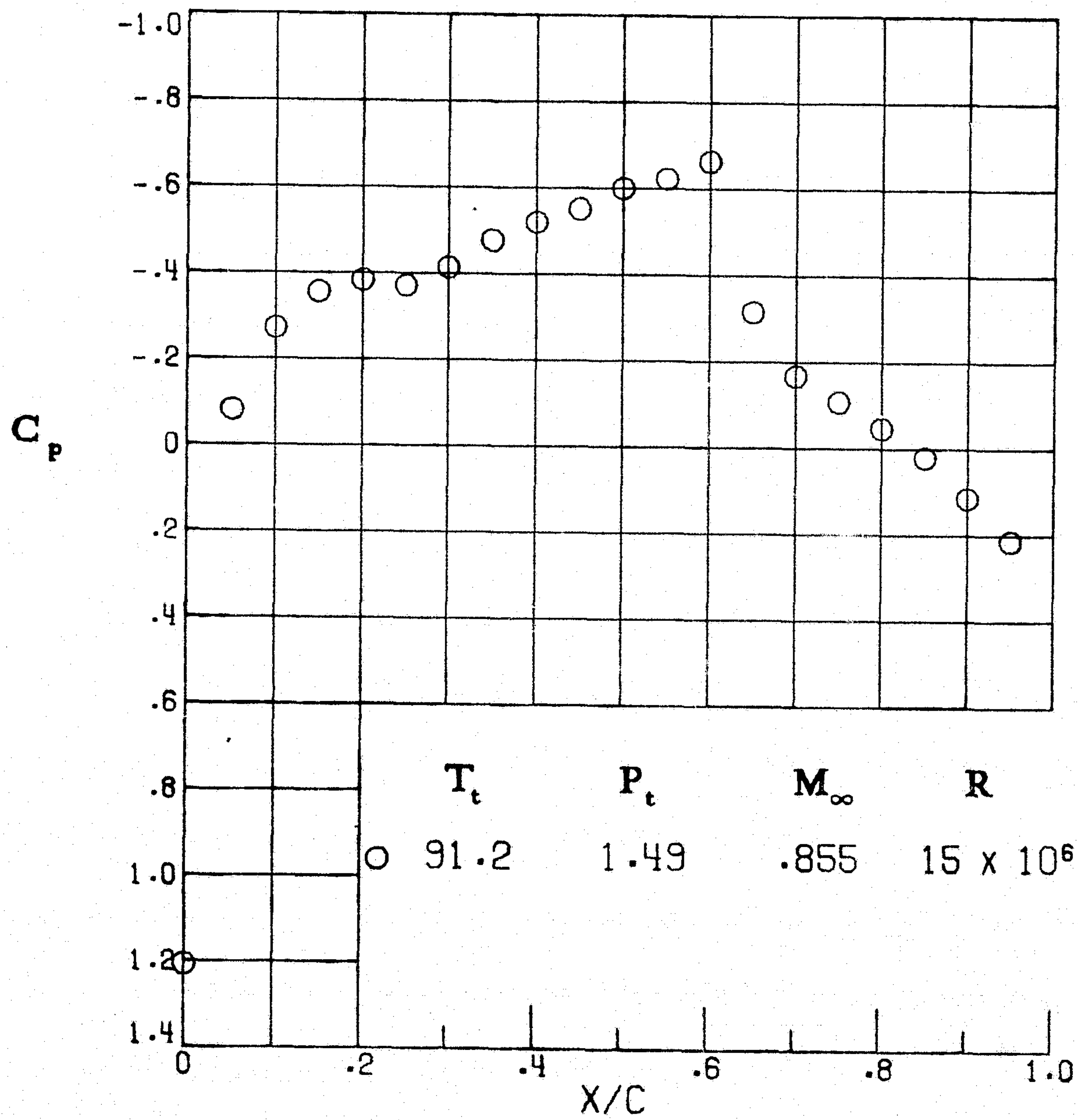

Figure A7.- Path 1, below local saturation.

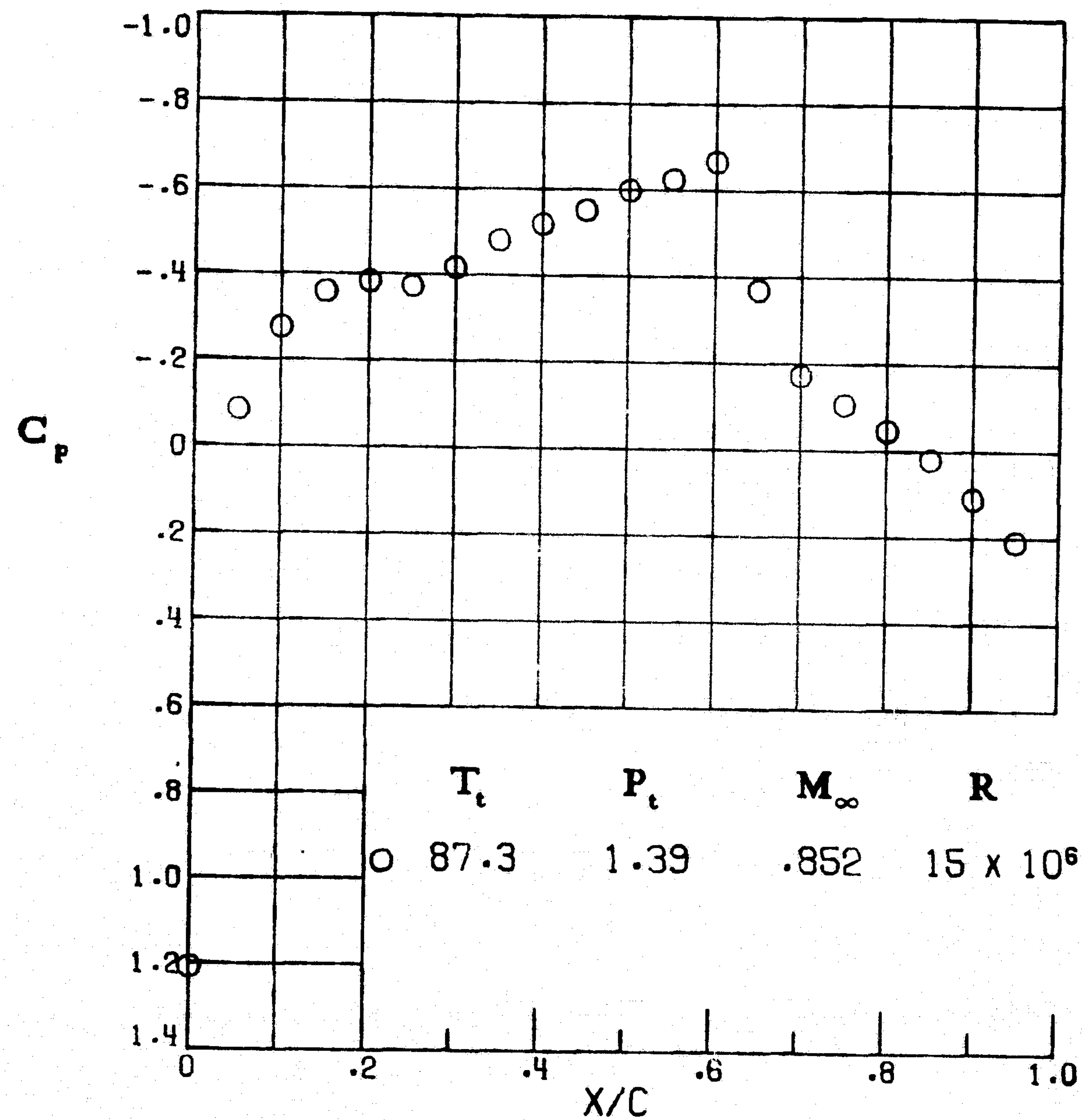

Figure A8.- Path 1, below local saturation.

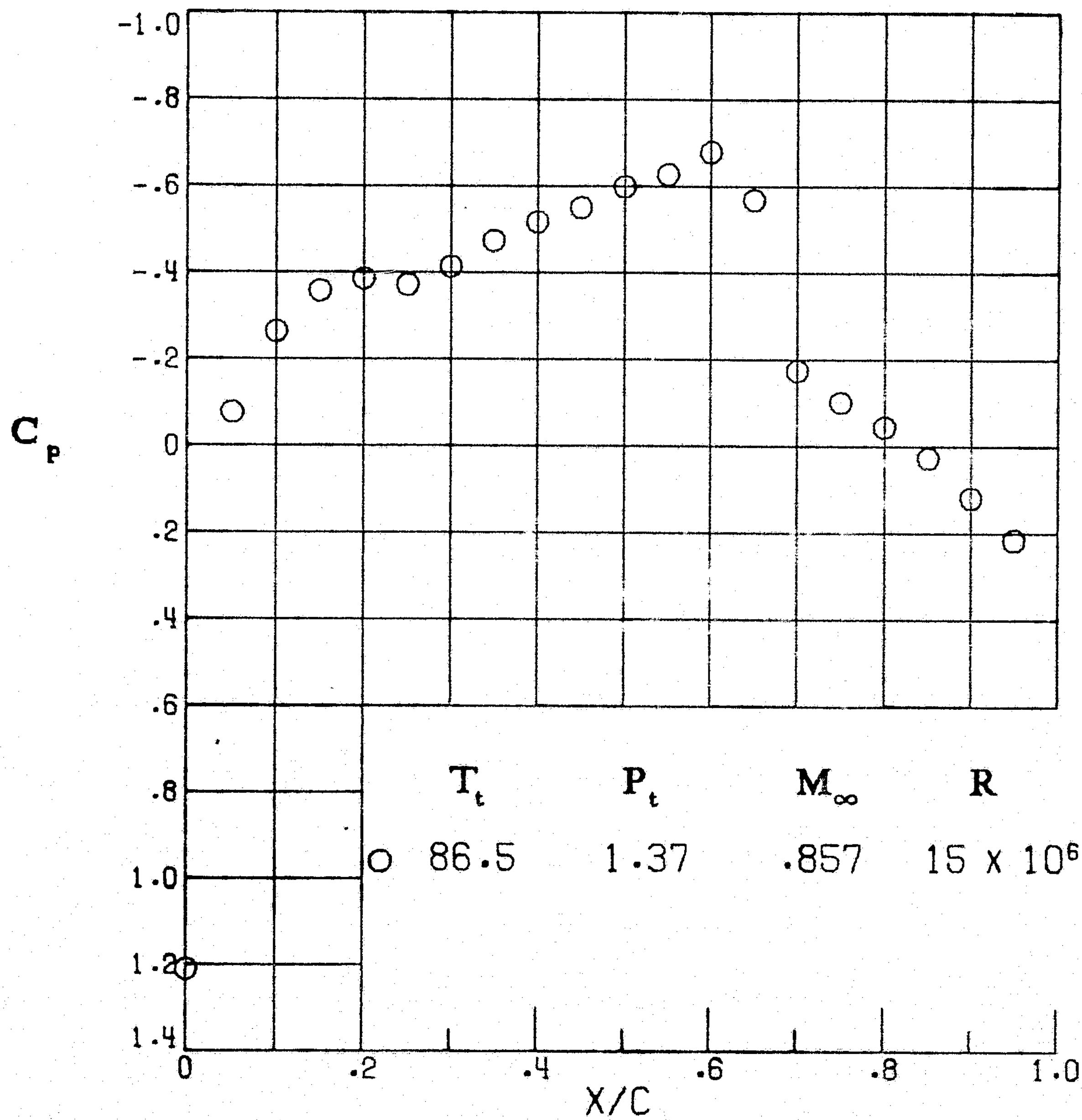

Figure A9.- Path 1, below free-stream saturation.

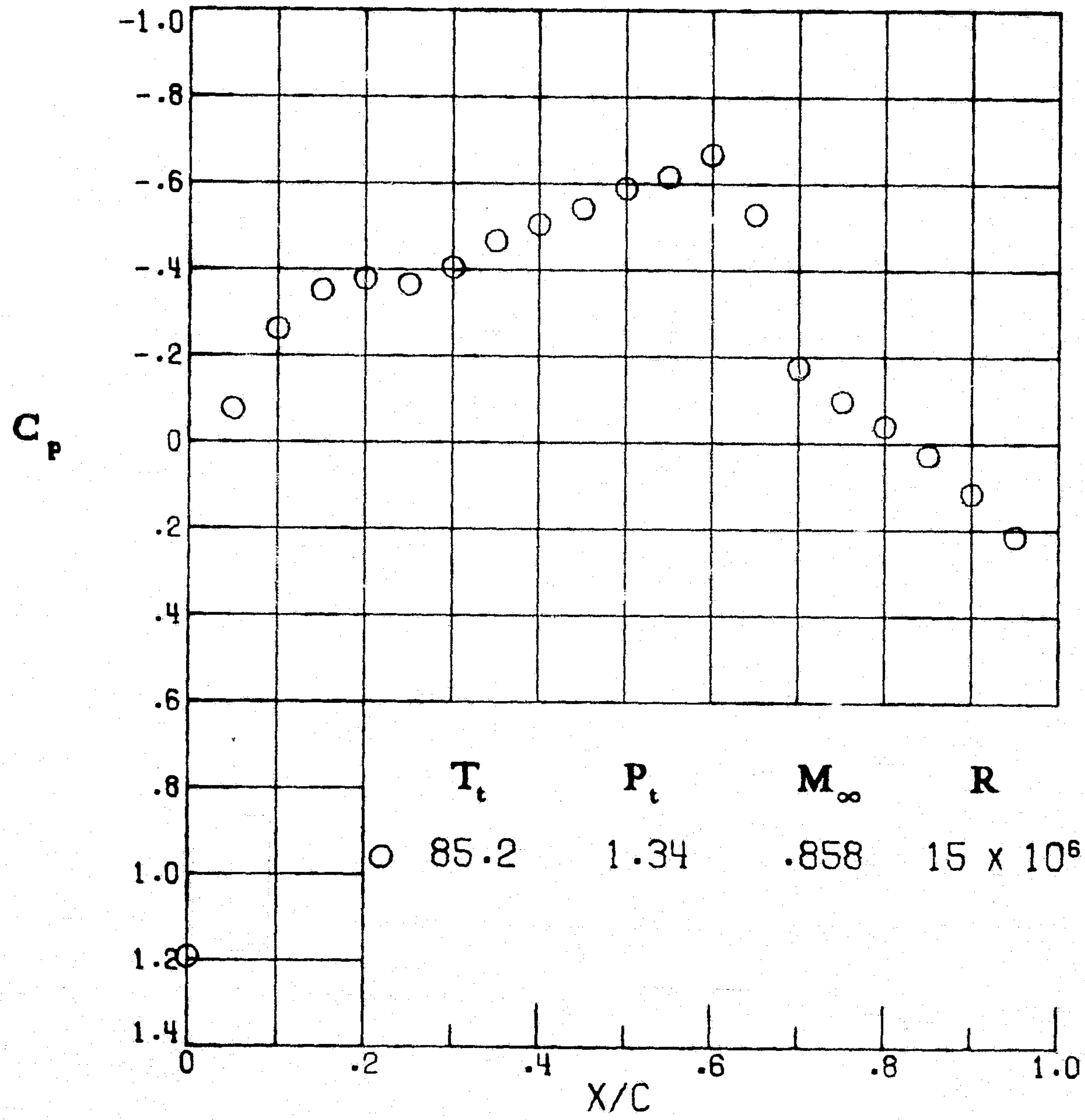

Figure A10.- Path 1, below free-stream saturation.

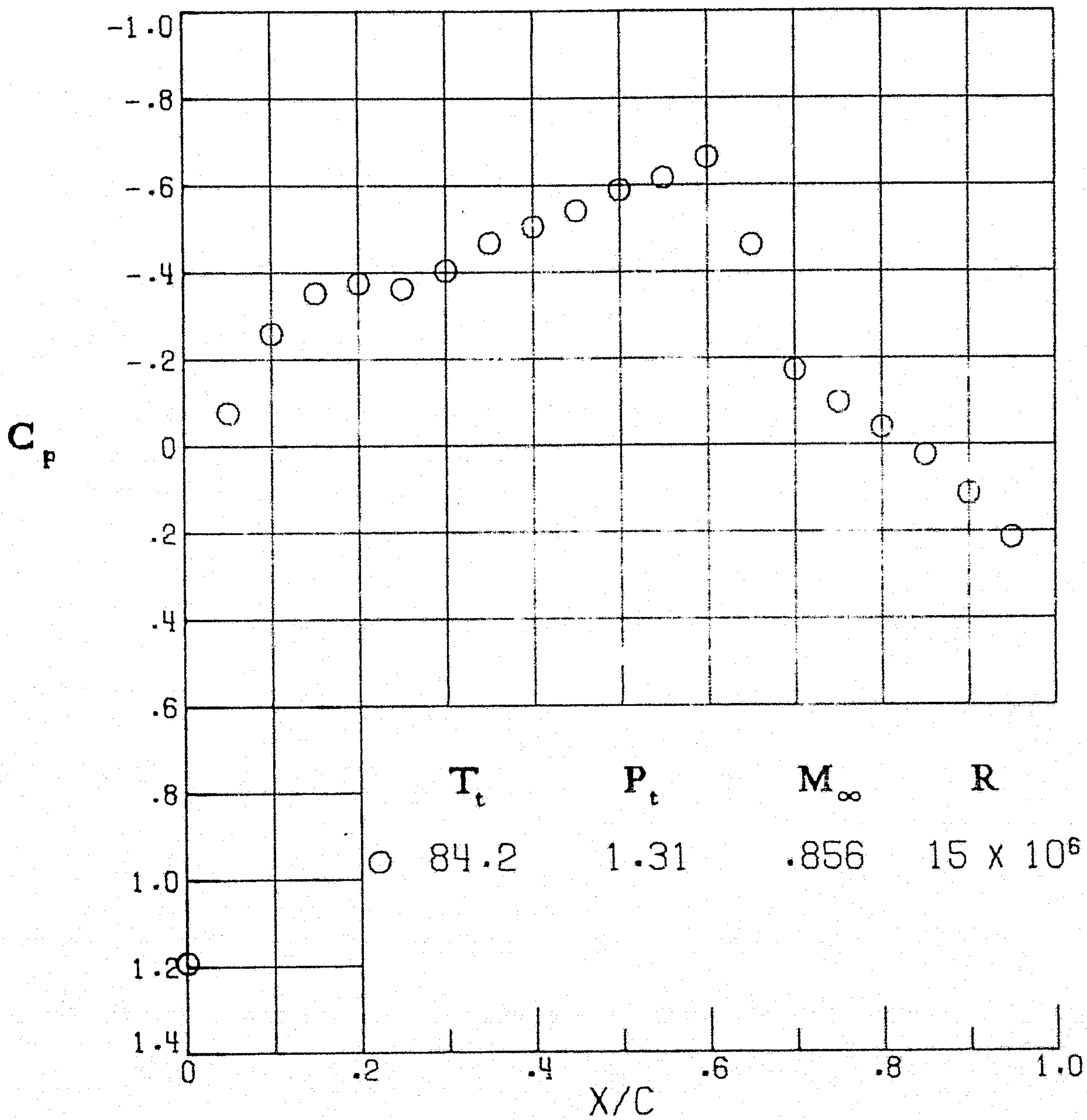

Figure A11.- Path 1, below free-stream saturation.

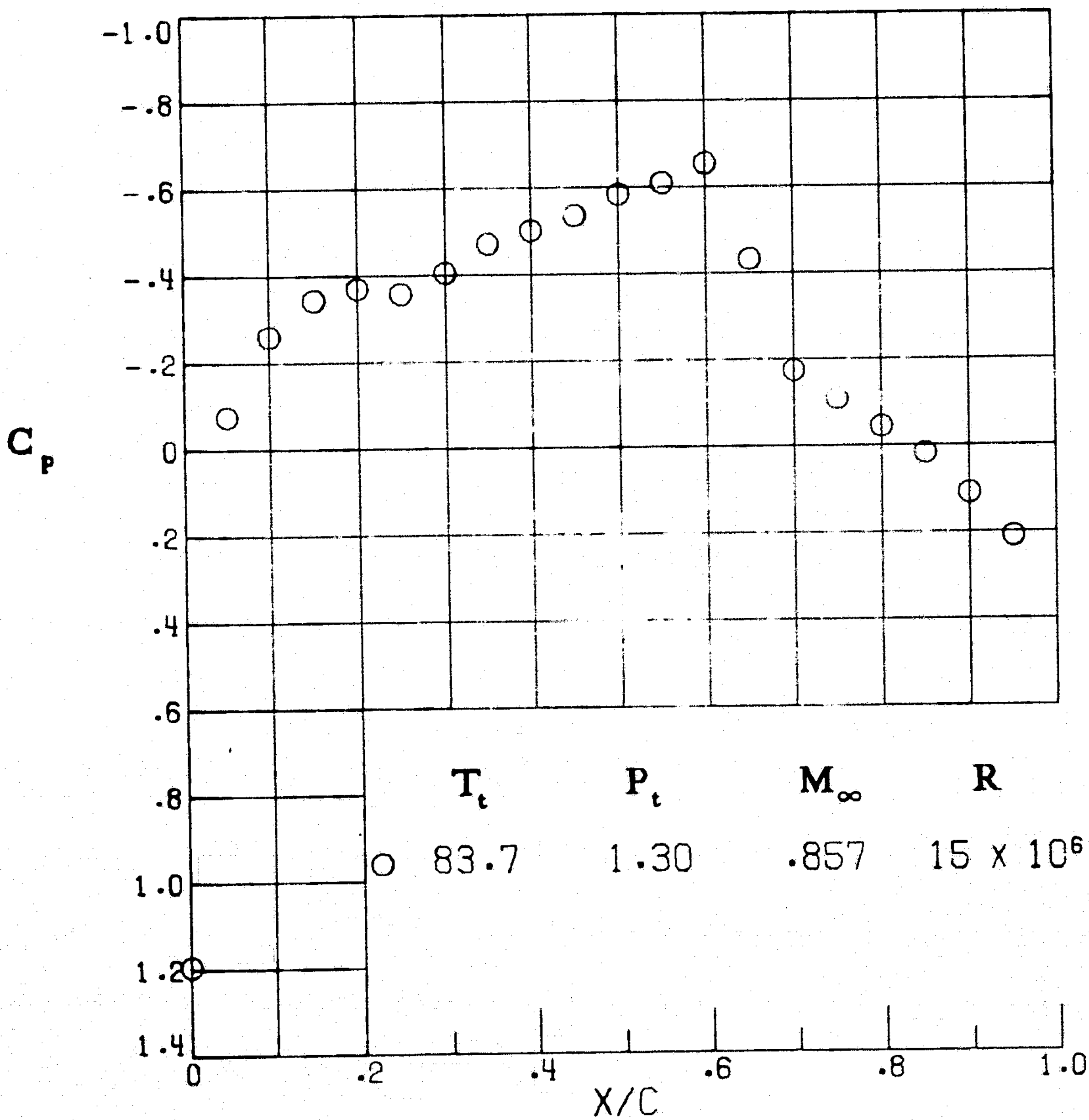

Figure A12.- Path 1, below free-stream saturation.

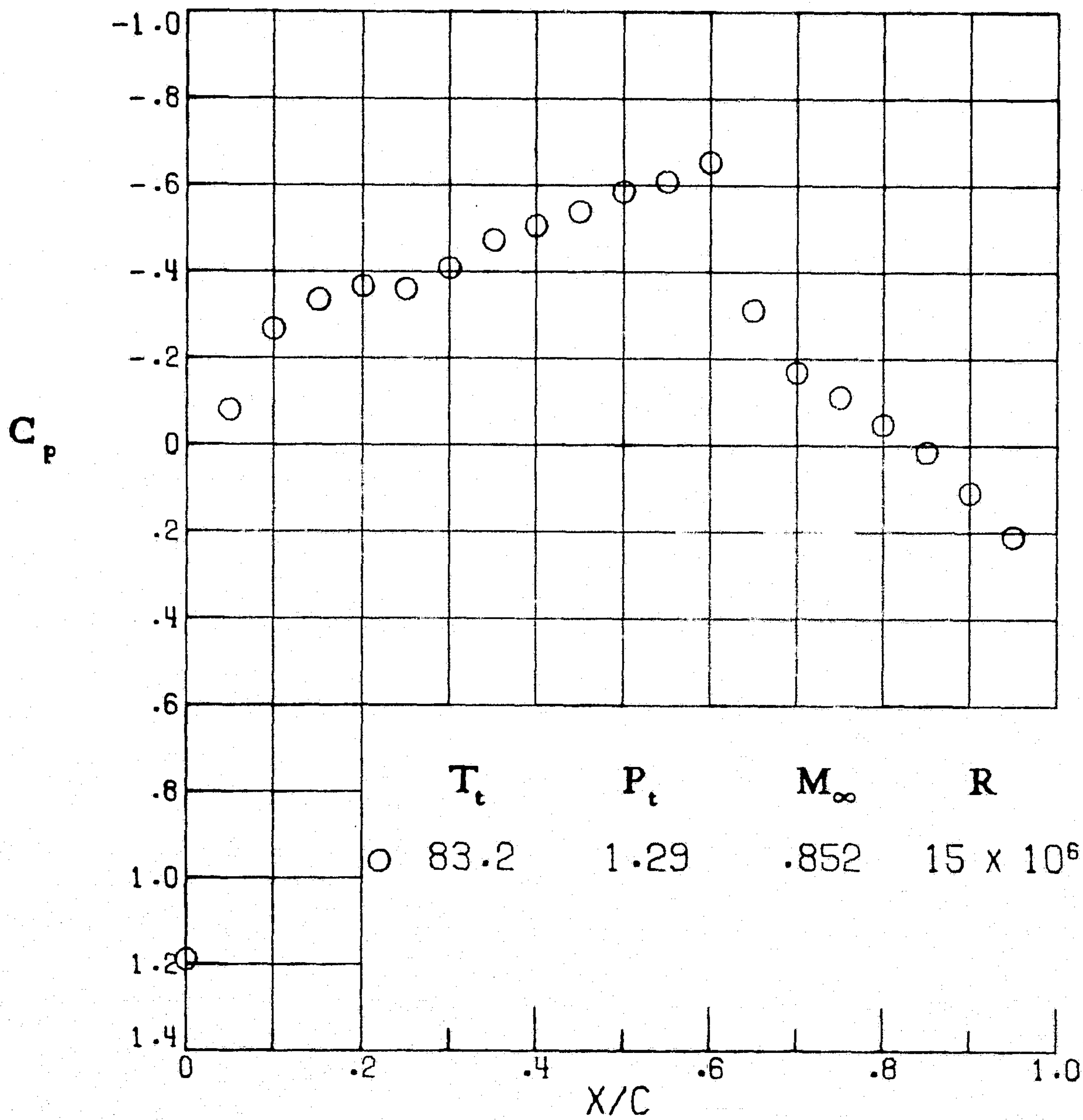

Figure A13.- Path 1, below free-stream saturation.

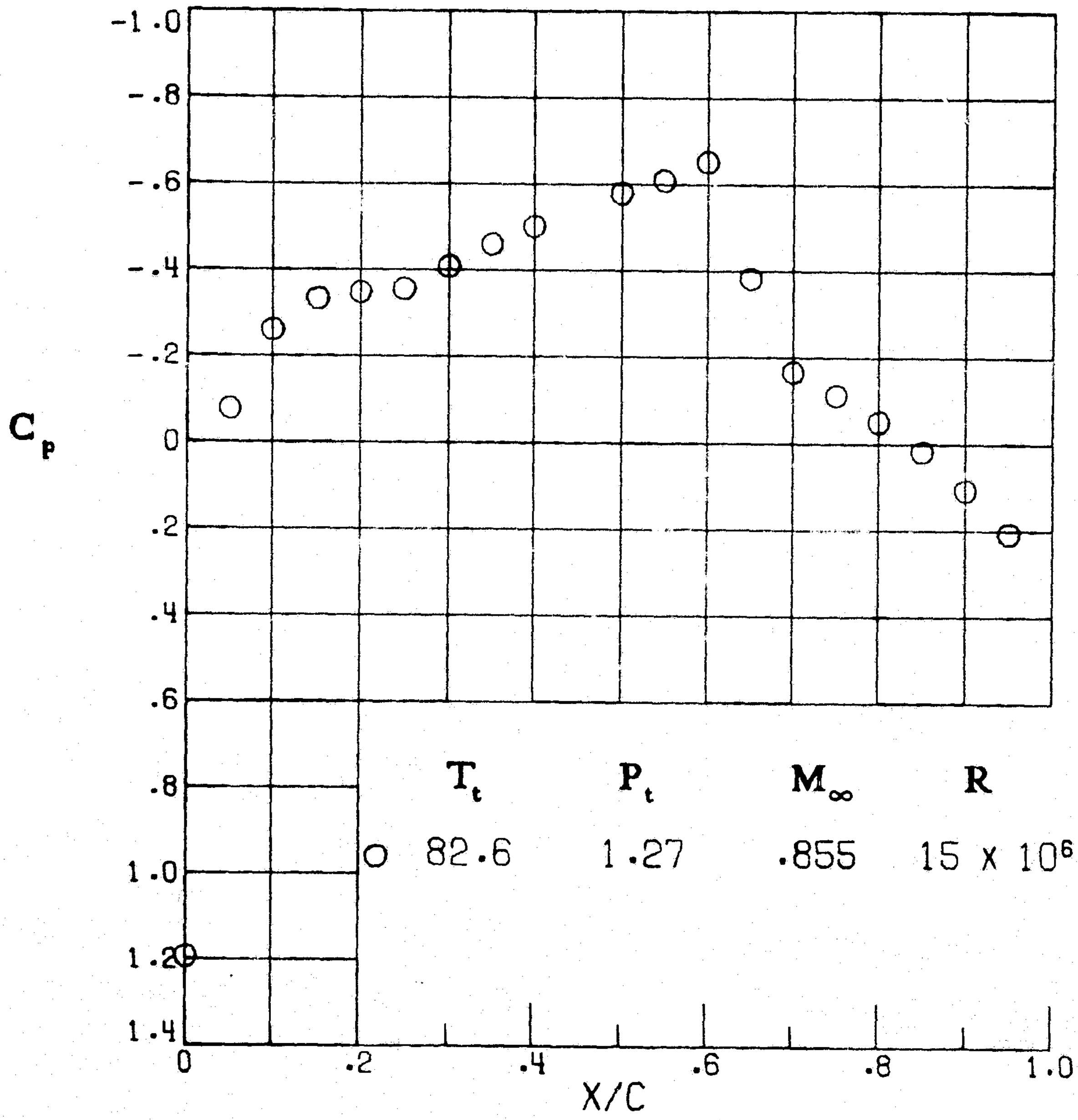

Figure A14.- Path 1, below free-stream saturation.

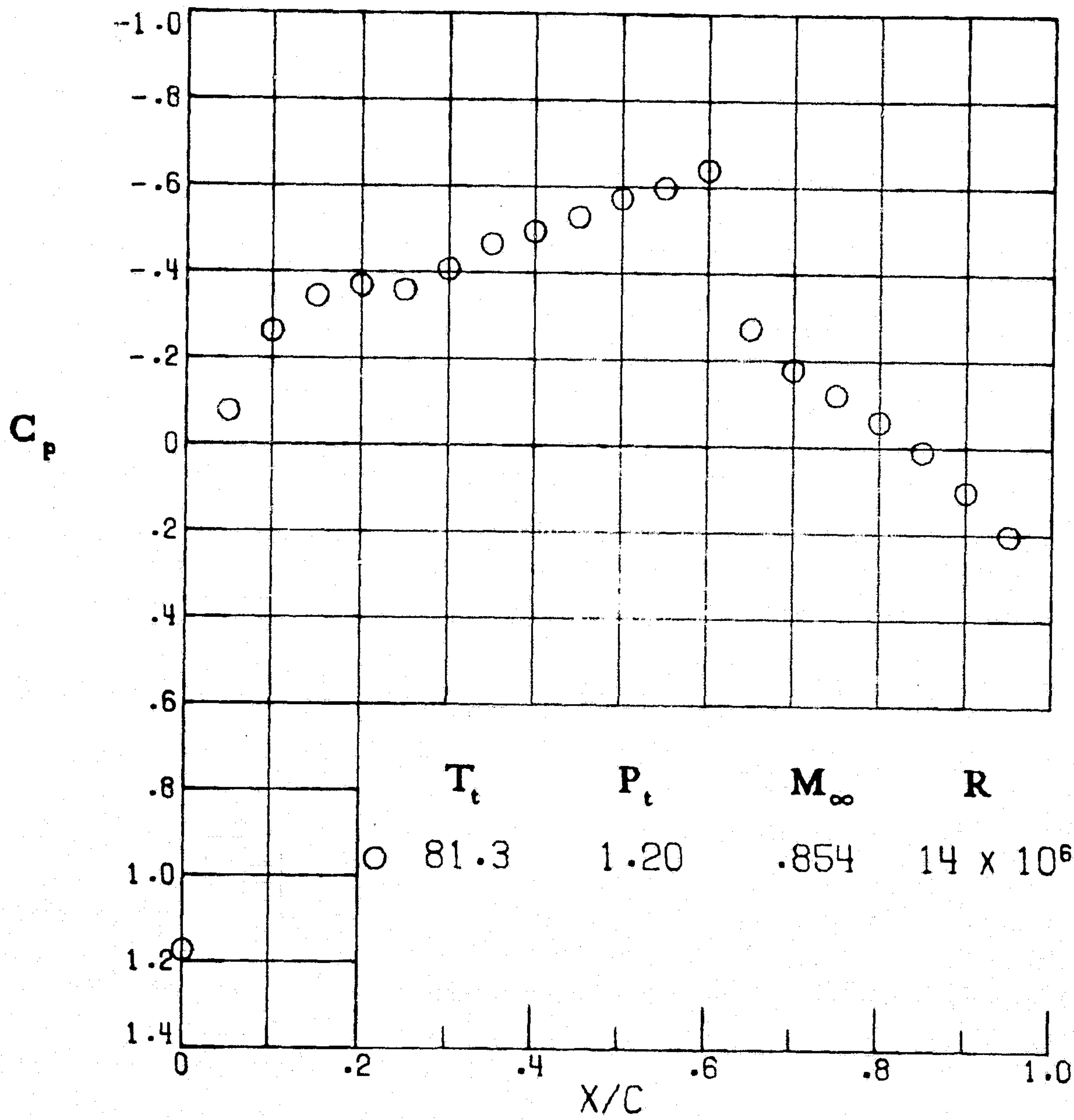

Figure A15.- Path 1, below free-stream saturation.

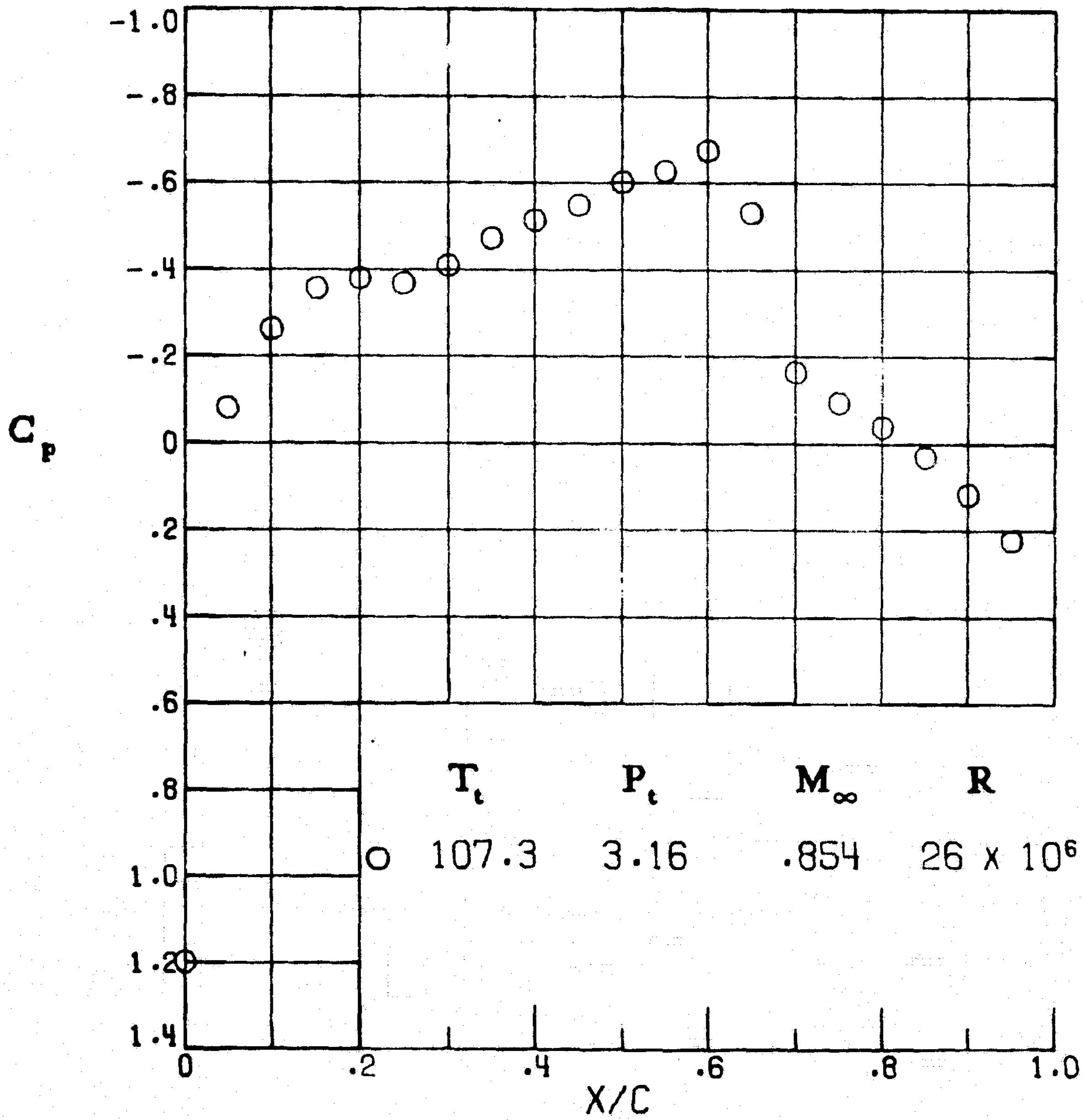

Figure A16.- Path 2, reference, above local saturation.

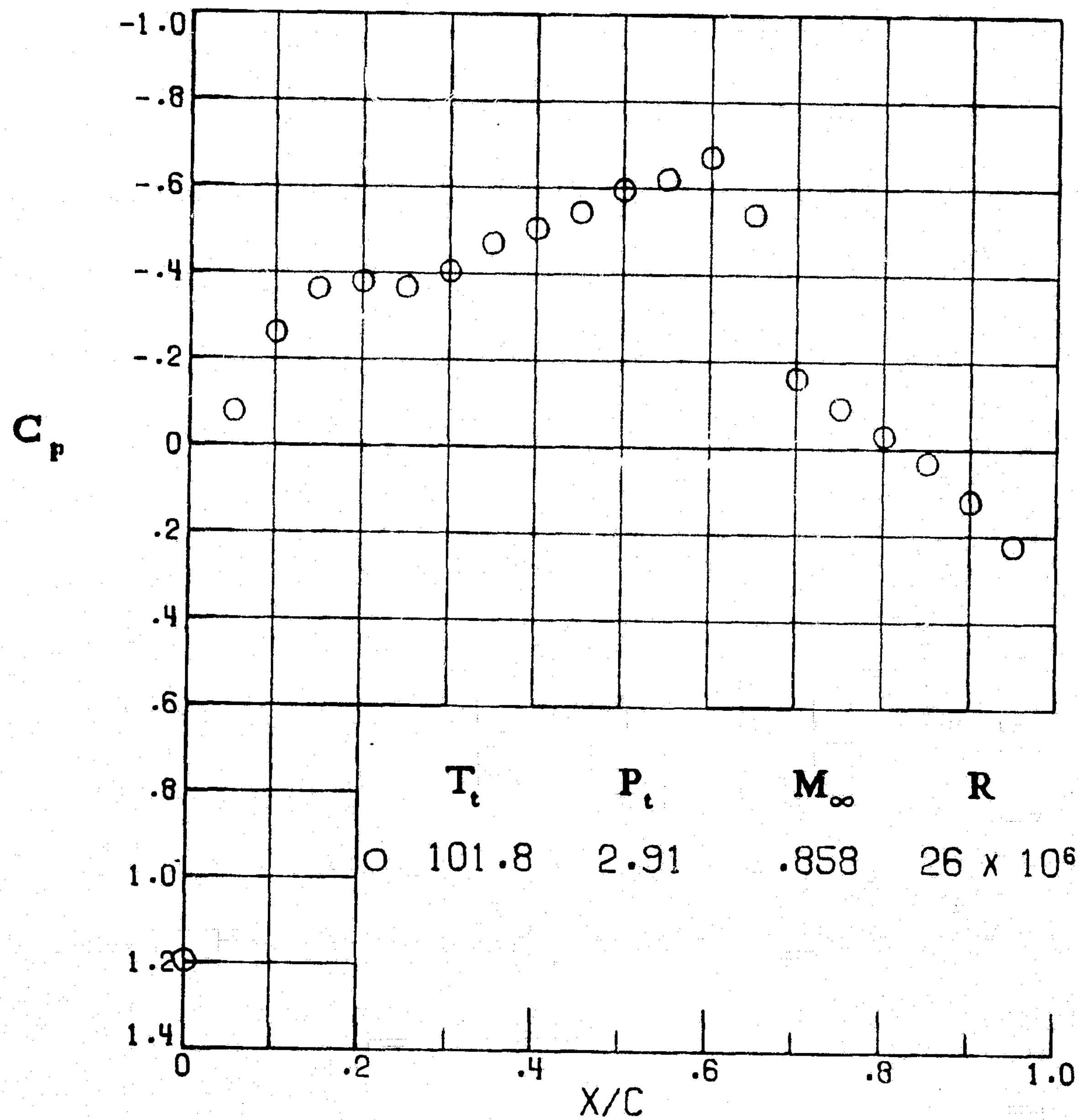

Figure A17.- Path 2, above local saturation.

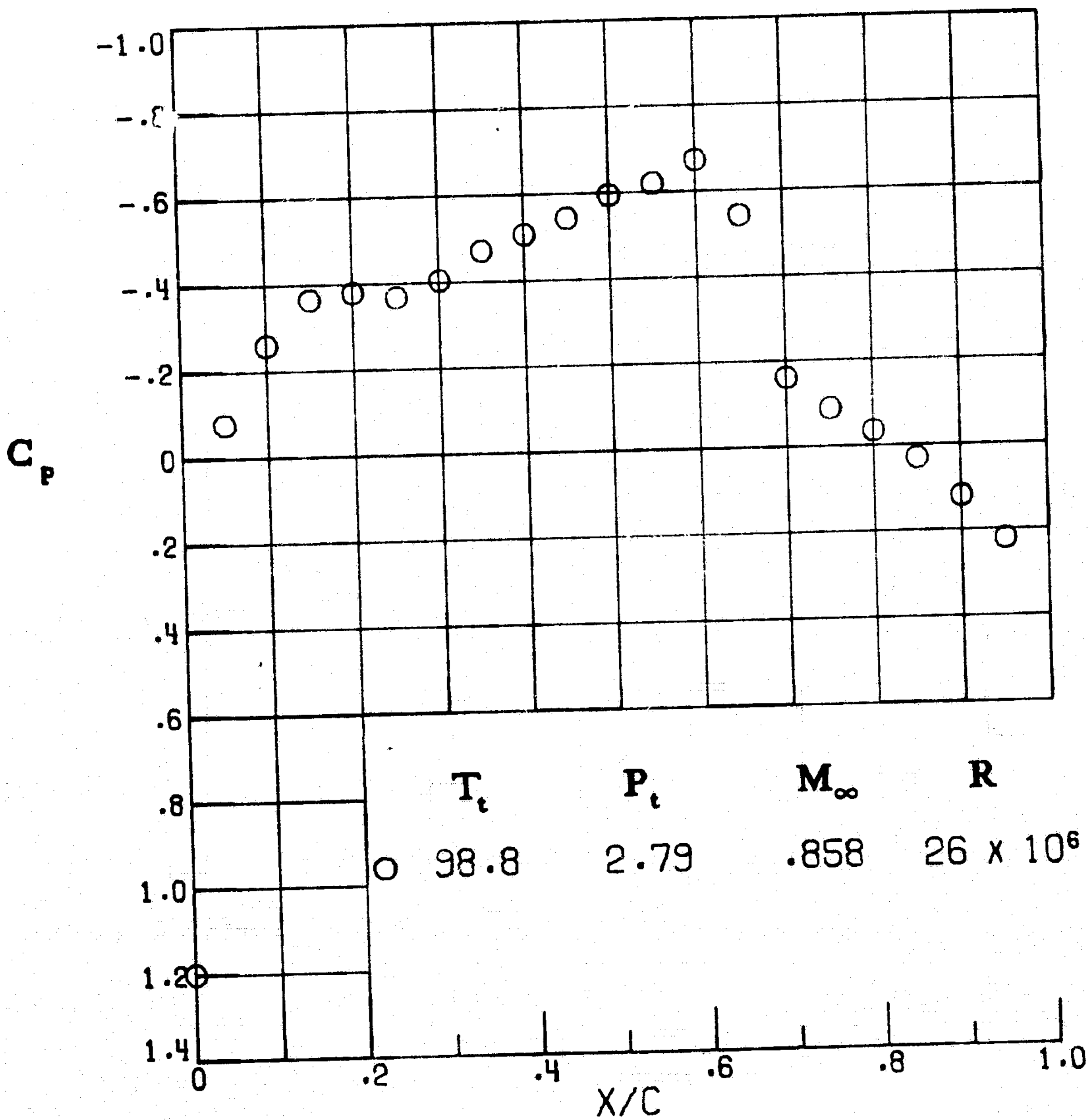

Figure A18.- Path 2, below local saturation.

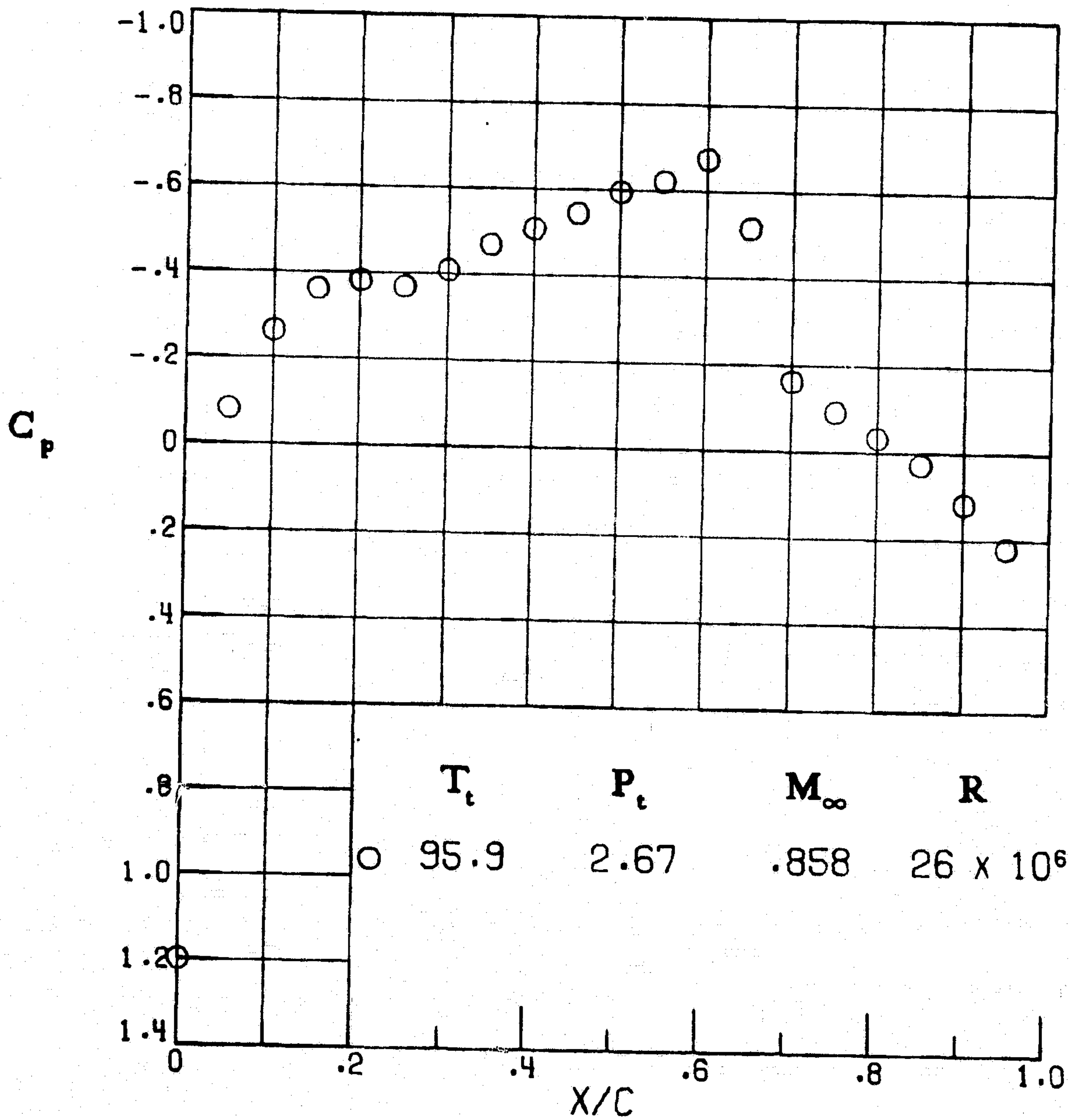

Figure A19.- Path 2, below local saturation.

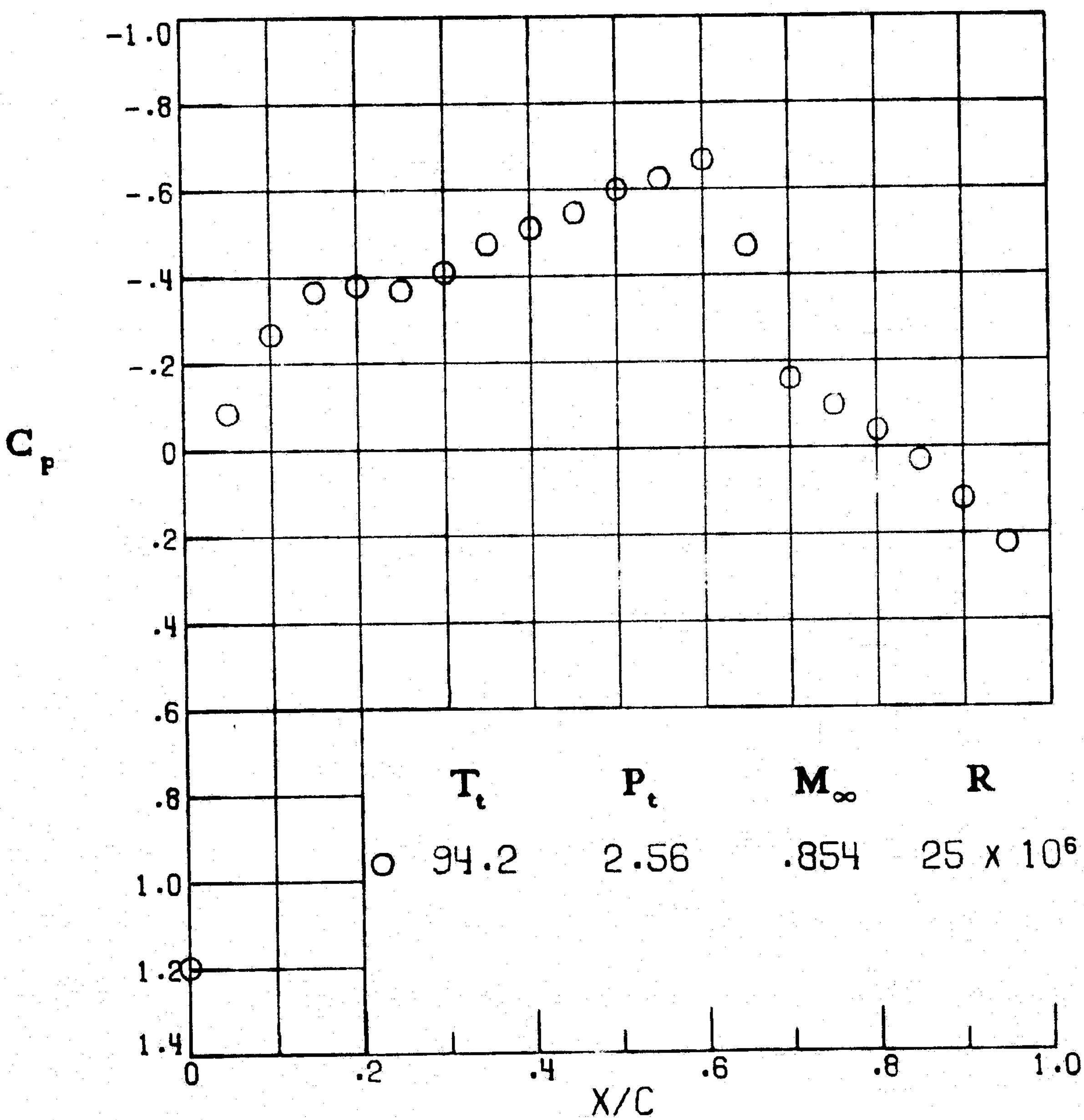

Figure A20.- Path 2, below local saturation.

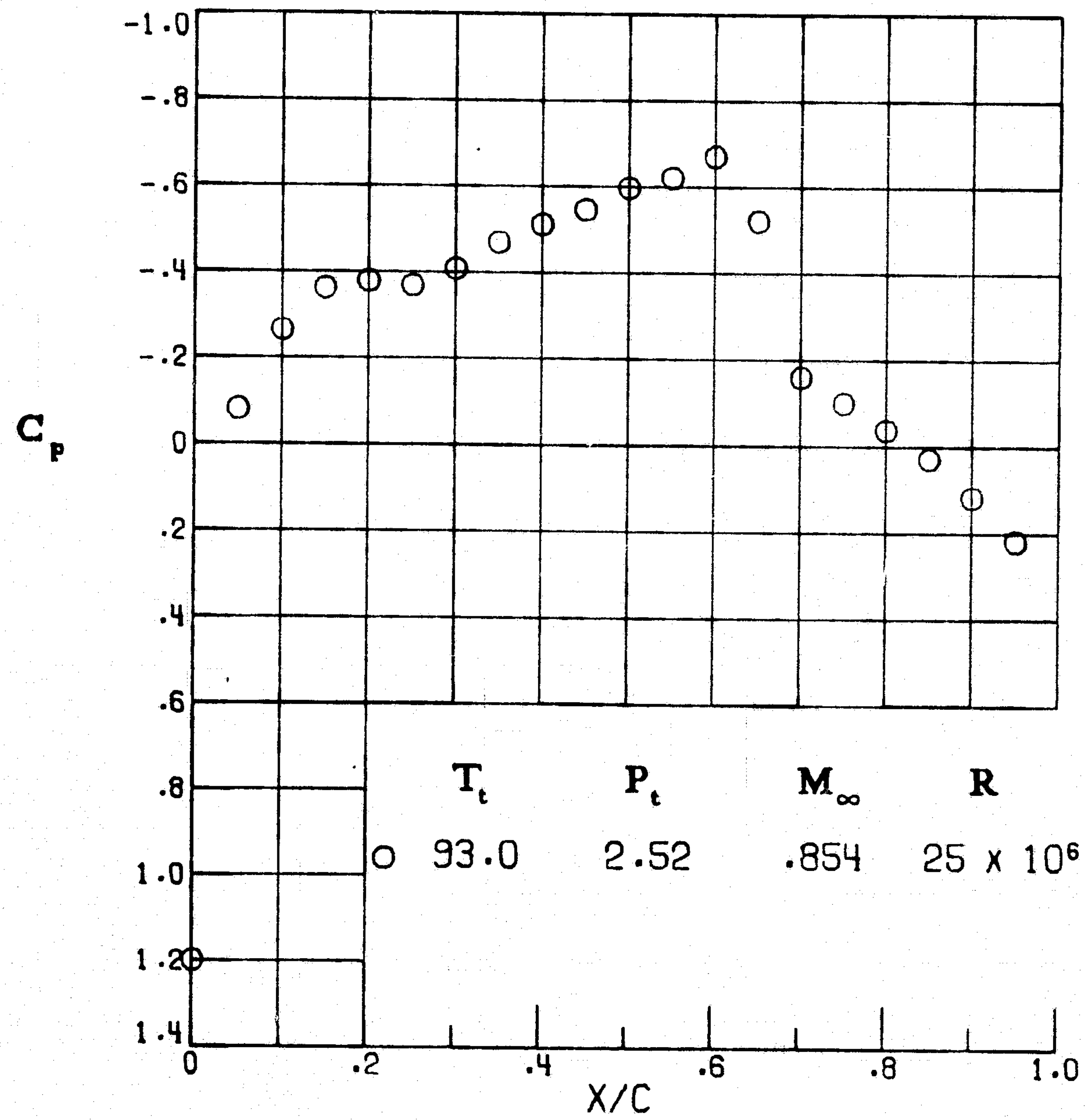

Figure A21.- Path 2, free-stream saturation.

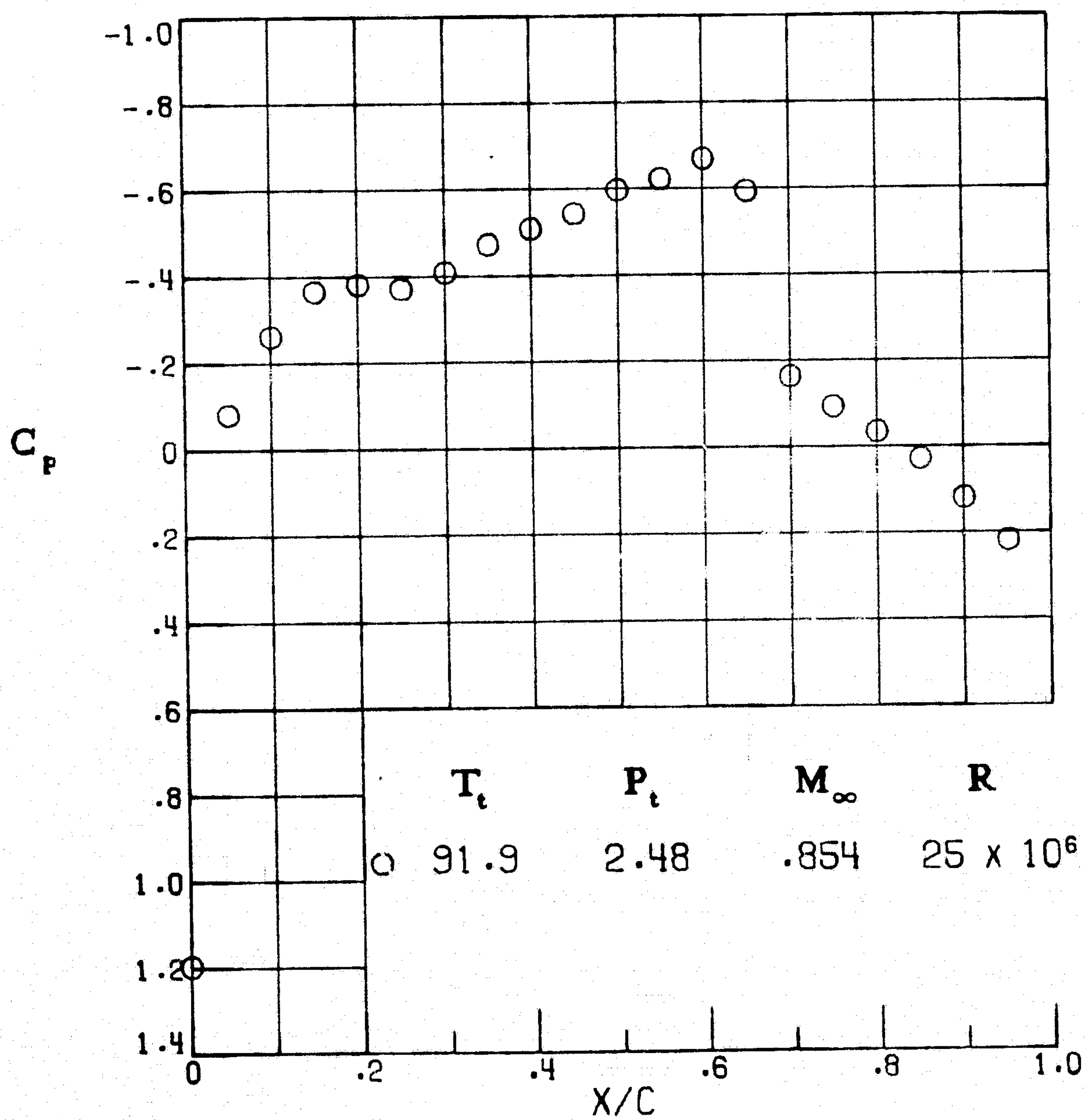

Figure A22.- Path 2, below free-stream saturation.

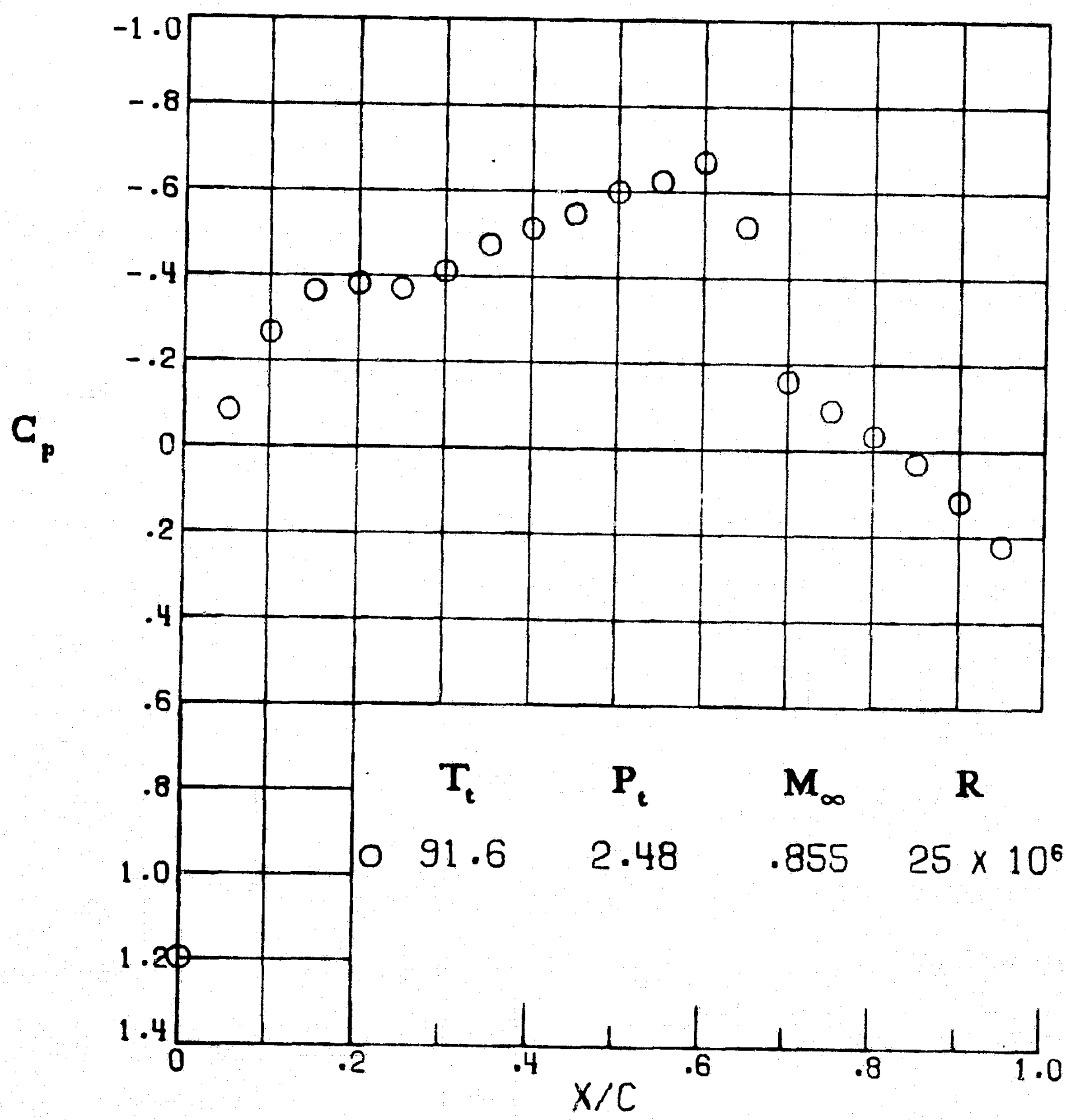

Figure A23.- Path 2, below free-stream saturation.

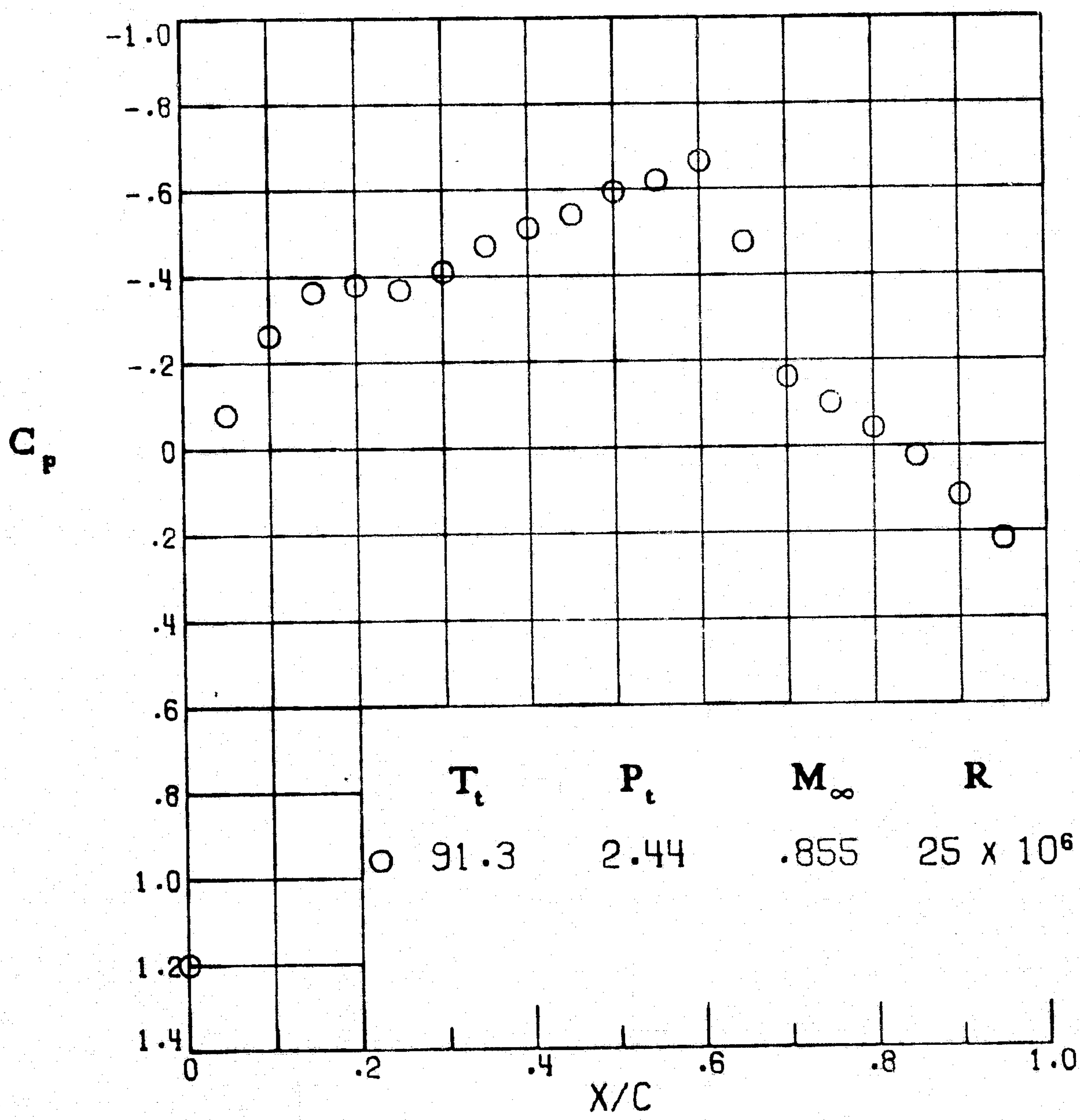

Figure A24.- Path 2, below free-stream saturation.

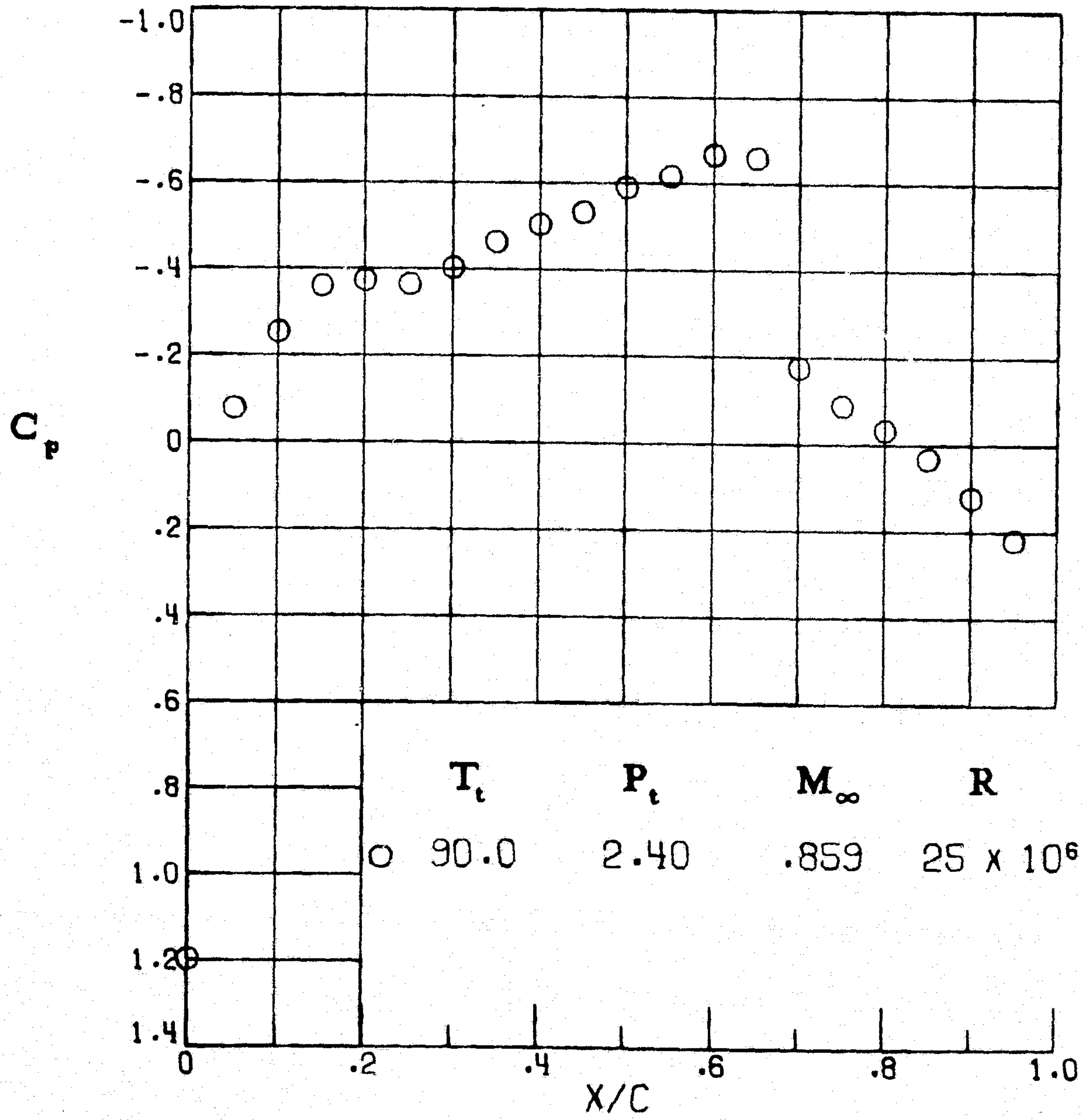

Figure A25.- Path 2, below free-stream saturation.

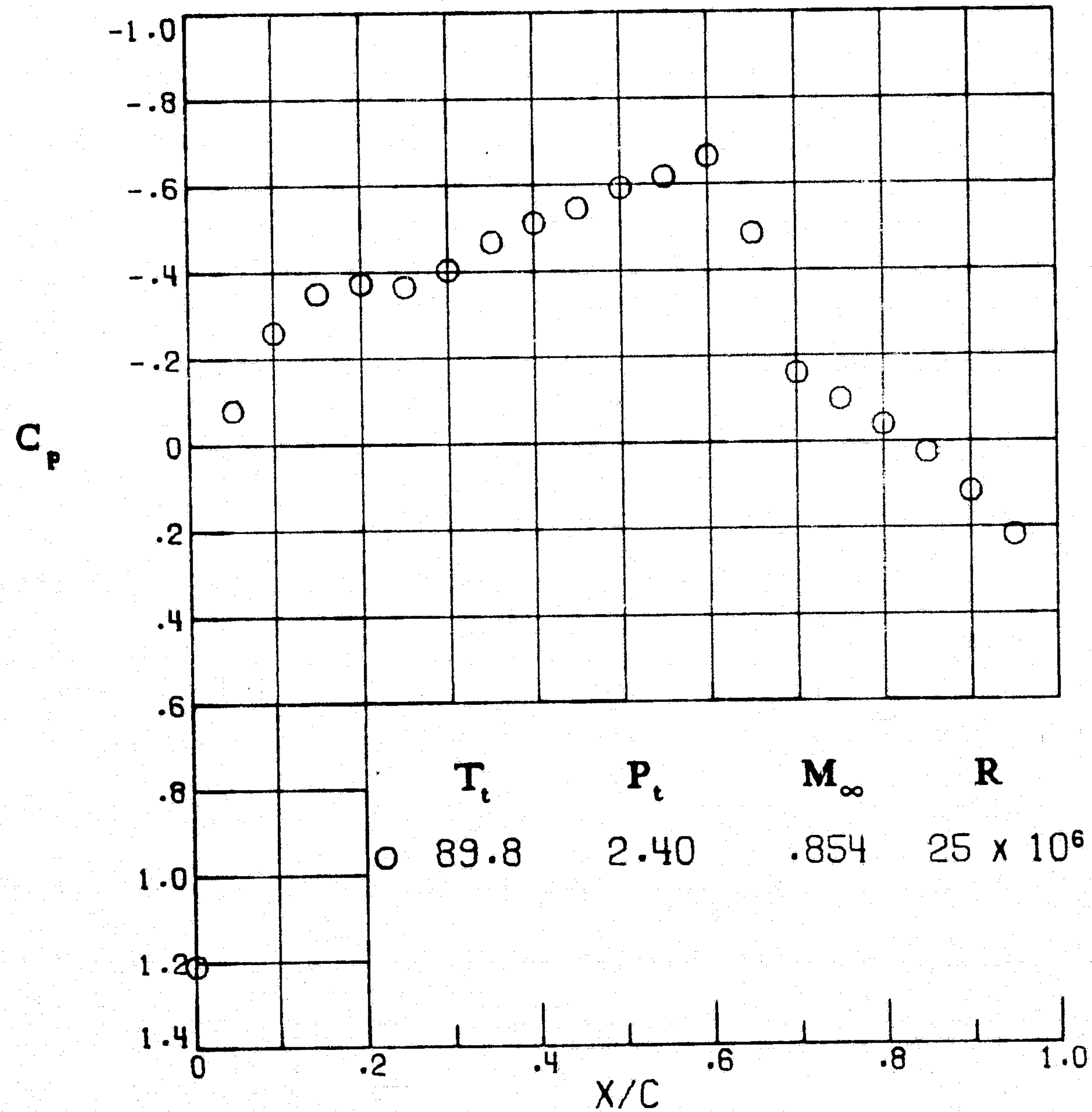

Figure A26.- Path 2, below free-stream saturation.

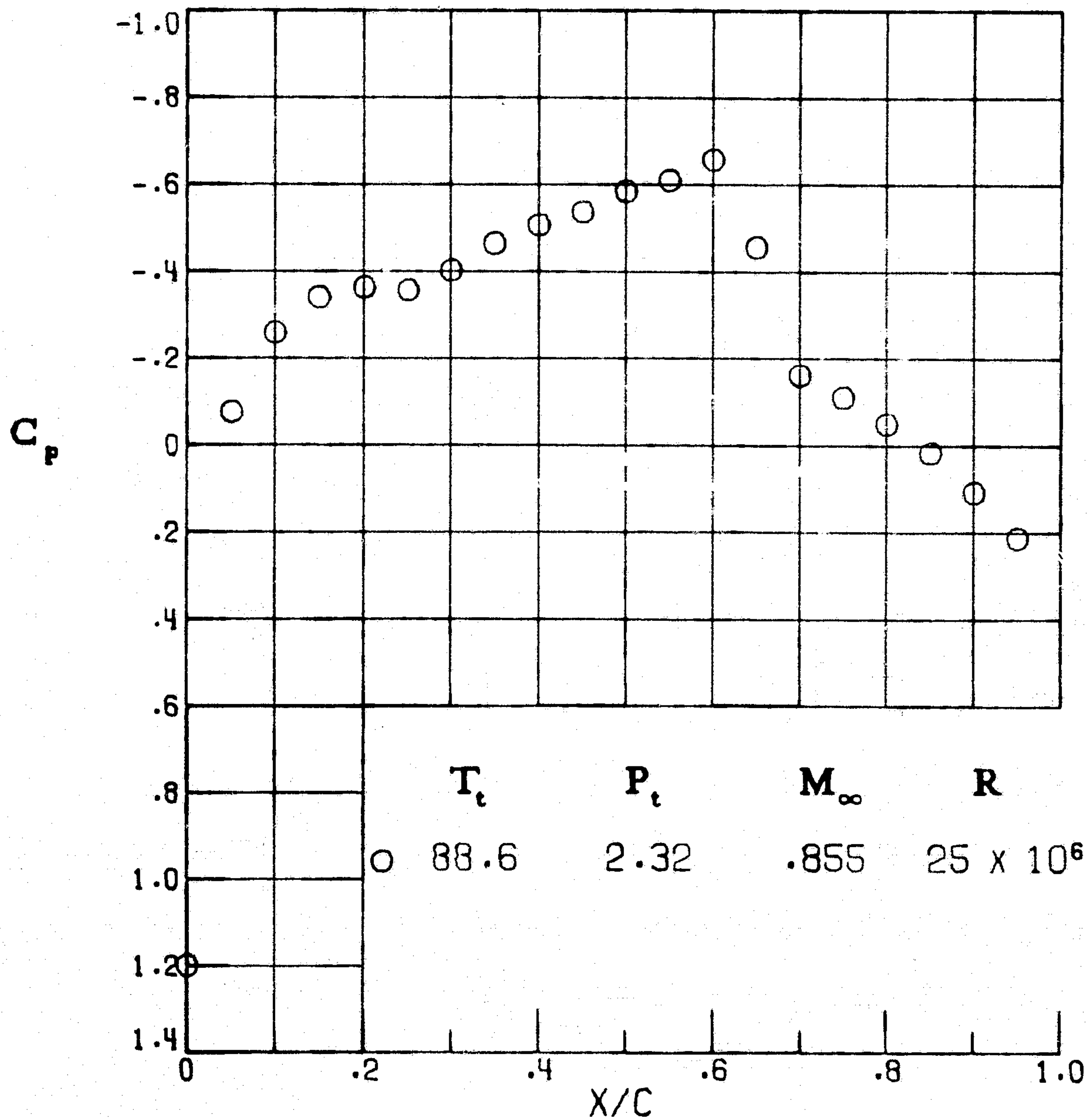

Figure A27.- Path 2, below free-stream saturation.

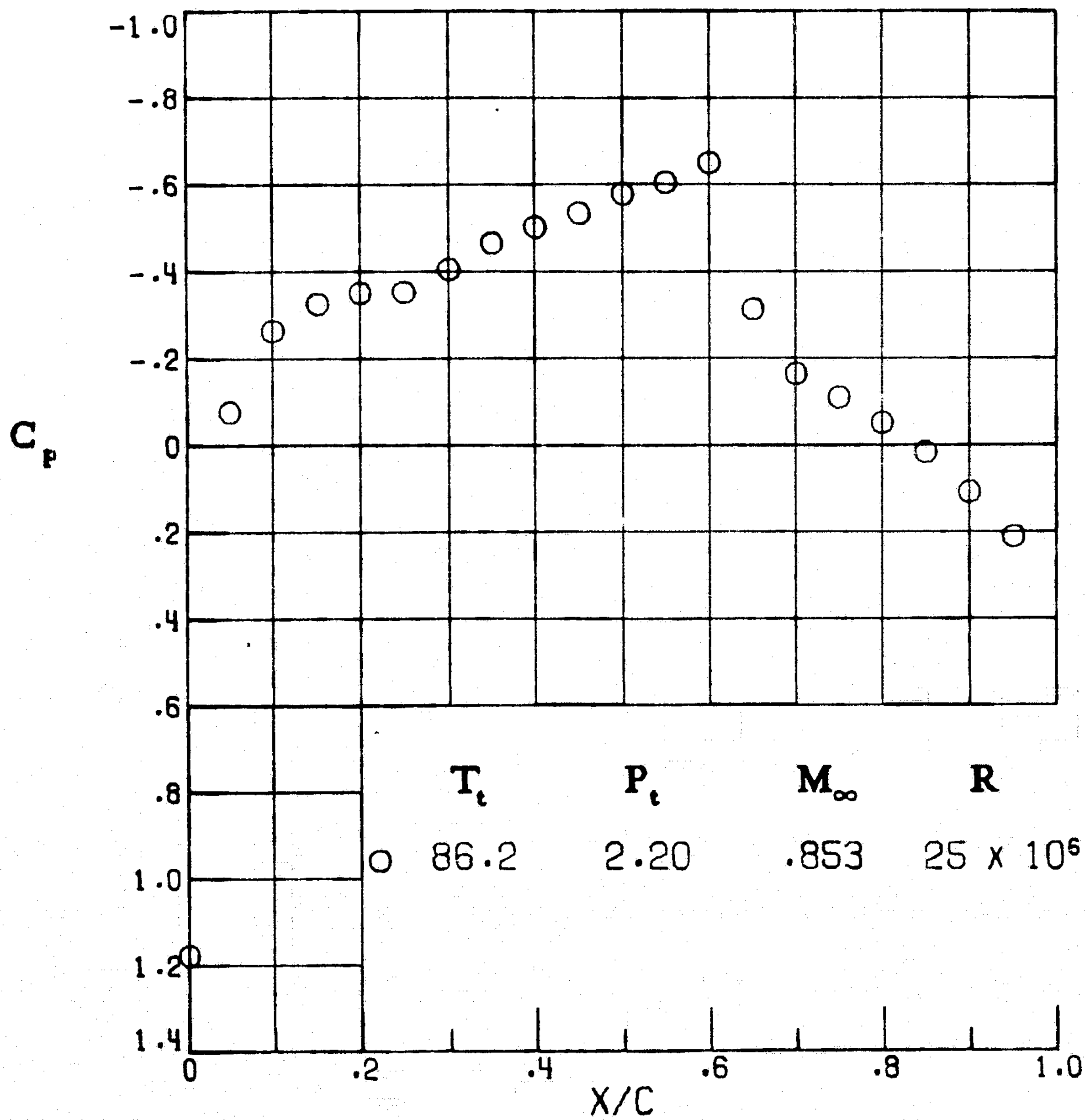

Figure A28.- Path 2, below free-stream saturation.

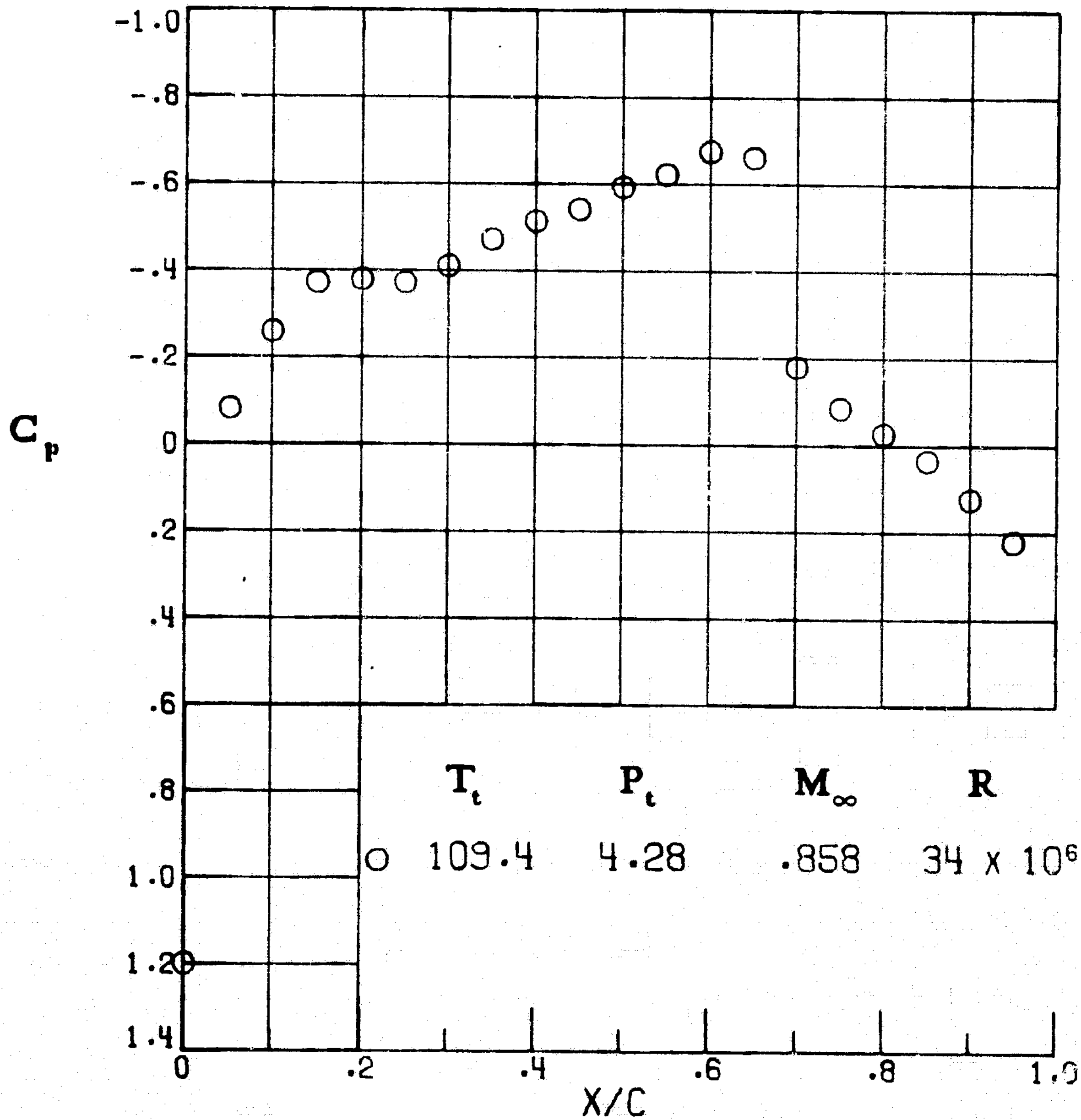

Figure A29.- Path 3, reference, above local saturation.

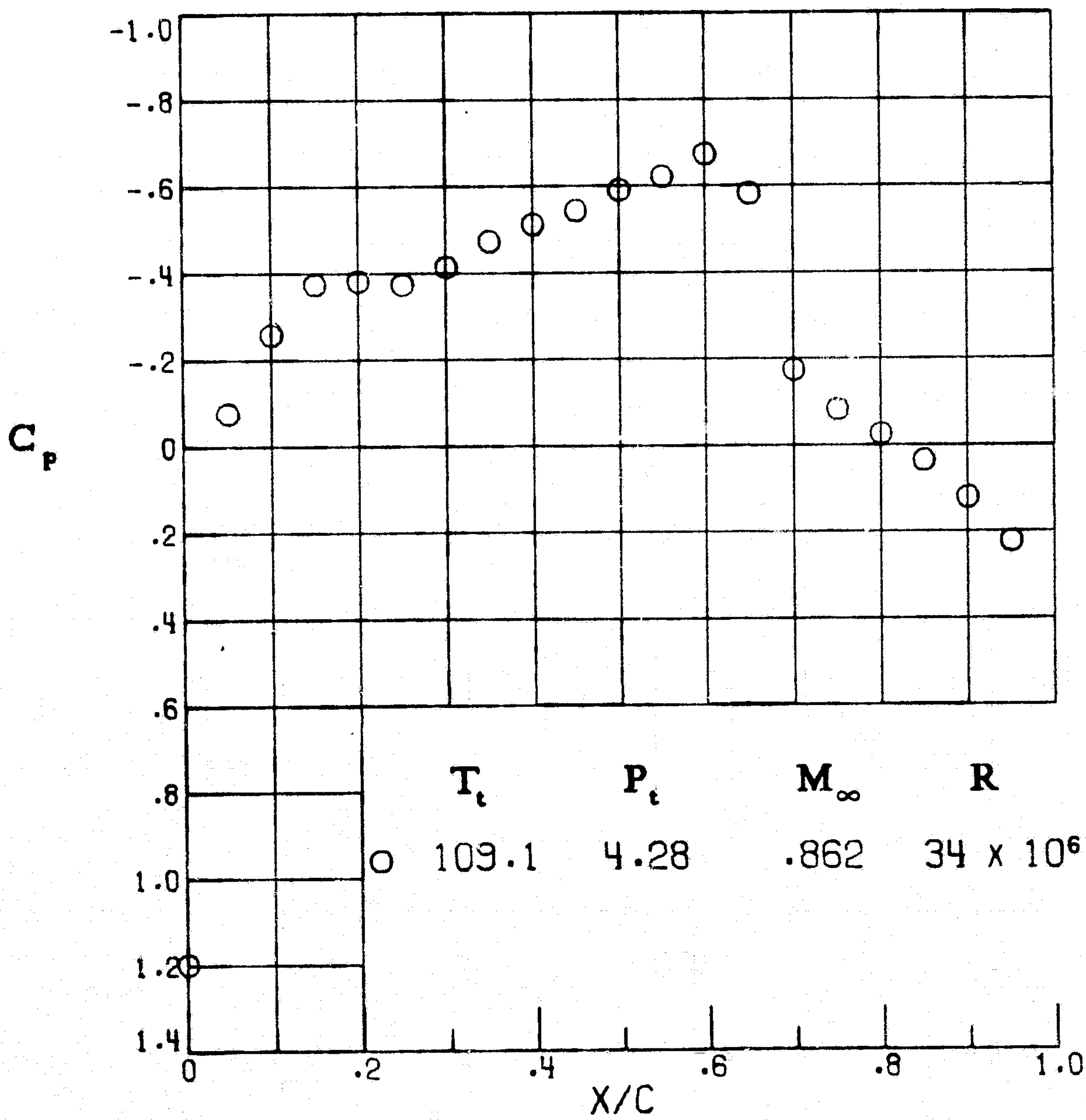

Figure A30.- Path 3, reference, above local saturation.

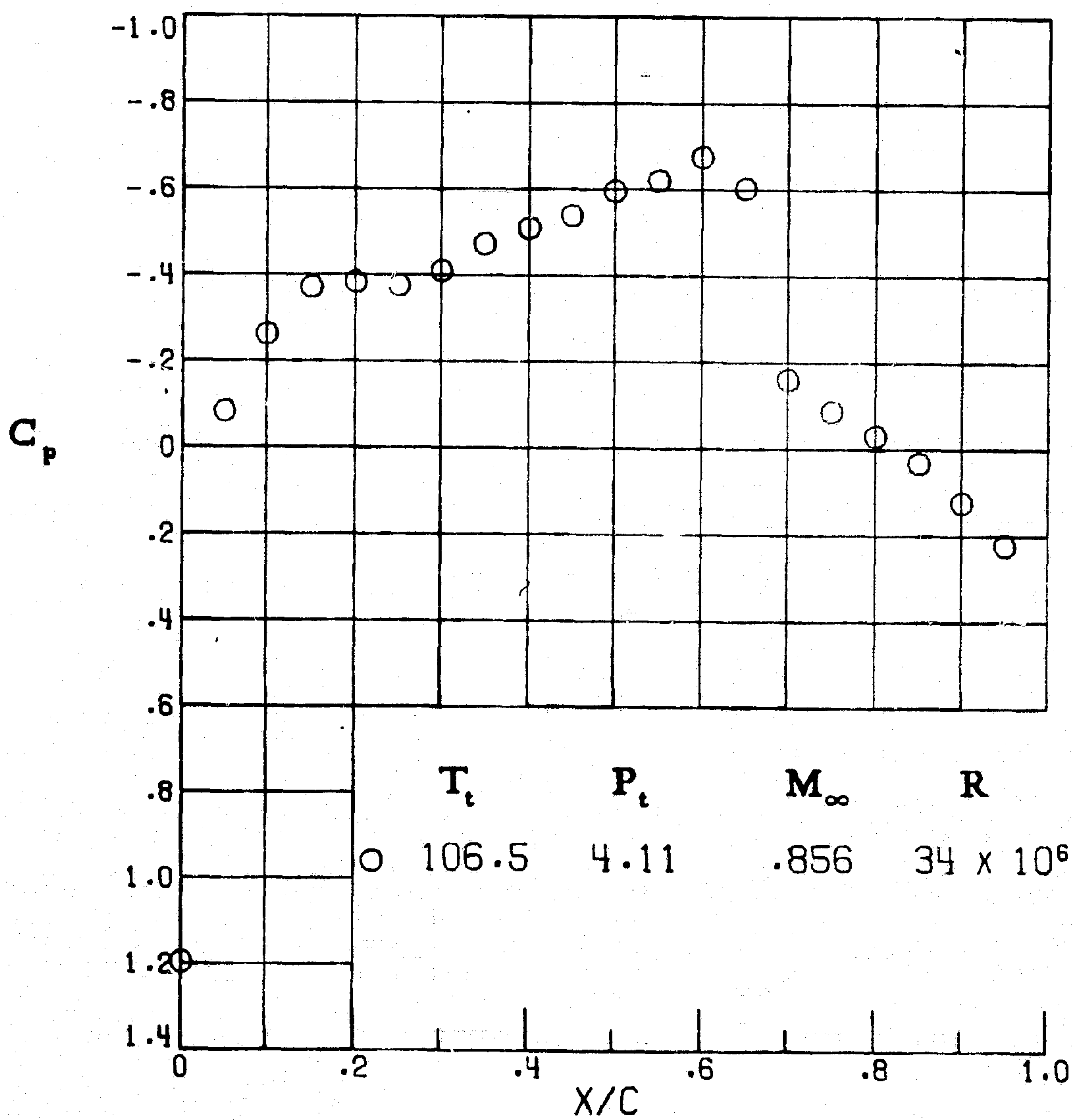

Figure A31.- Path 3, above local saturation.

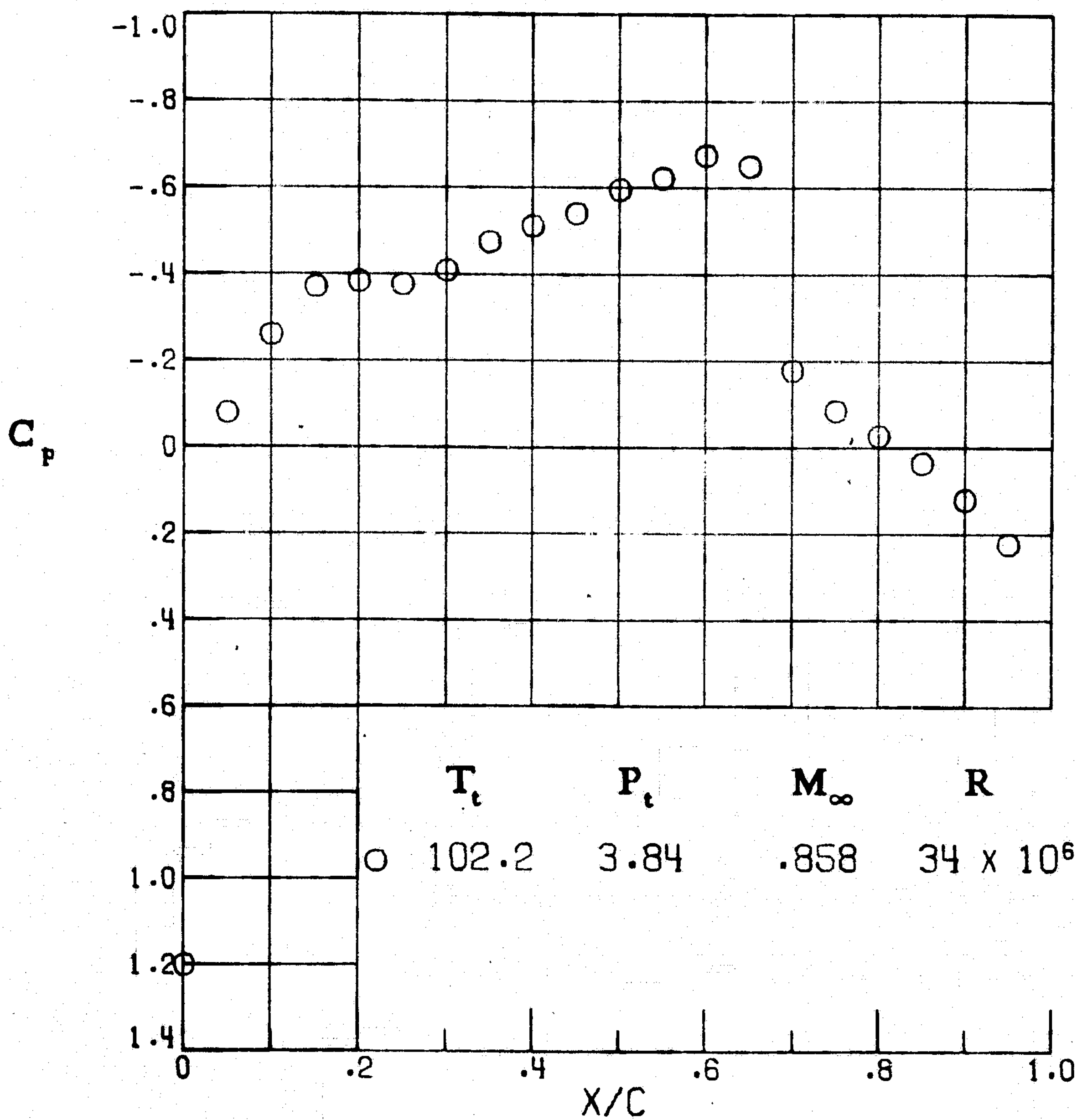

Figure A32. - Path 3, below local saturation.

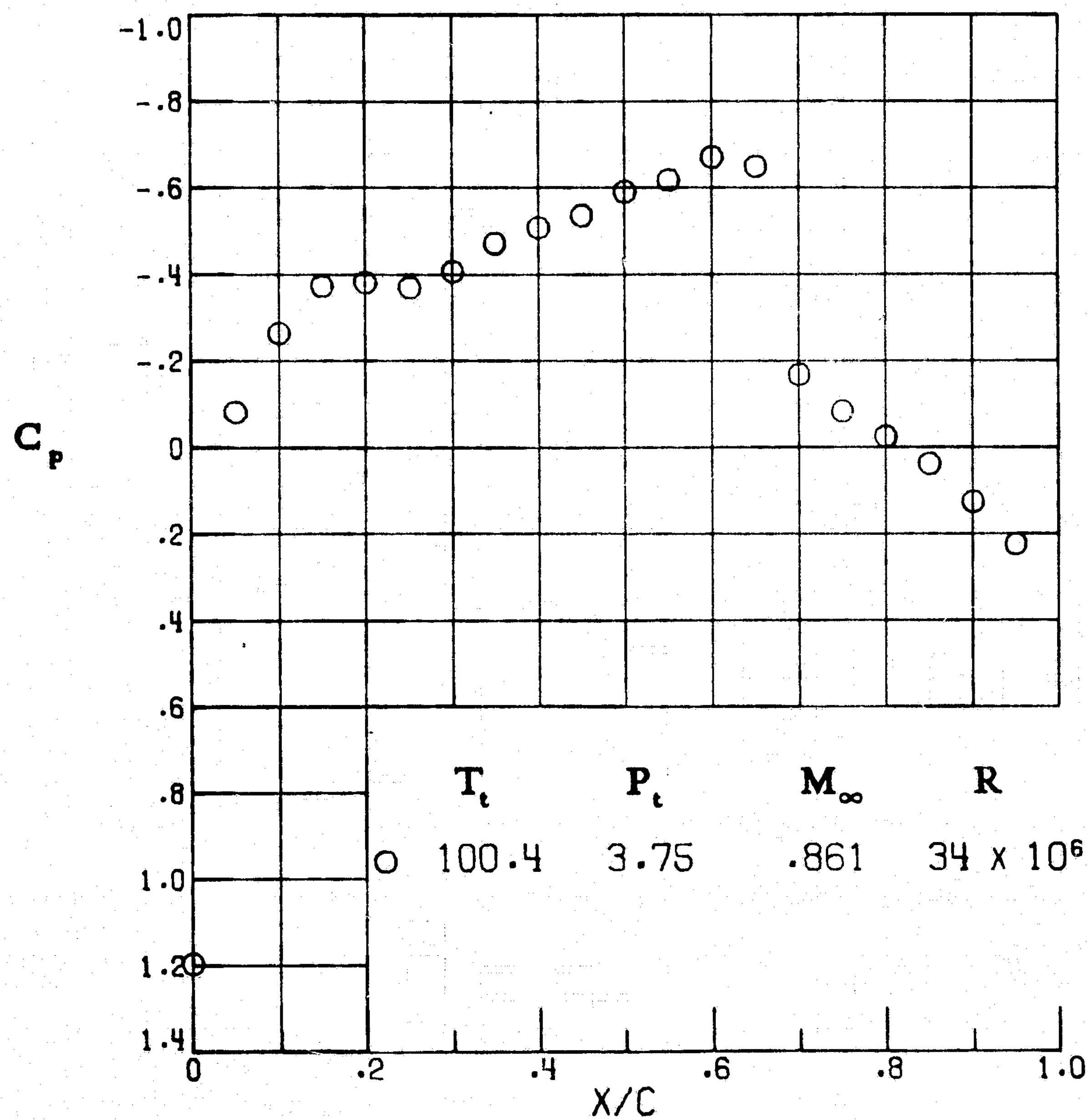

Figure A33.- Path 3, below local saturation.

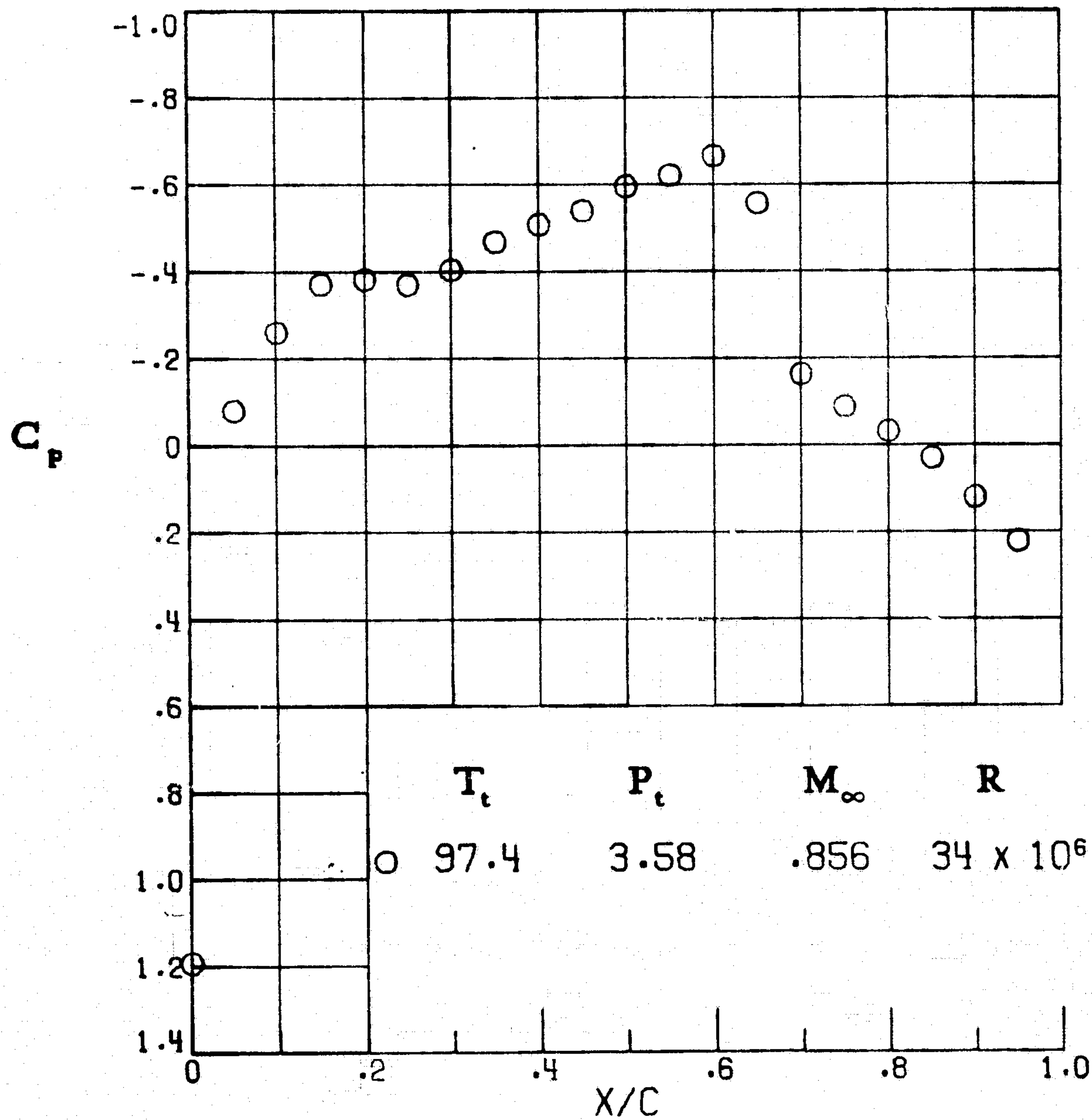

Figure A34.- Path 3, below local saturation.

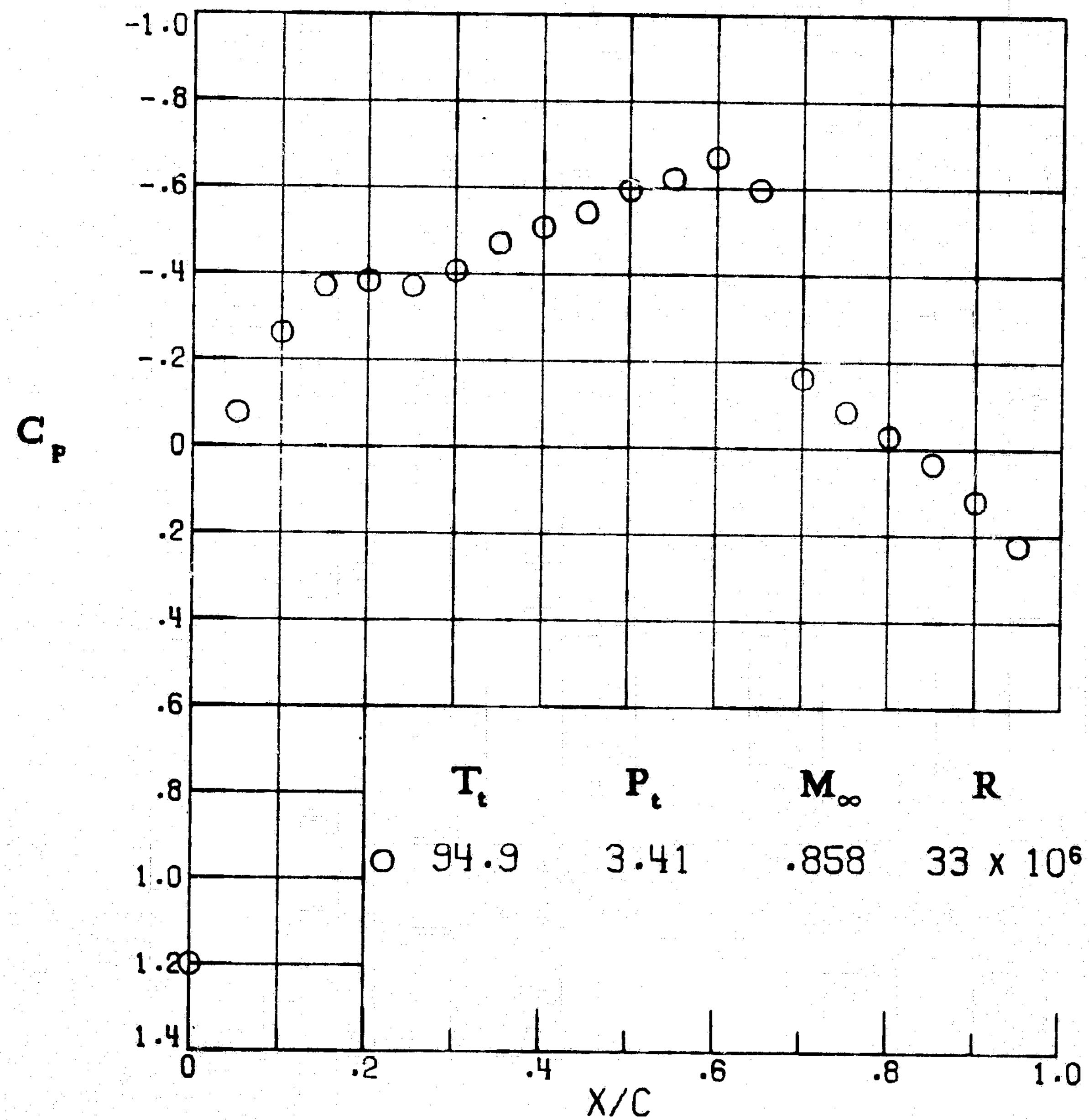

Figure A35.- Path 3, below free-stream saturation.

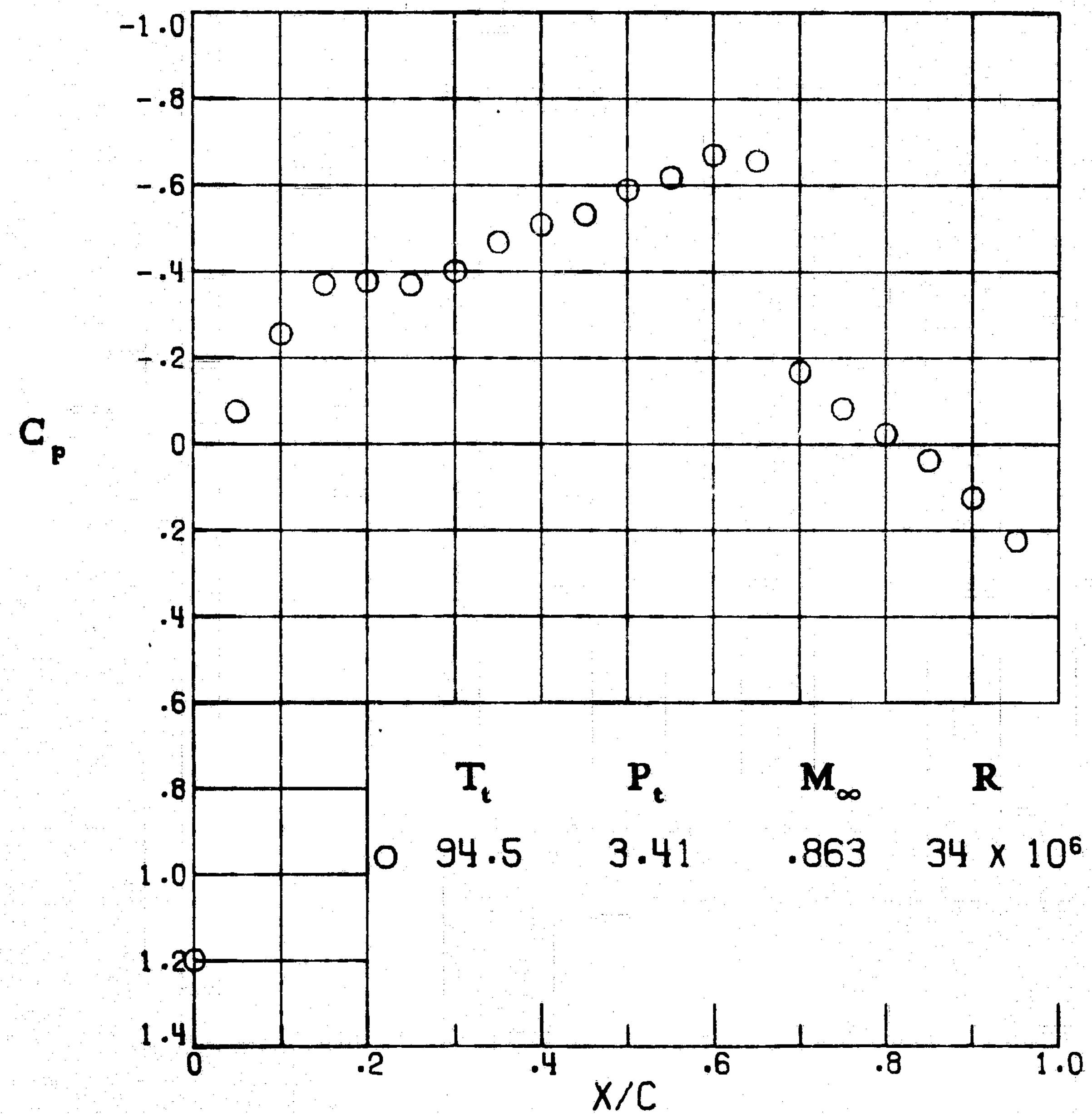

Figure A36.- Path 3, below free-stream saturation.

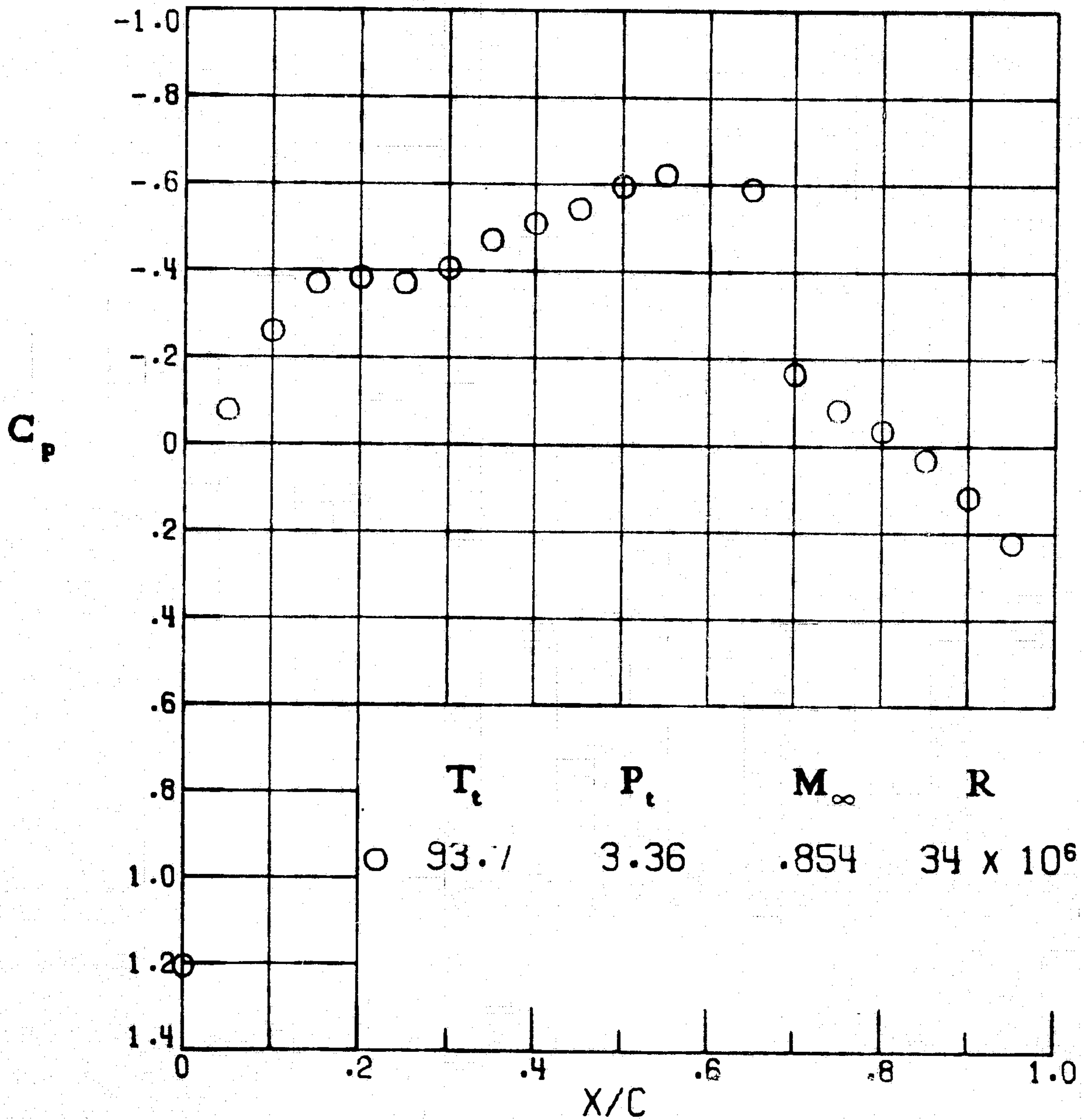

Figure A37.- Path 3, below free-stream saturation.

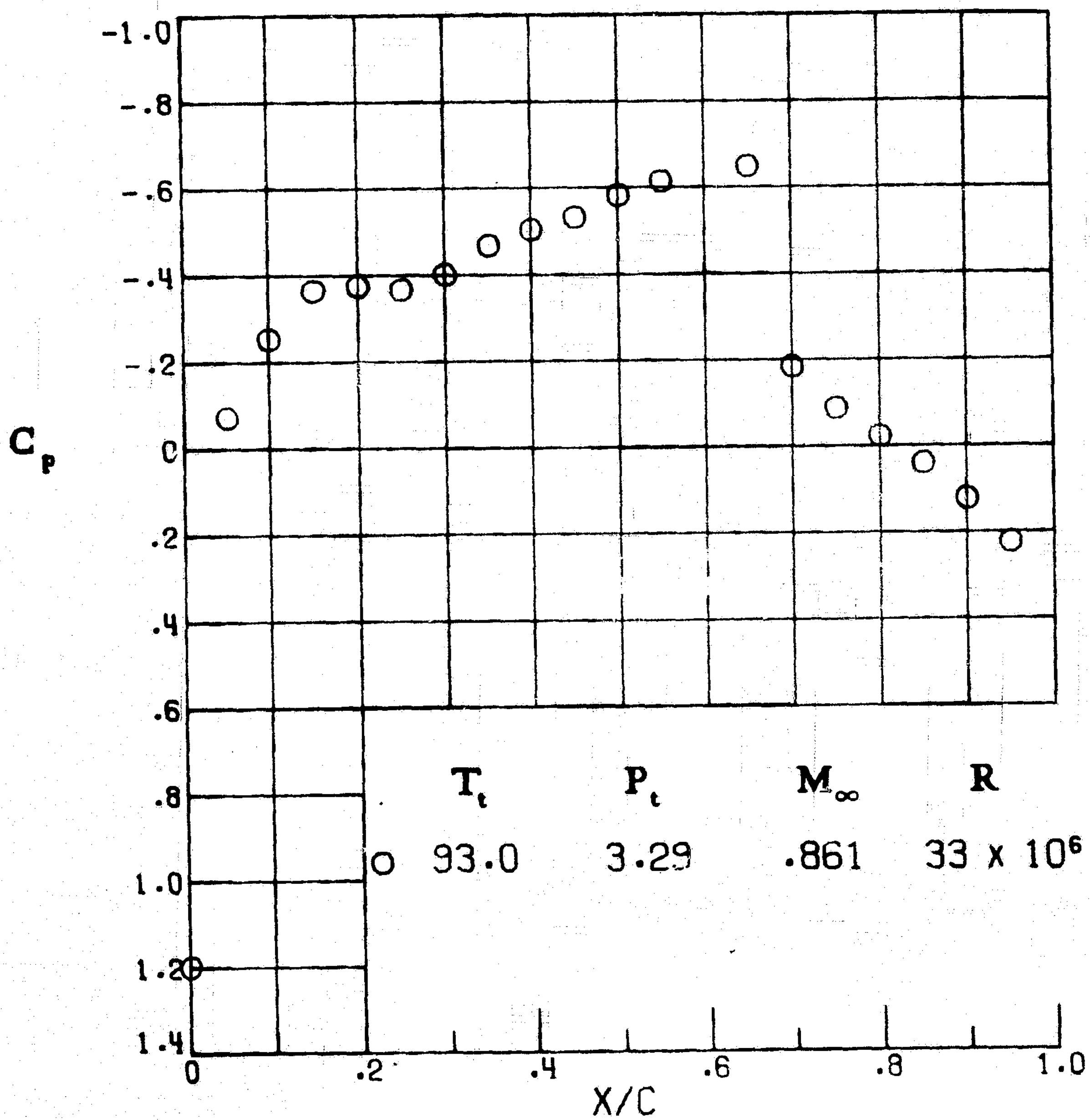

Figure A38.- Path 3, below free-stream saturation.

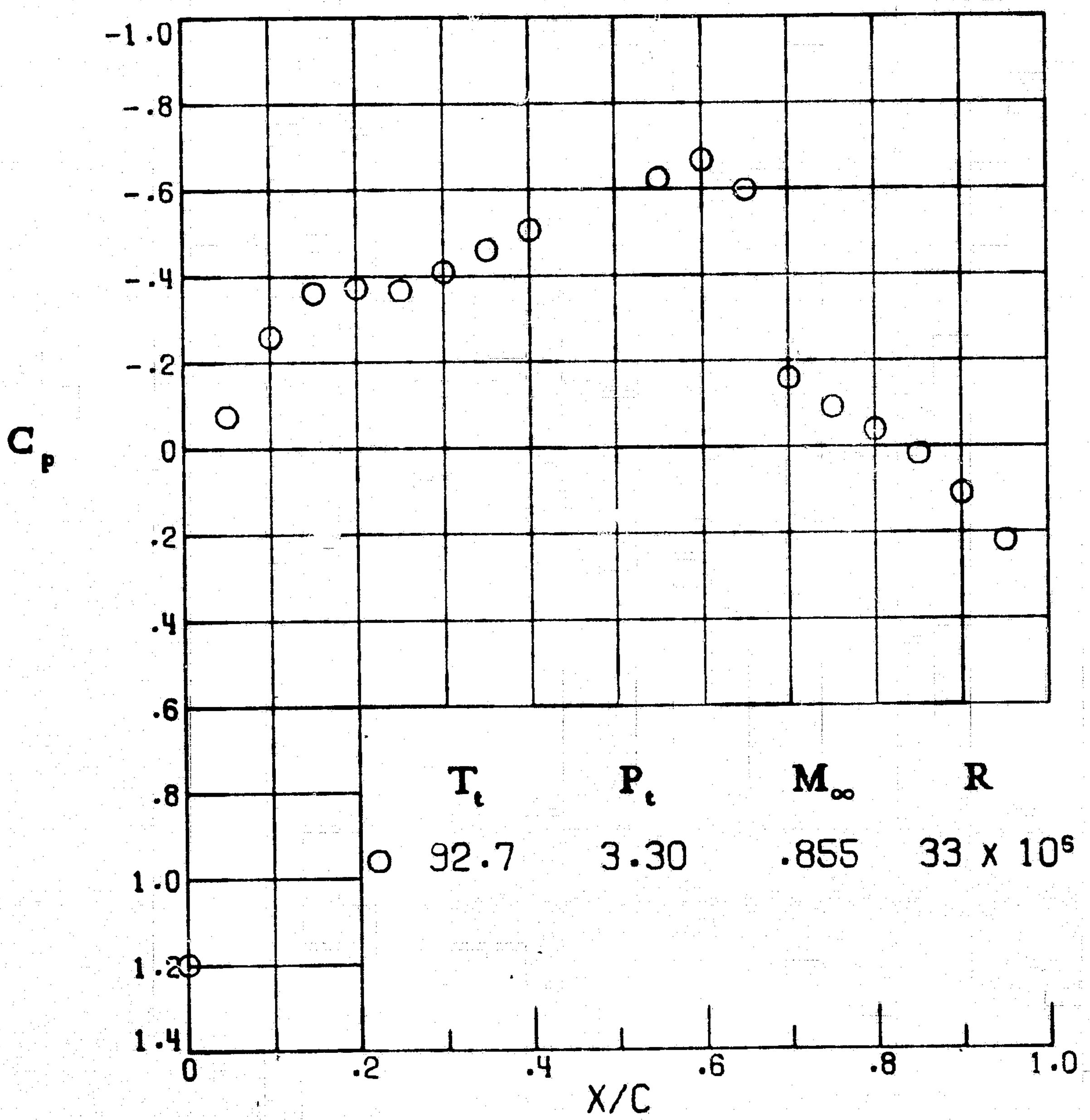

Figure A39.- Path 3, below free-stream saturation.

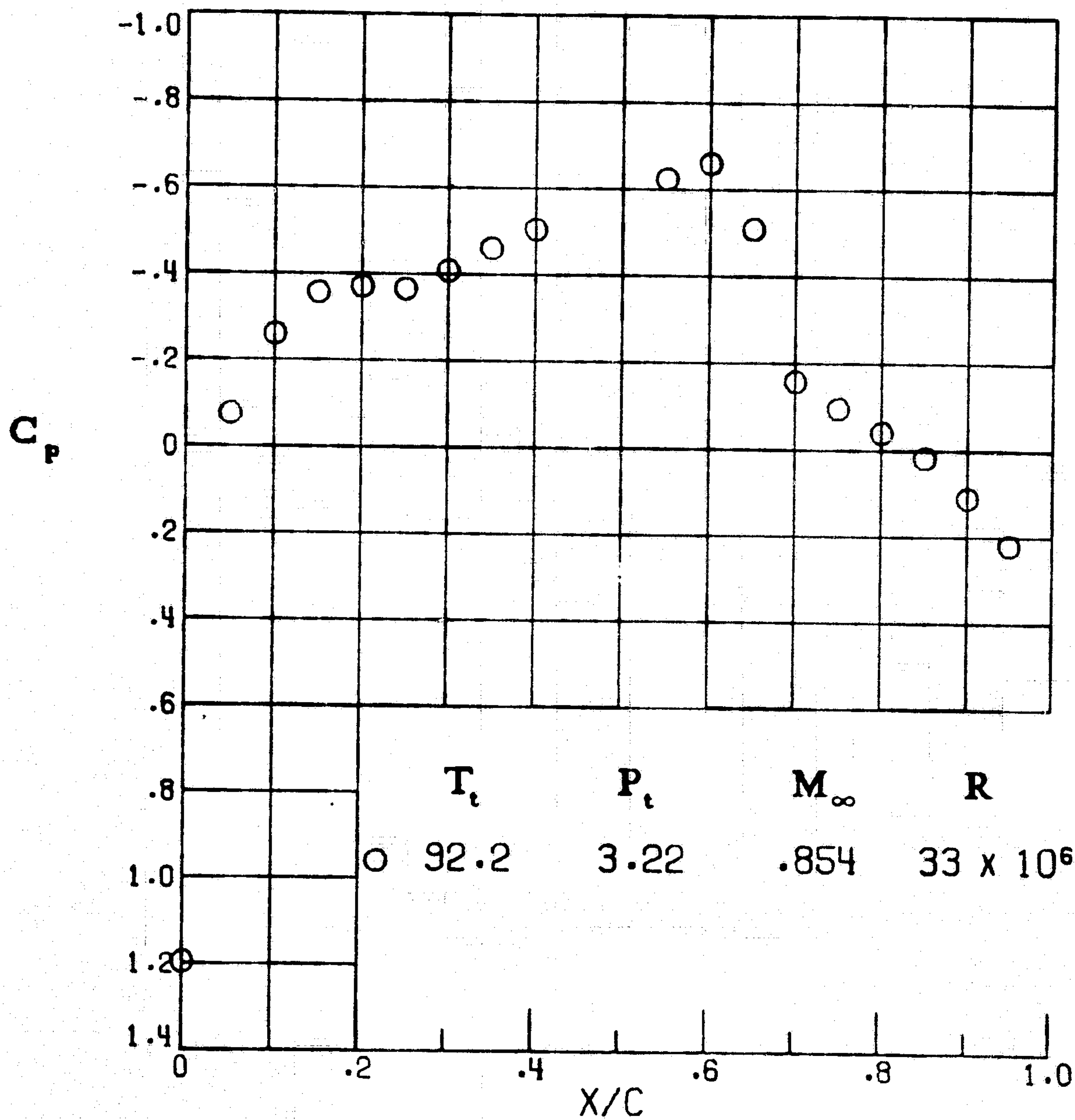

Figure A40.- Path 3, below free-stream saturation.

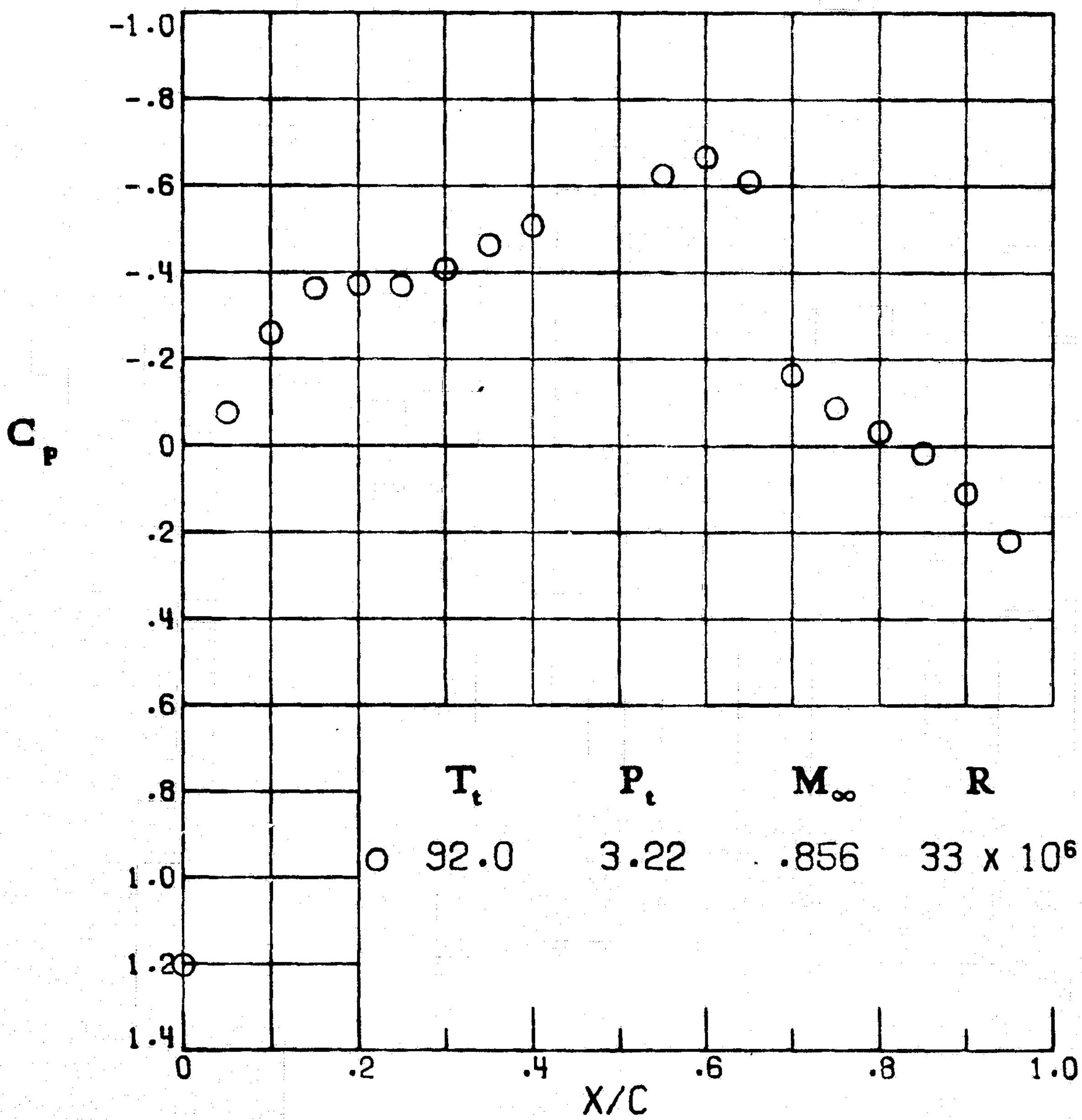

Figure A41.- Path 3, below free-stream saturation.

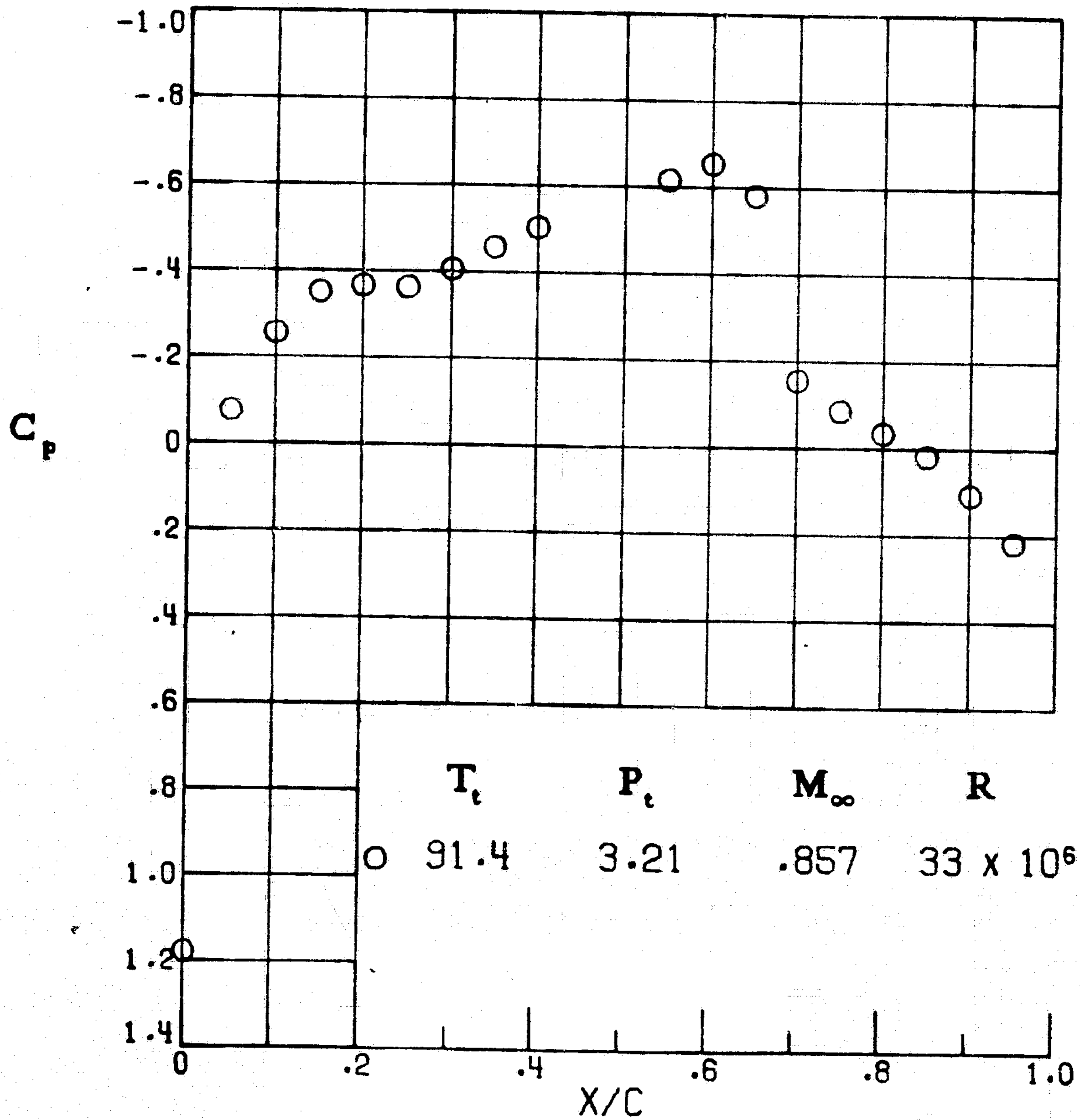

Figure A42.- Path 3, below free-stream saturation.

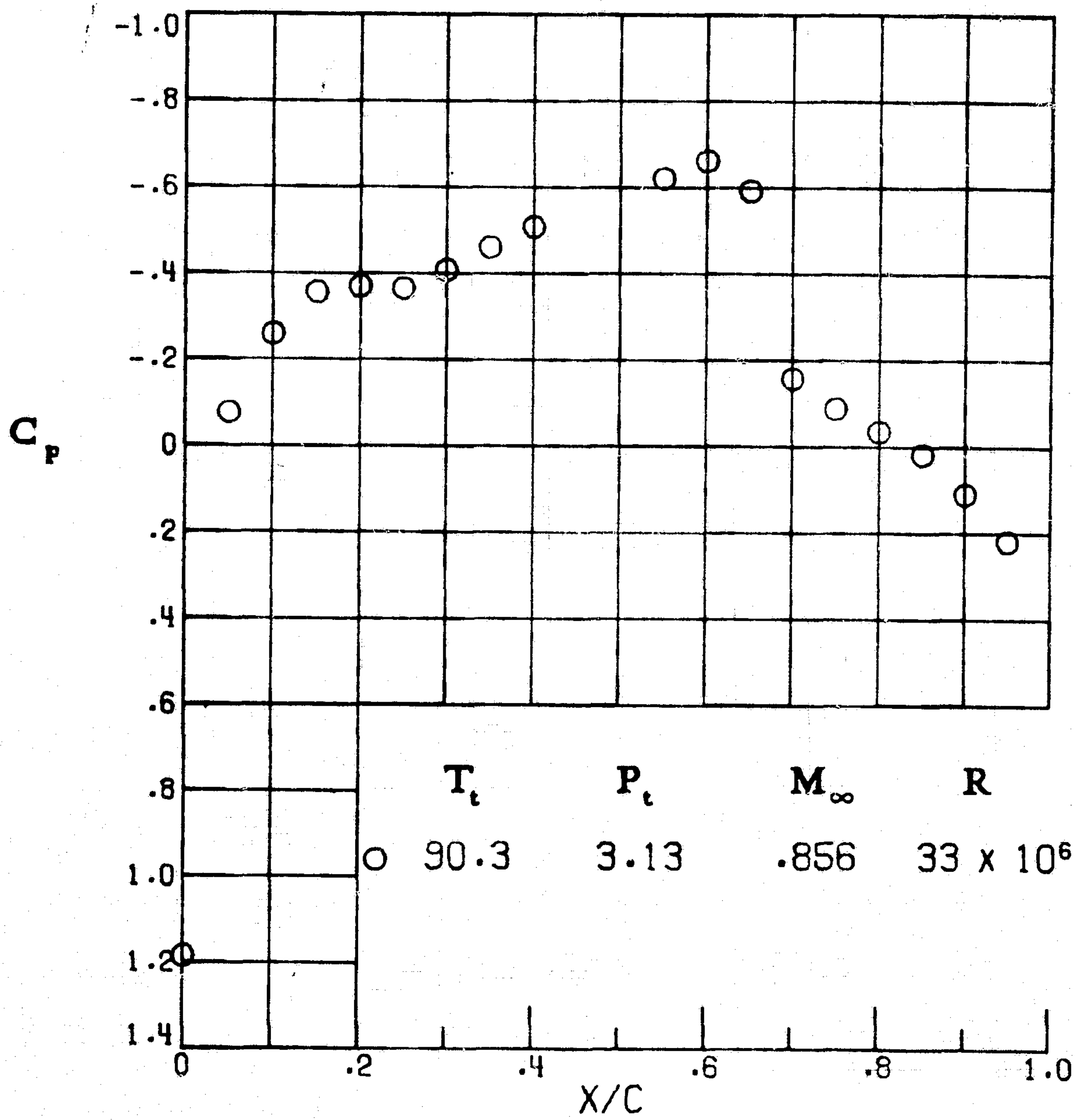

Figure A43.- Path 3, below free-stream saturation.

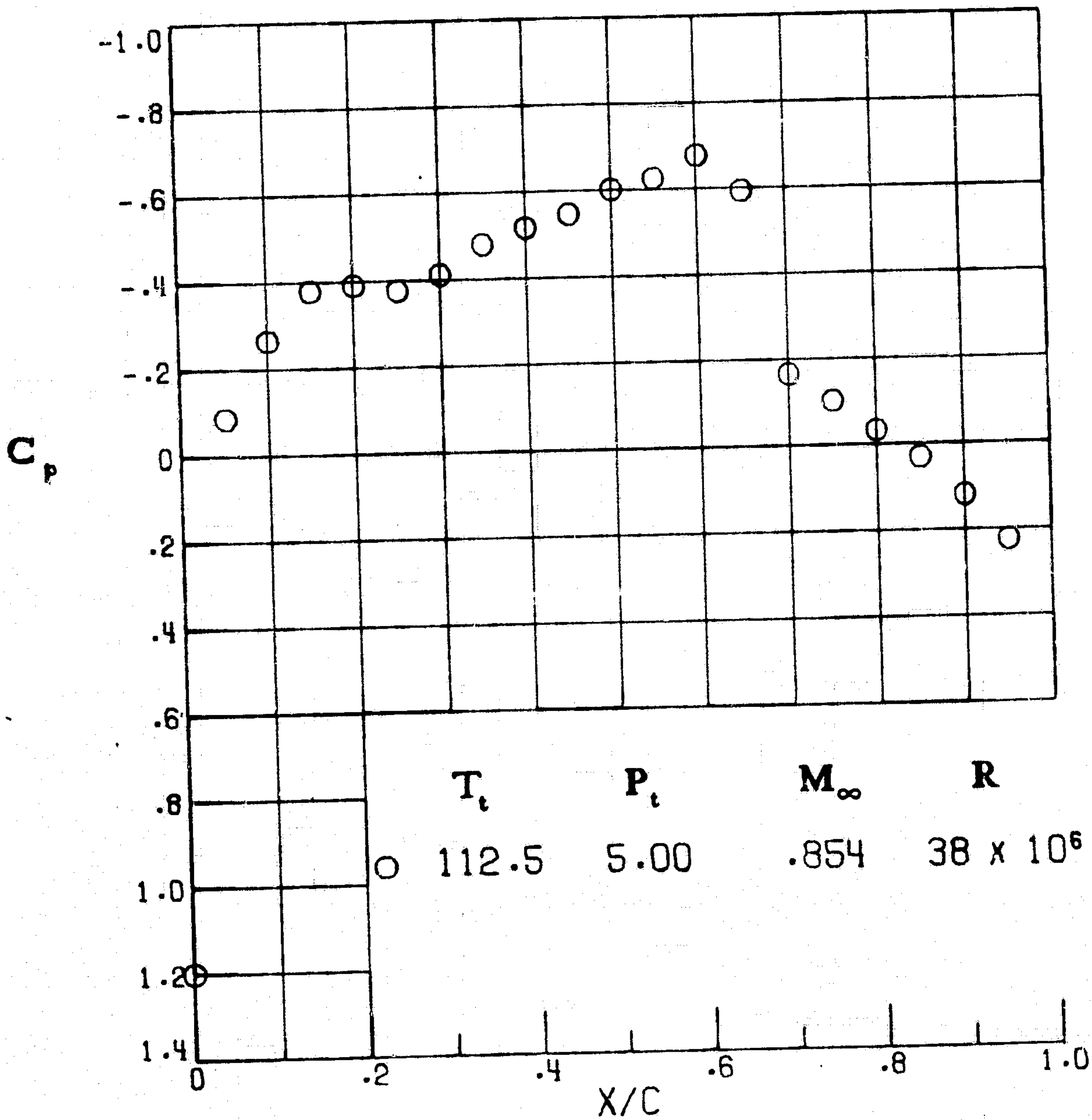

Figure A44.- Path 4, reference, above local saturation.

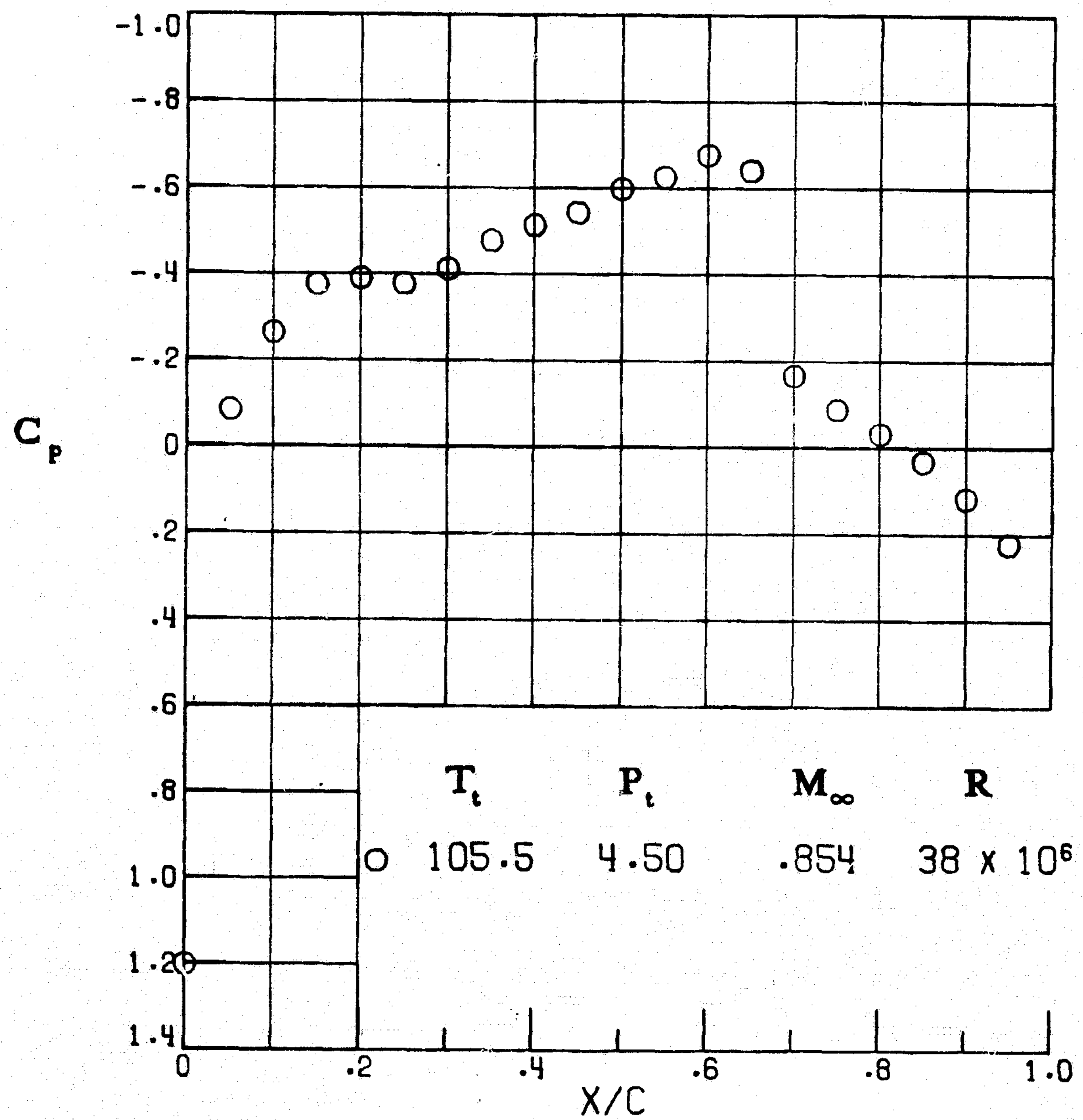

Figure A45.- Path 4, below local saturation.

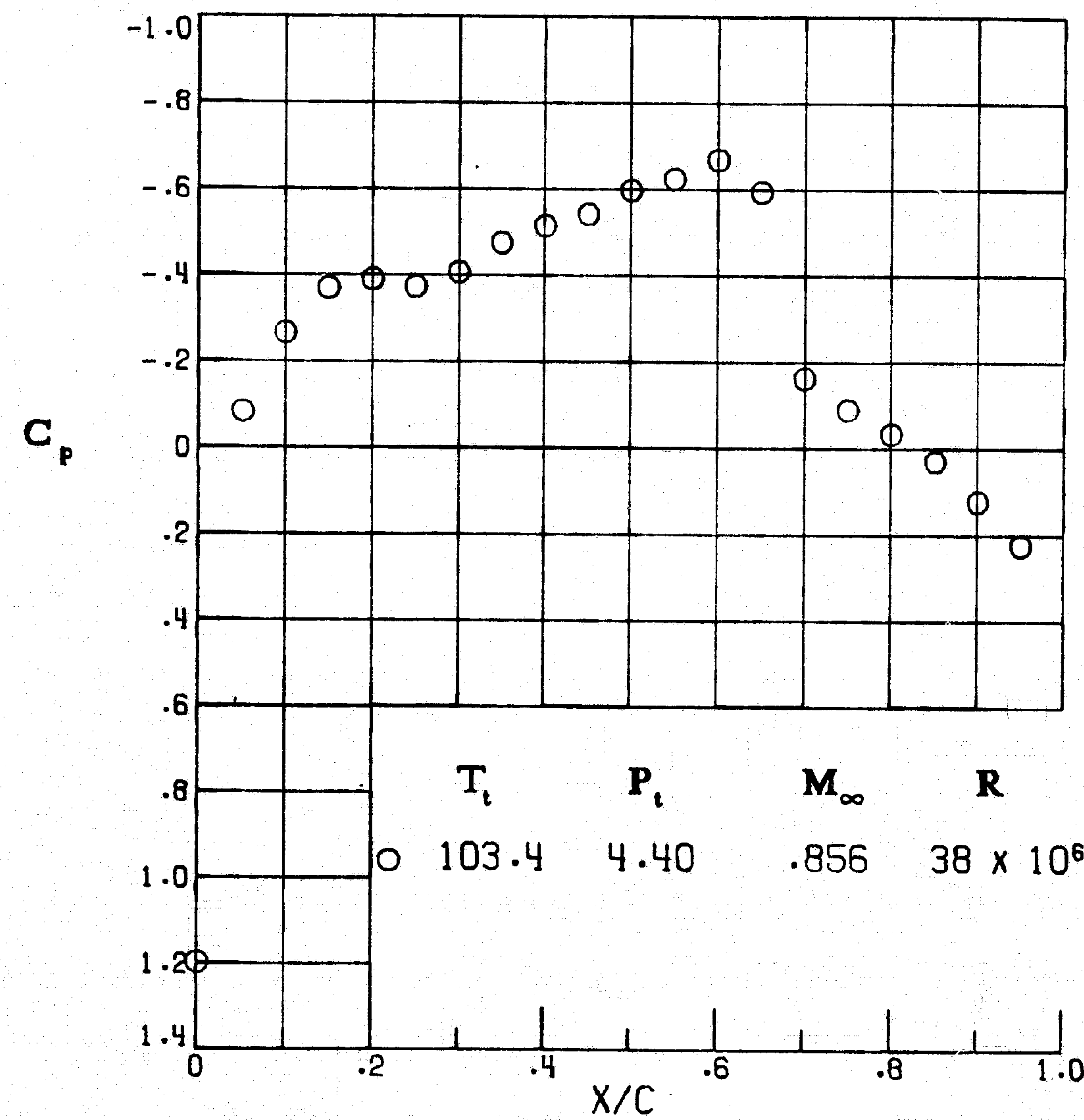

Figure A46.- Path 4, below local saturation.

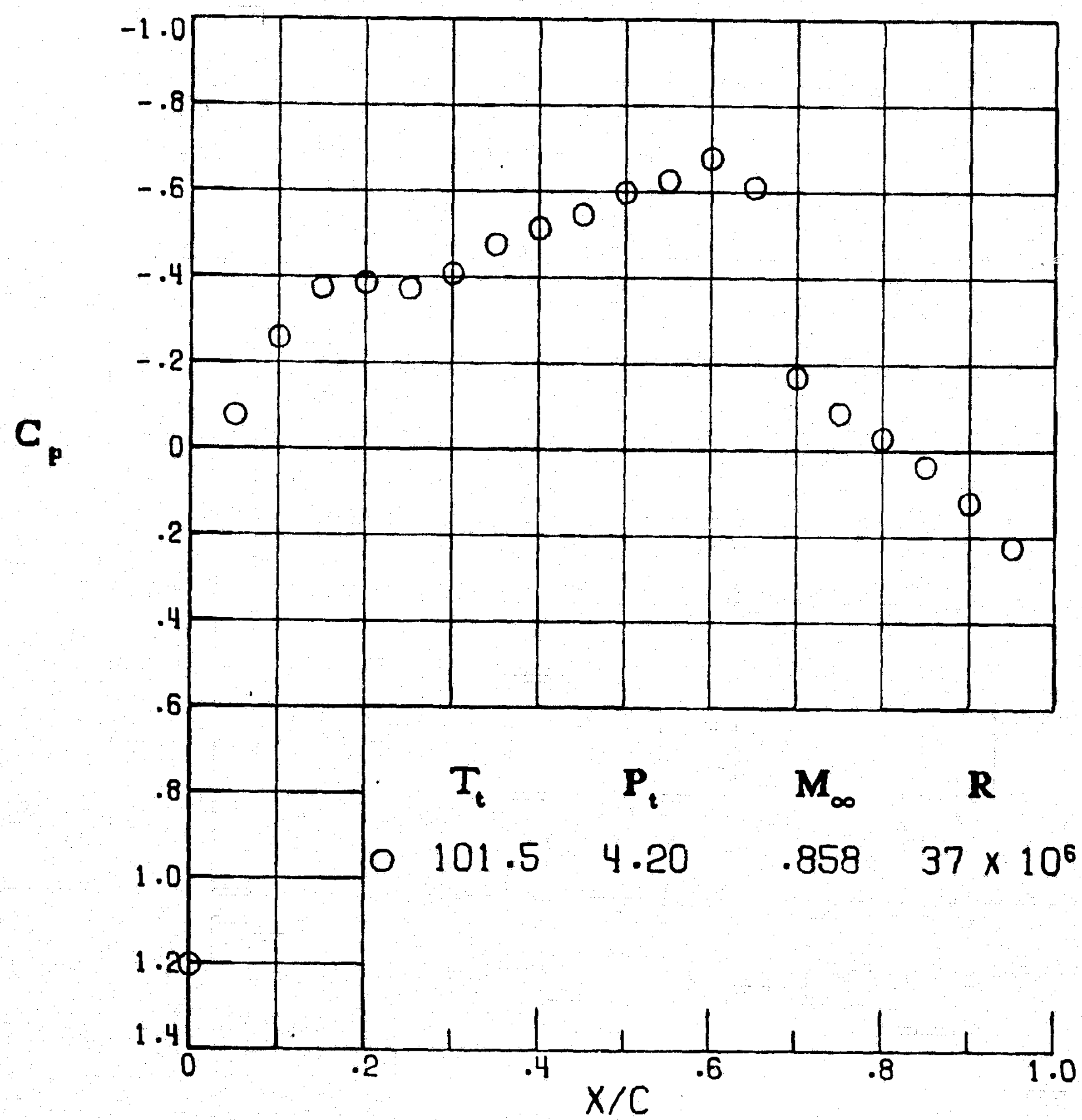

Figure A47.- Path 4, below local saturation.

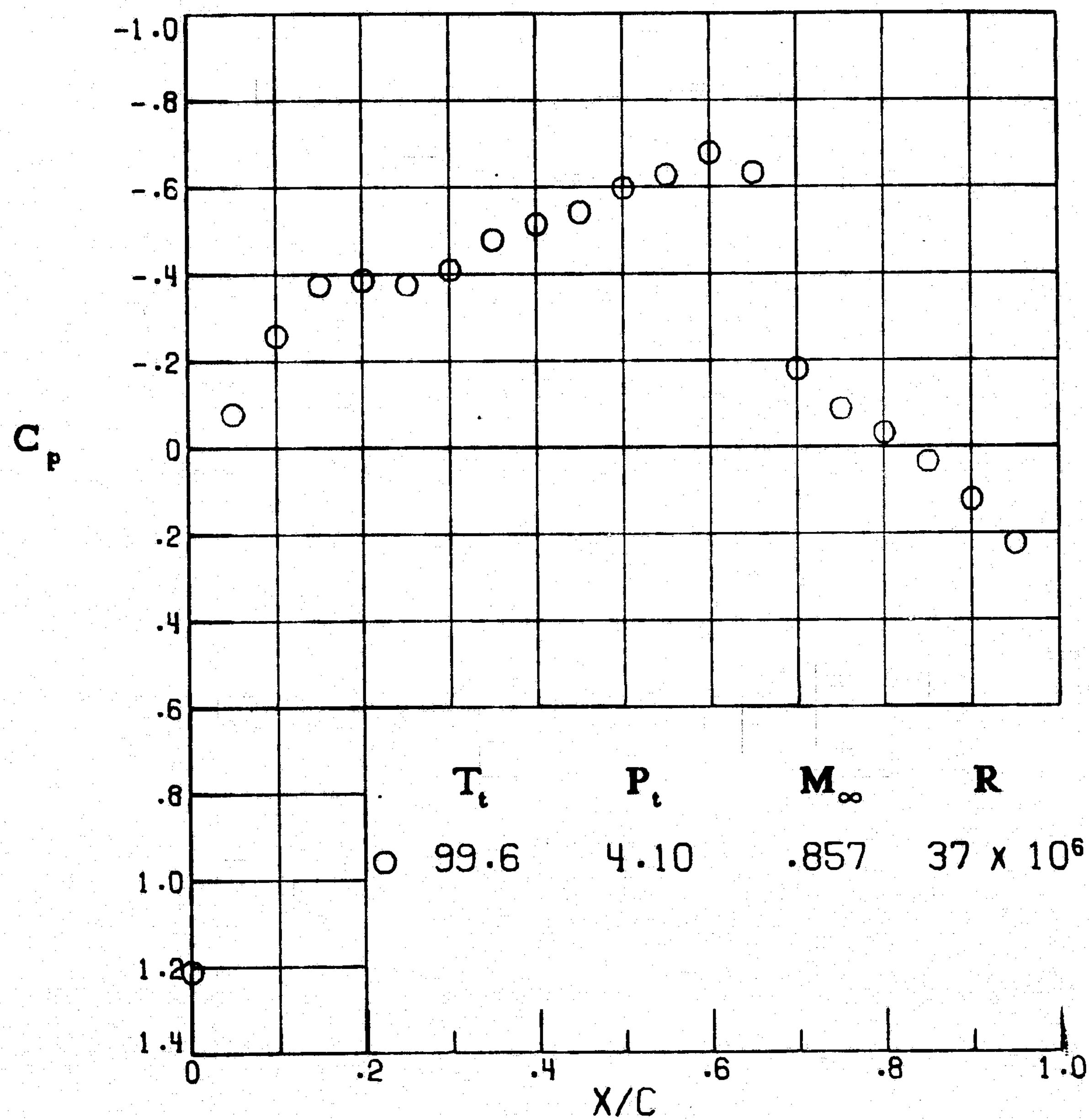

Figure A48.- Path 4, below local saturation.

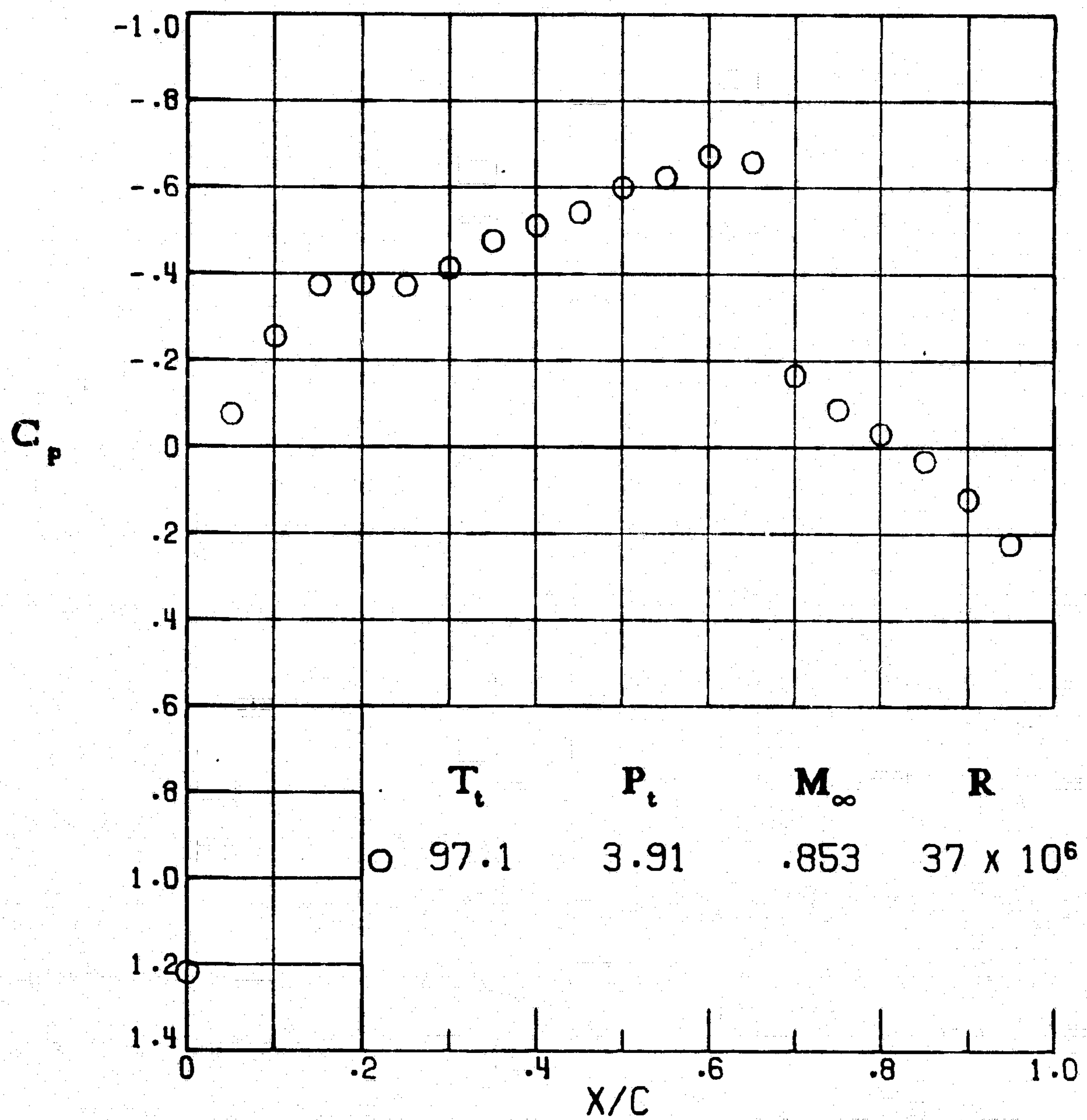

Figure A49.- Path 4, below free-stream saturation.

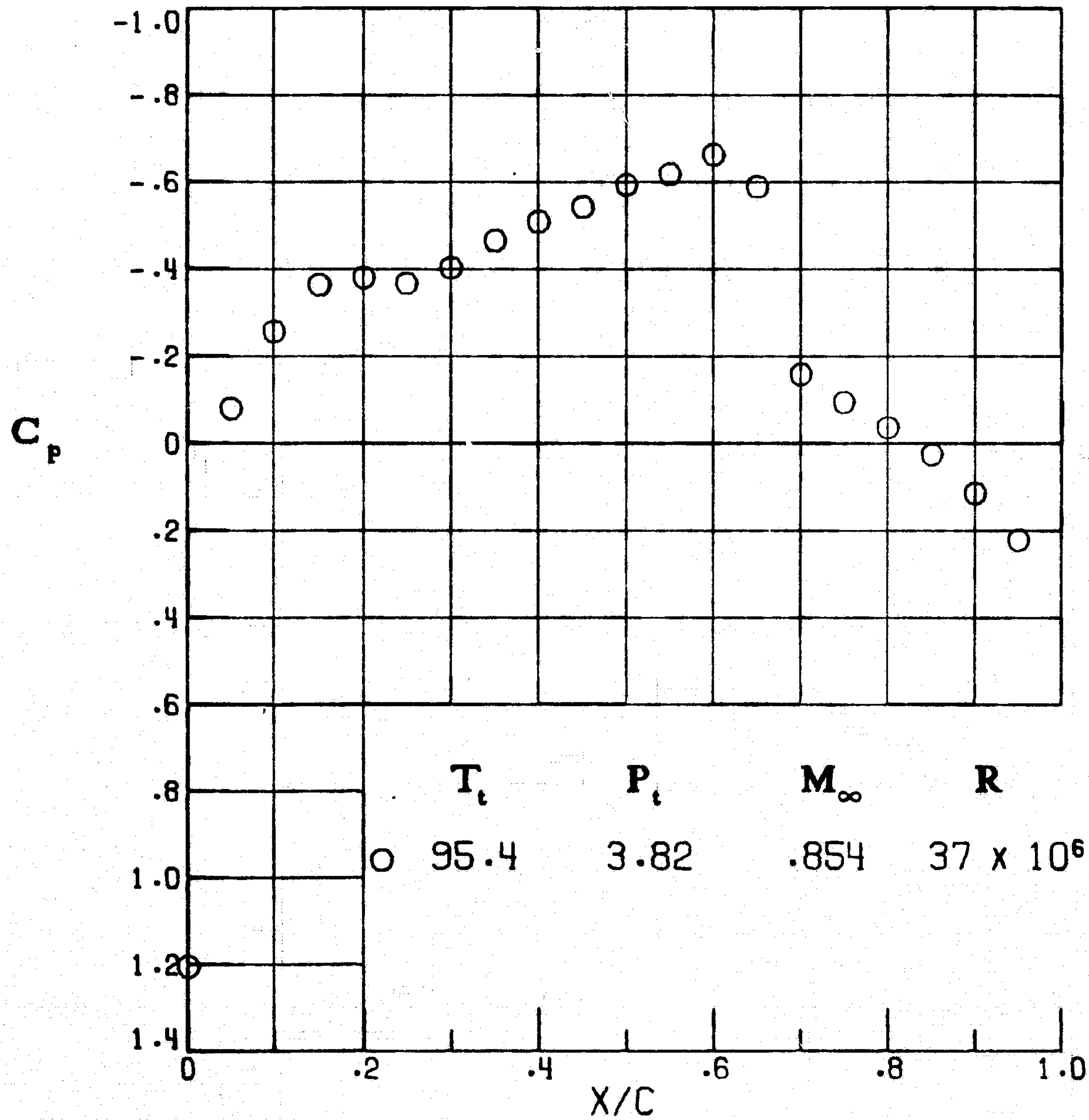

Figure A50.- Path 4, below free-stream saturation.

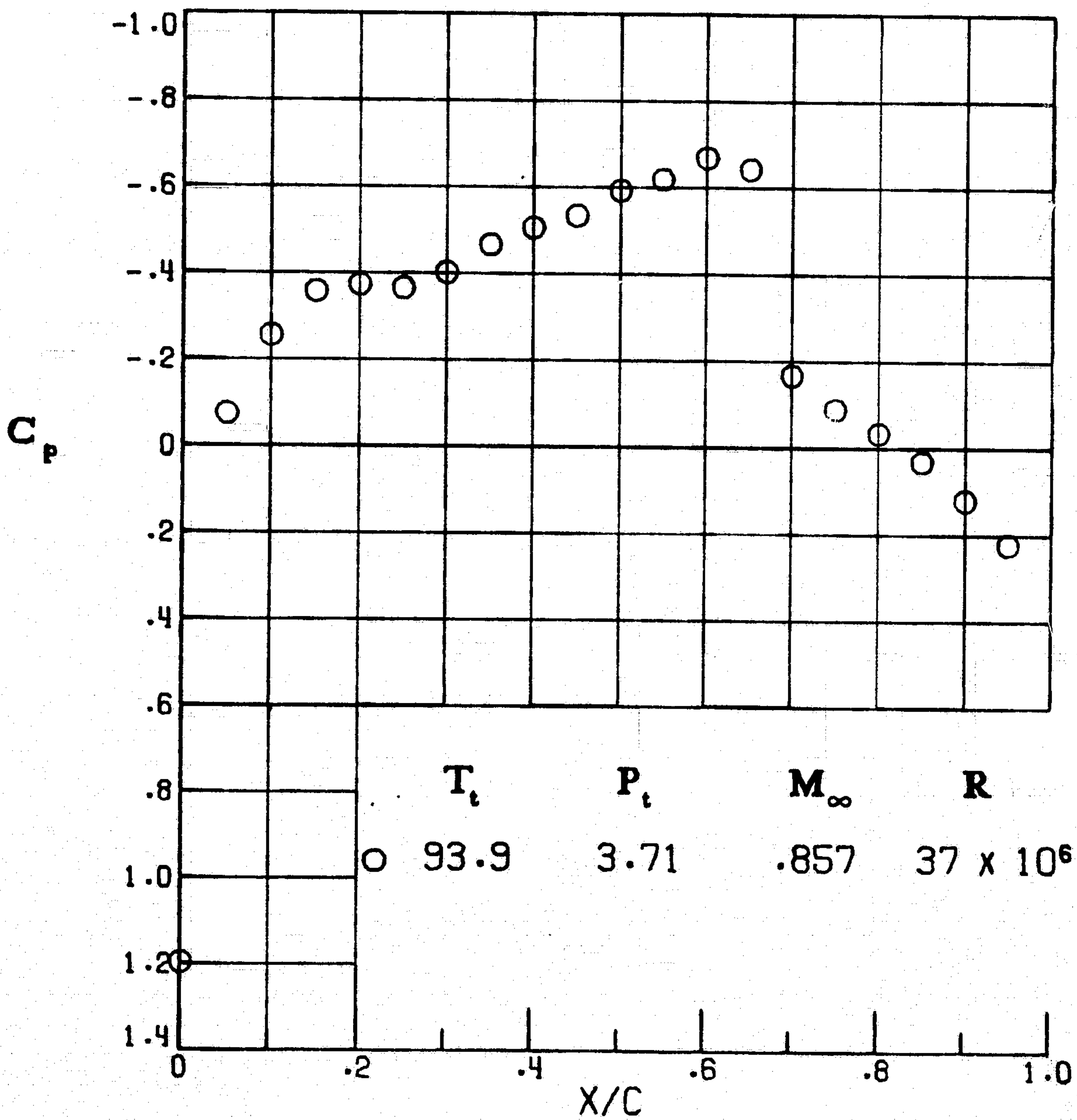

Figure A51.- Path 4, below free-stream saturation.

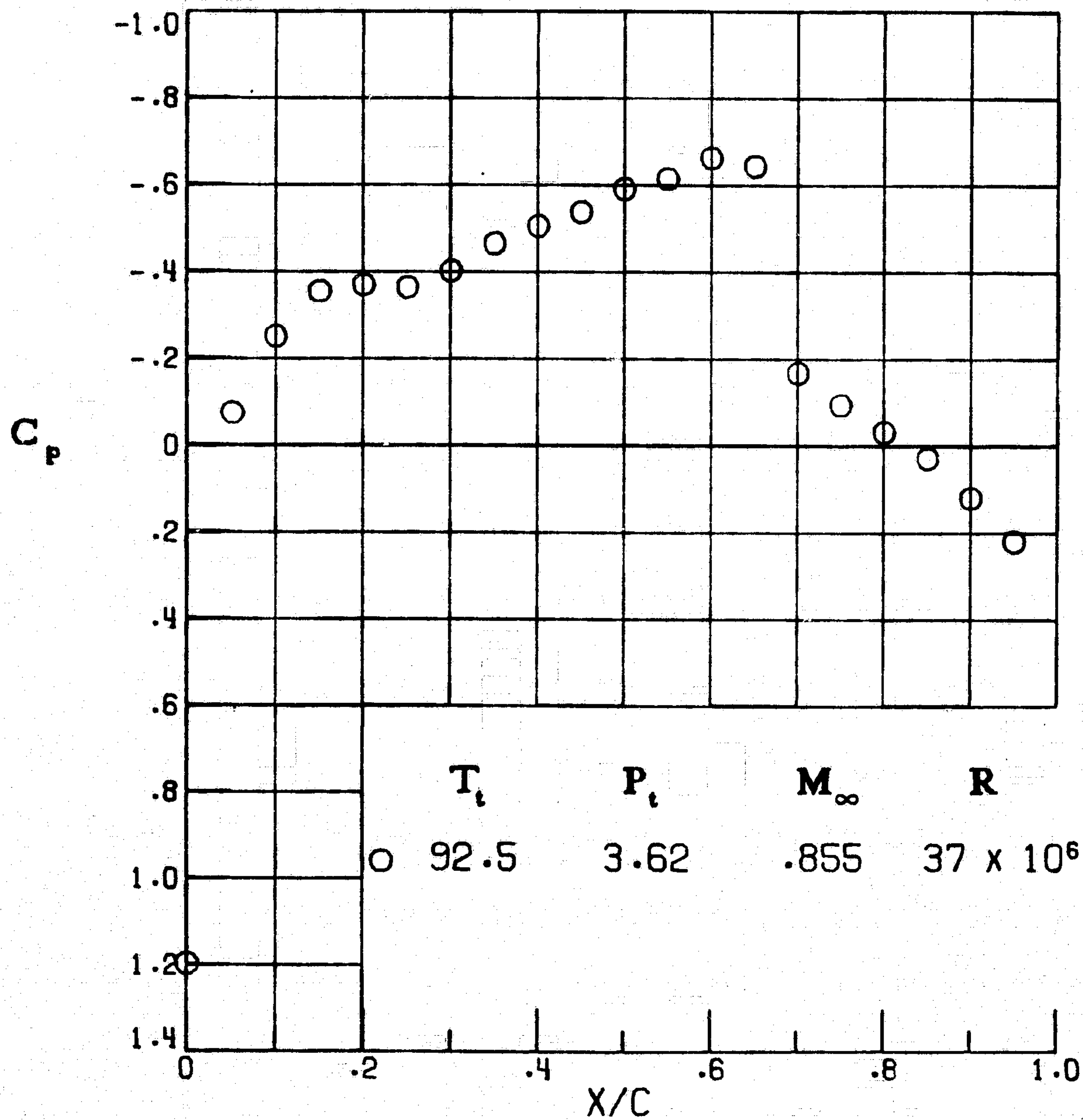

Figure A52.- Path 4, below free-stream saturation.

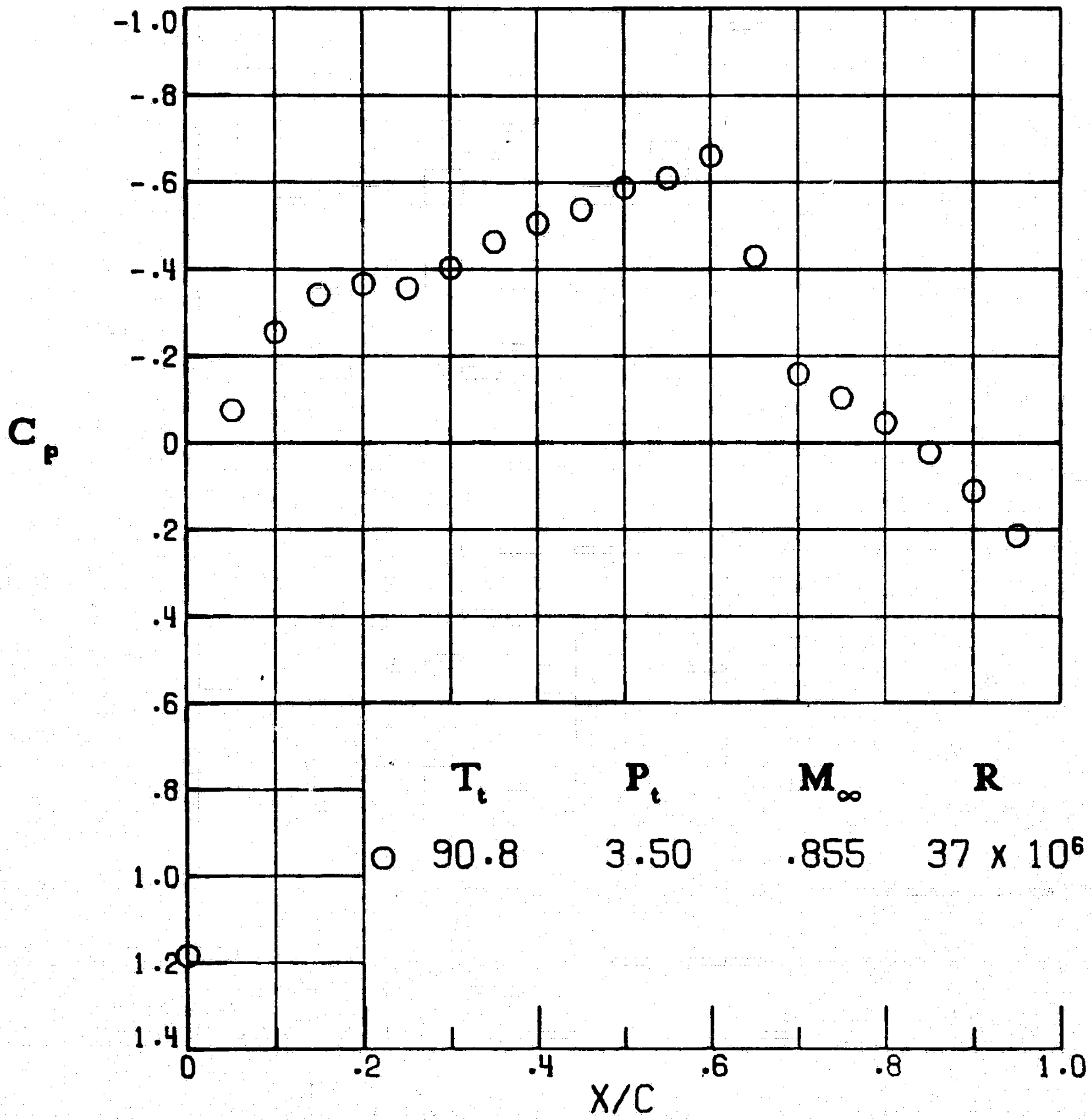

Figure A53.- Path 4, below free-stream saturation.

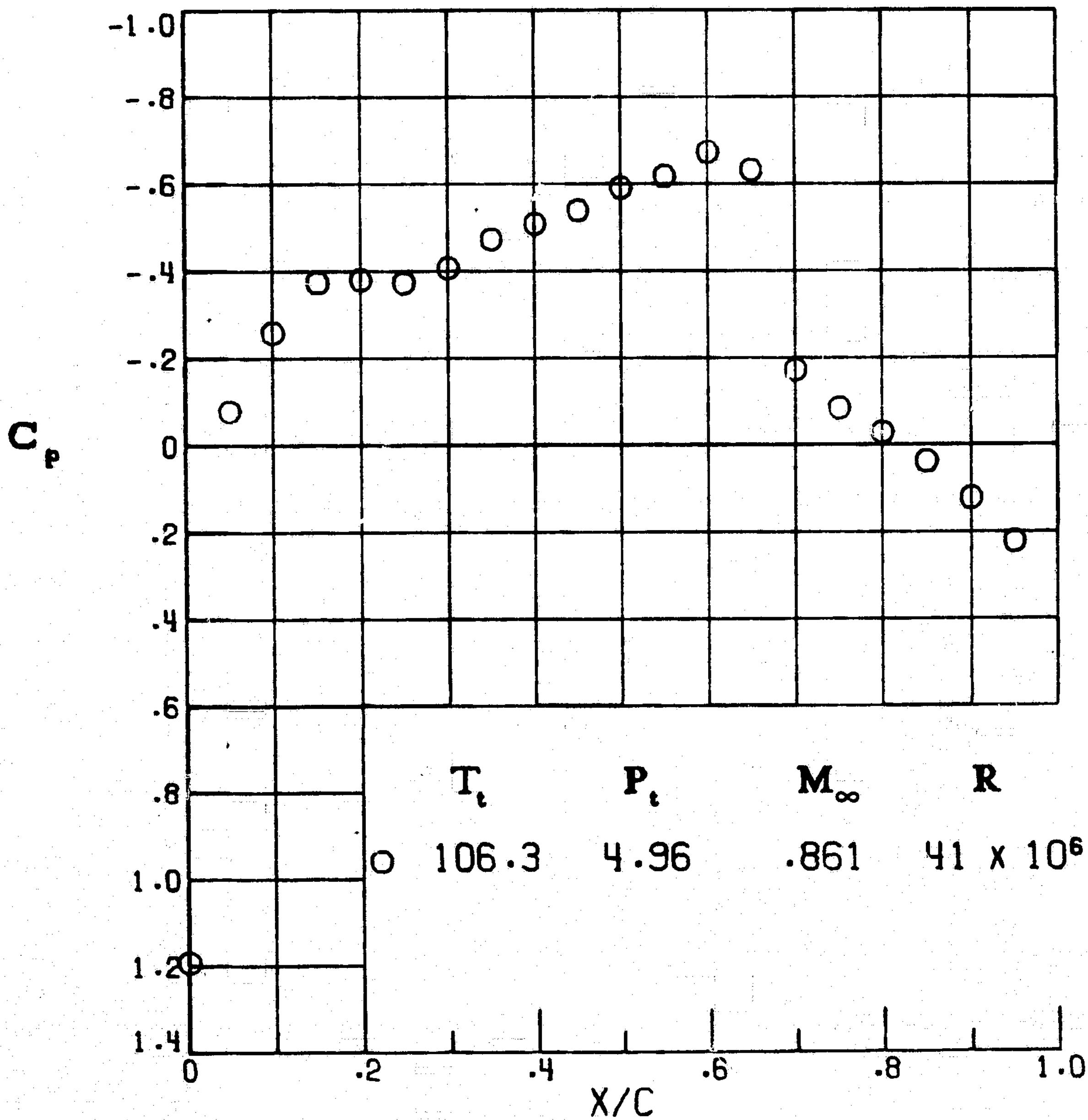

Figure A54. - Path 5, reference, below local saturation.

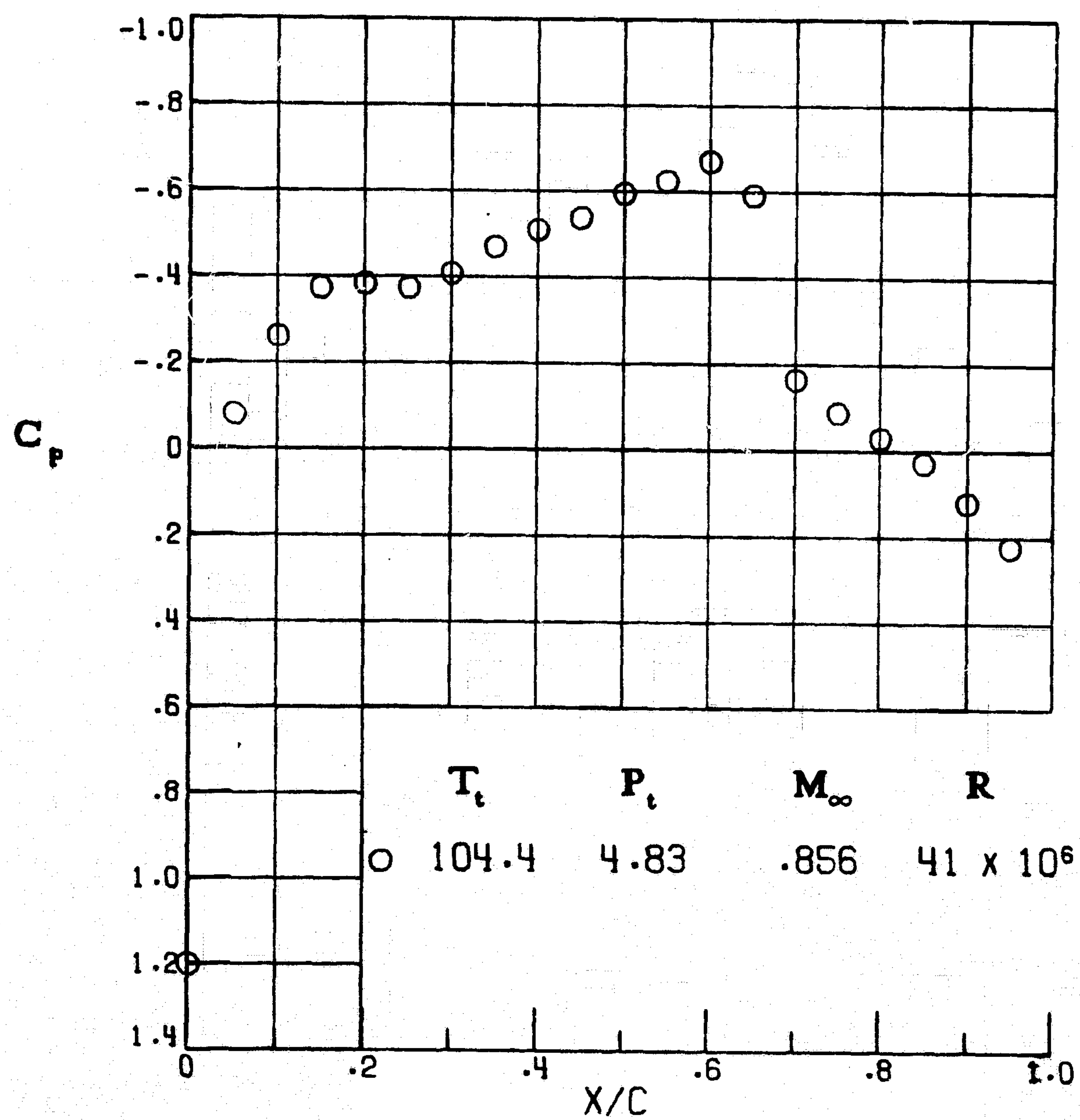

Figure A55.- Path 5, below local saturation.

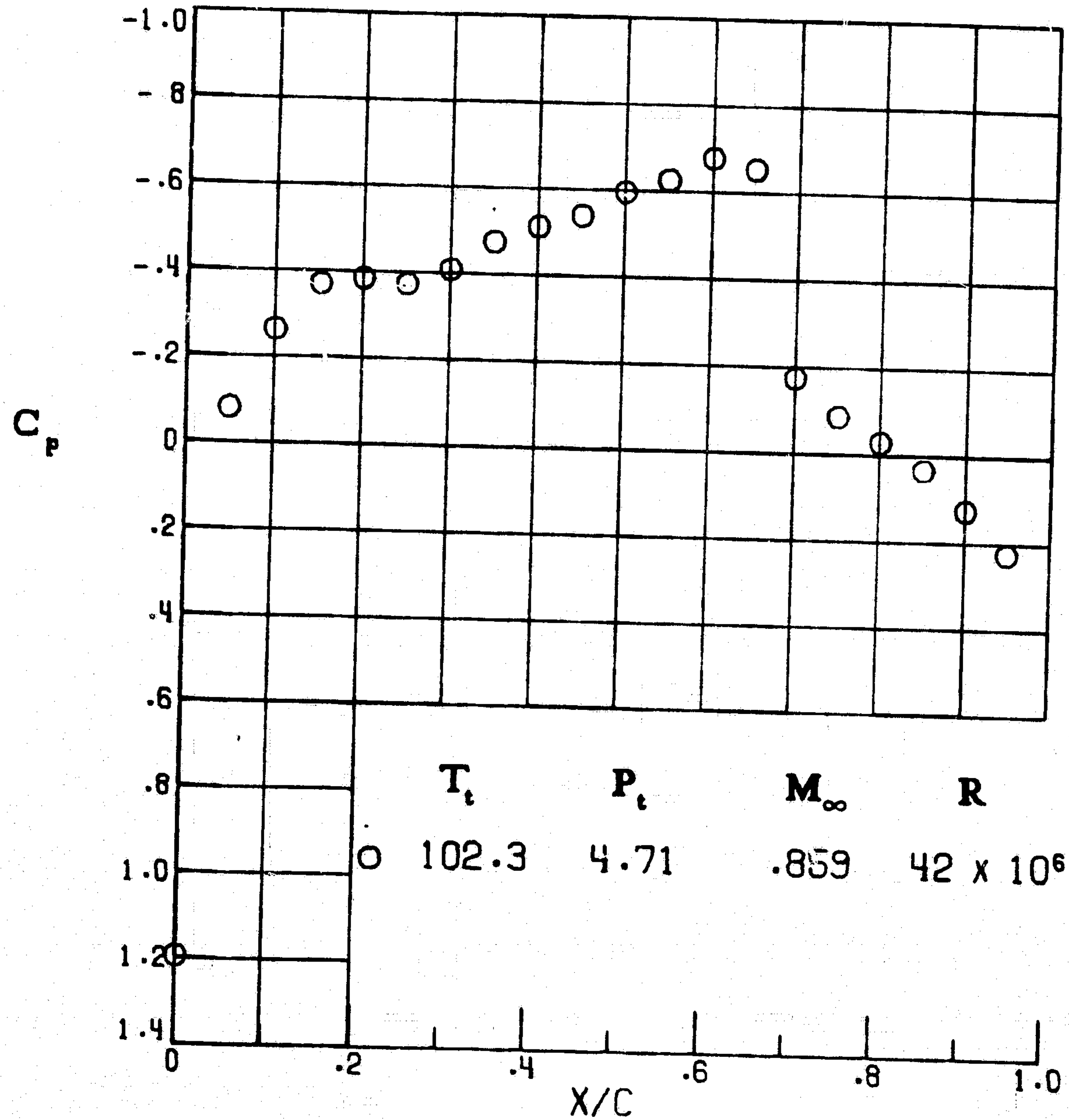

Figure A56.- Path 5, below local saturation.

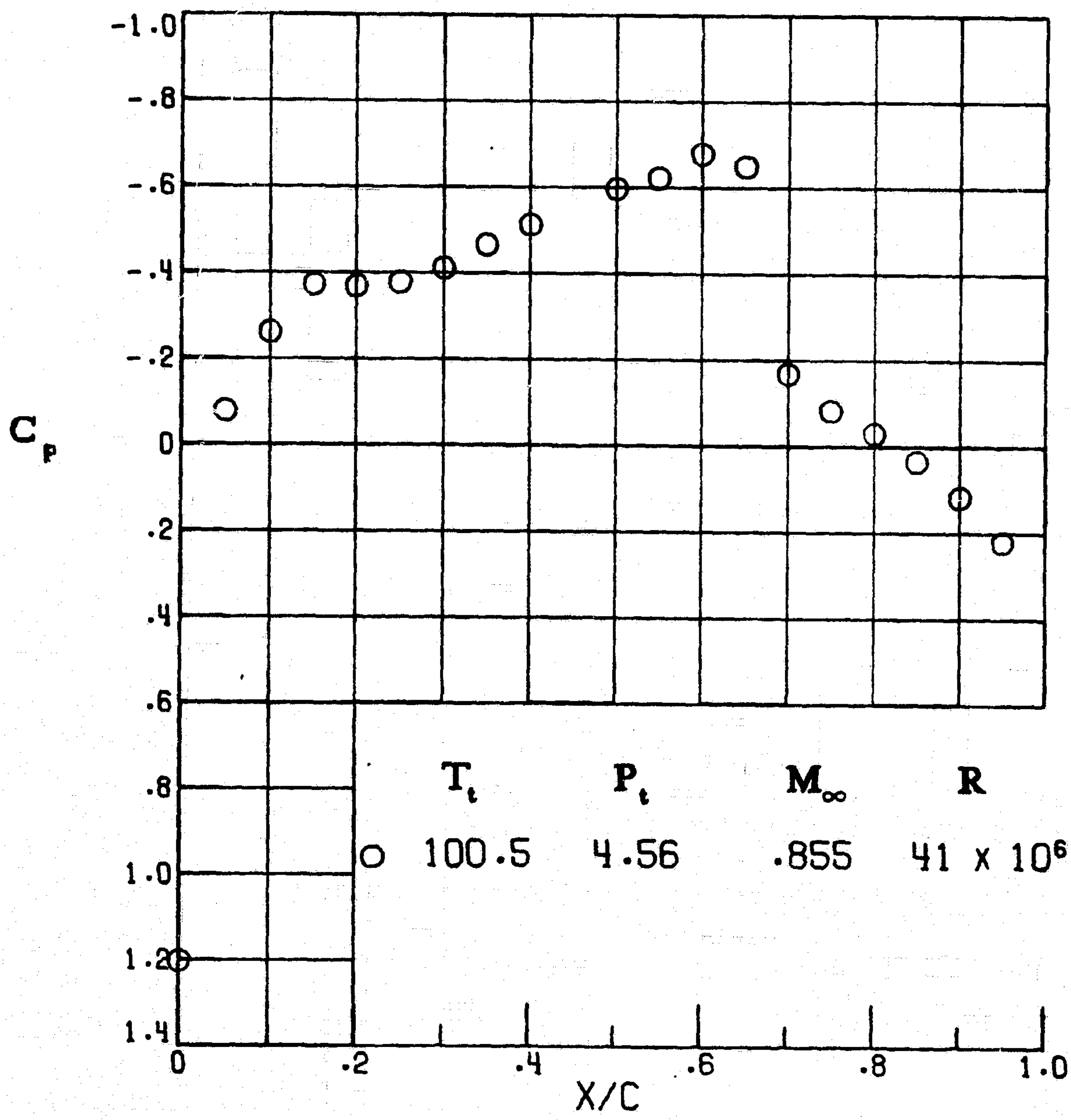

Figure A57.- Path 5, below local saturation.

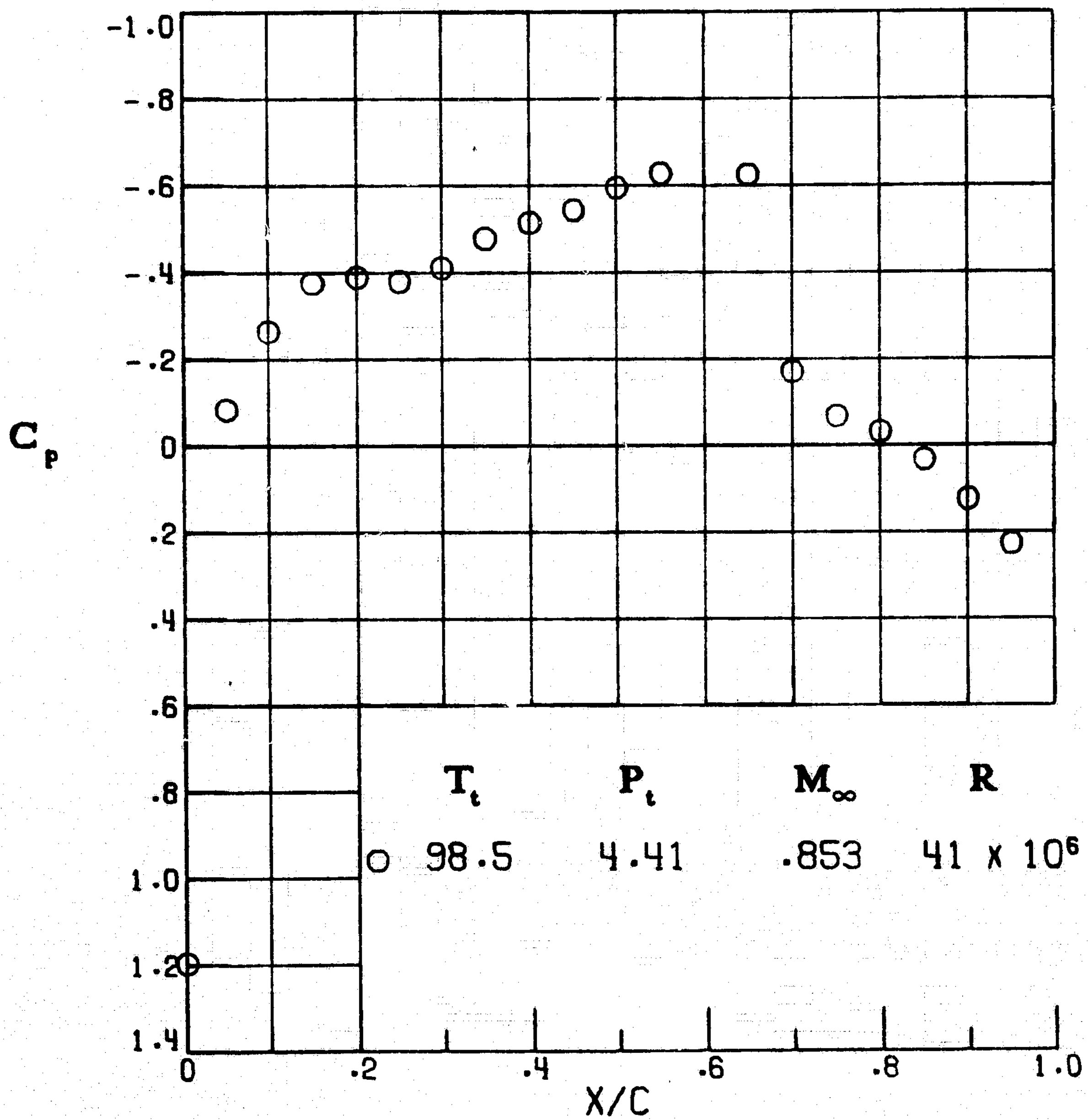

Figure A58.- Path 5, below free-stream saturation.

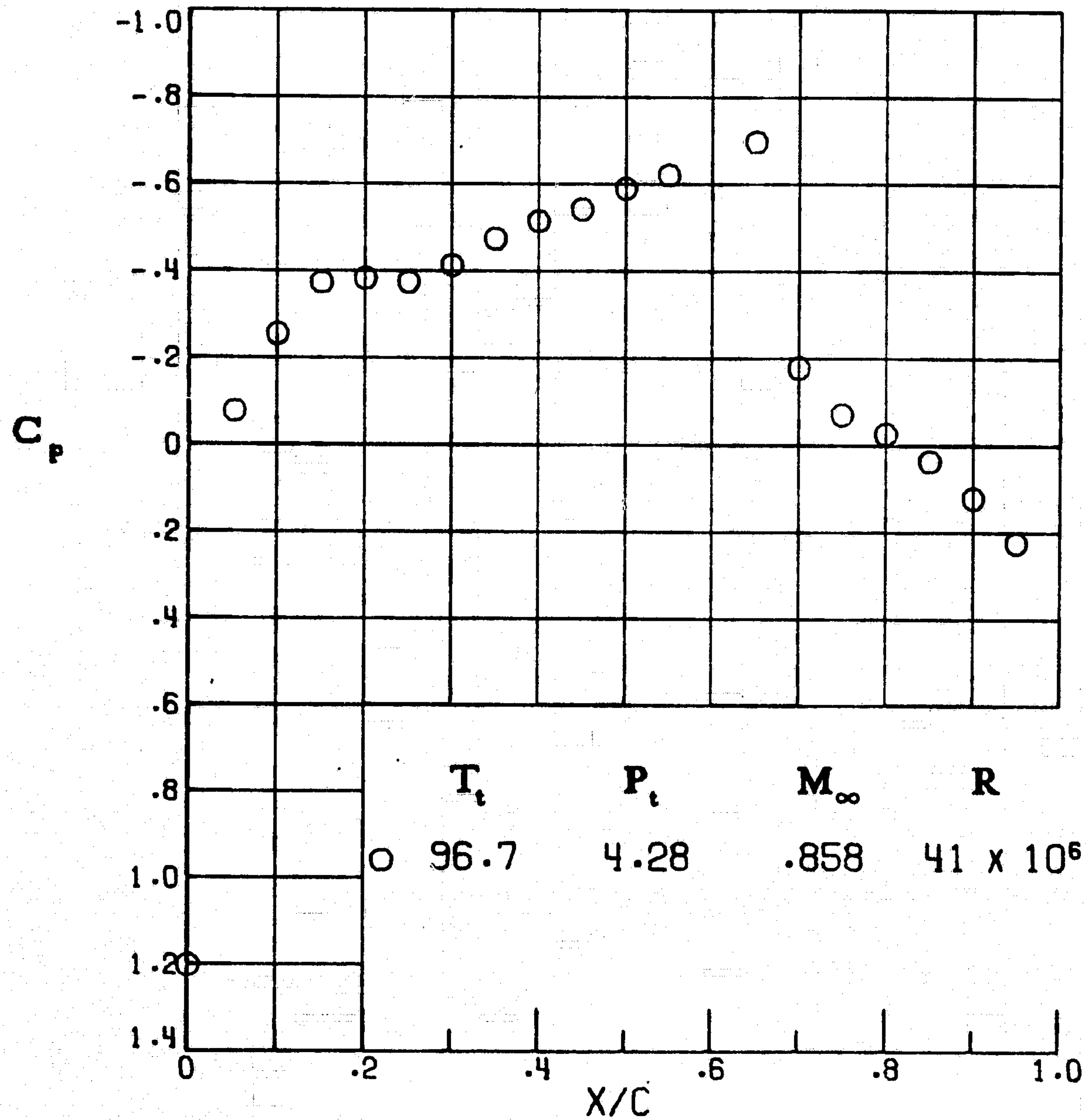

Figure A59.- Path 5, below free-stream saturation.

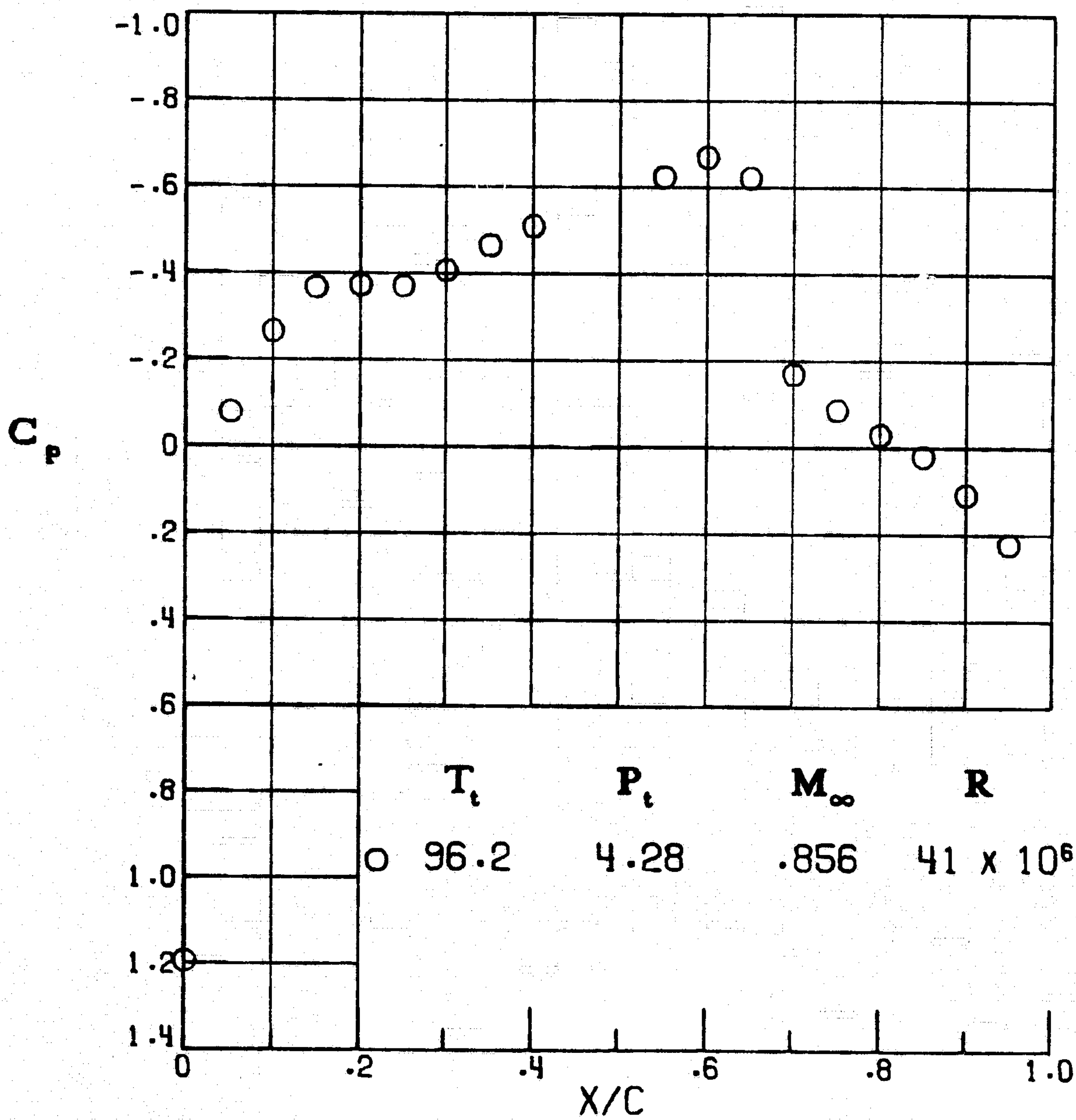

Figure A60.- Path 5, below free-stream saturation.

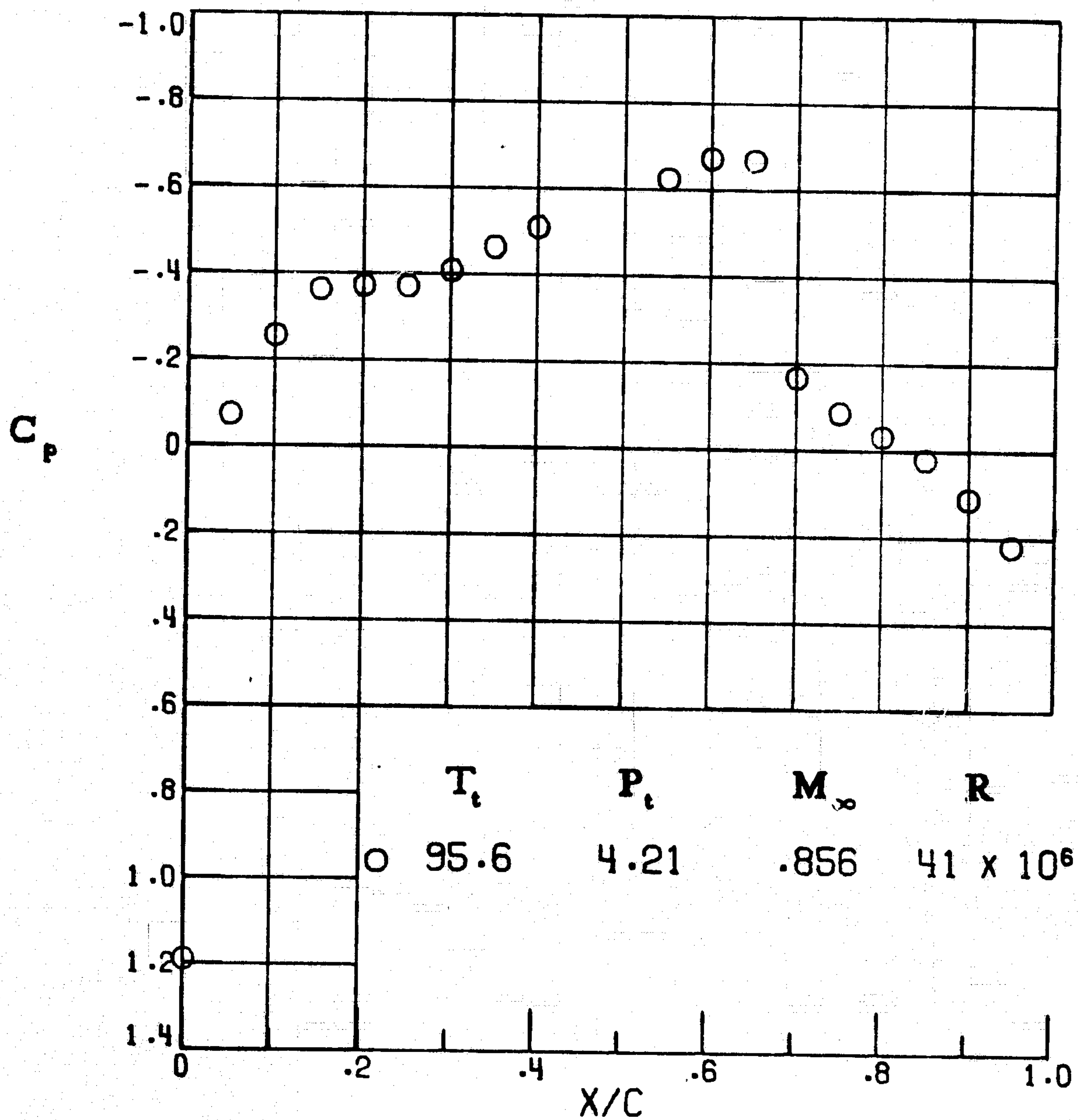

Figure A61.- Path 5, below free-stream saturation.

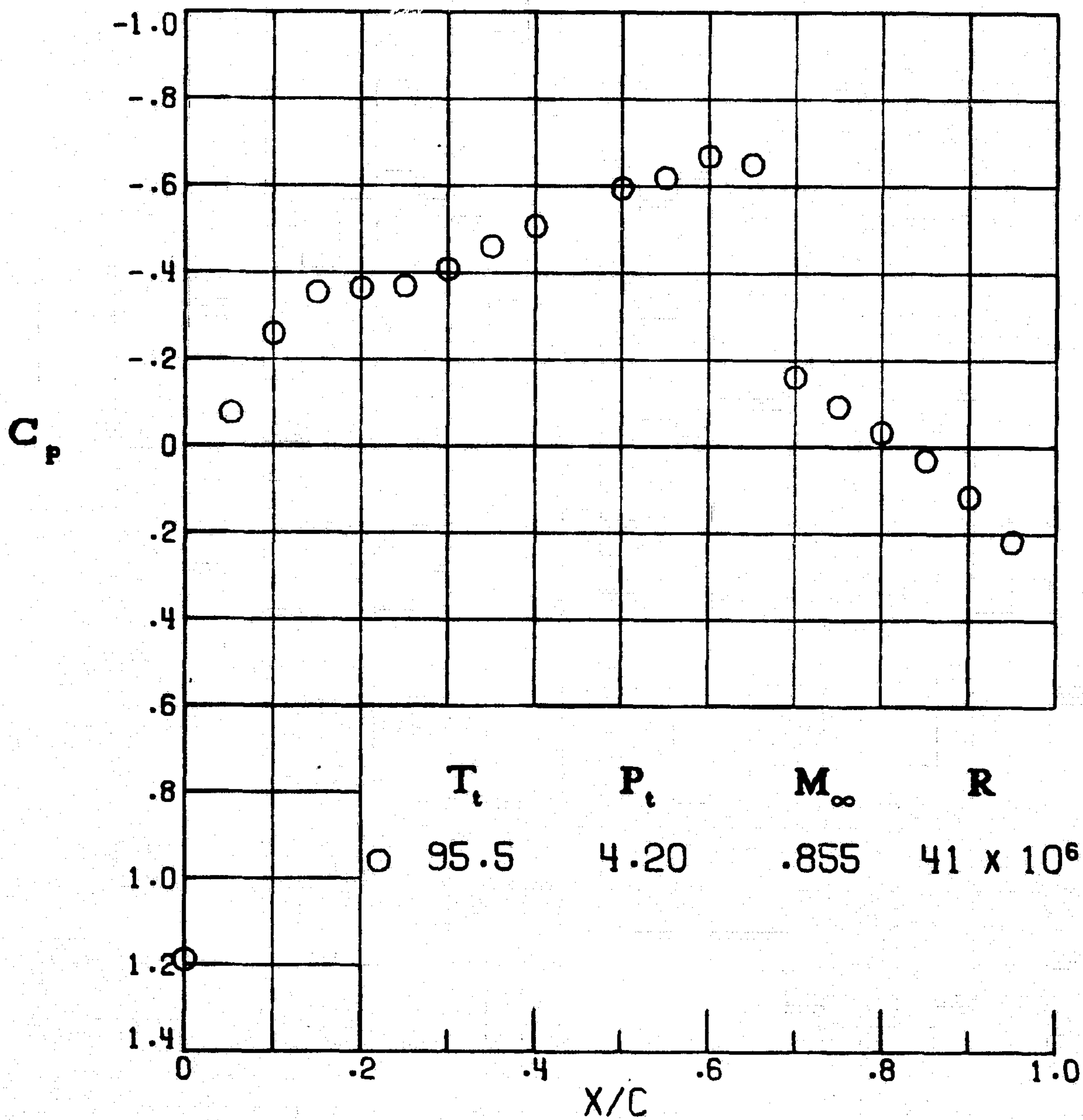

Figure A62.- Path 5, below free-stream saturation.

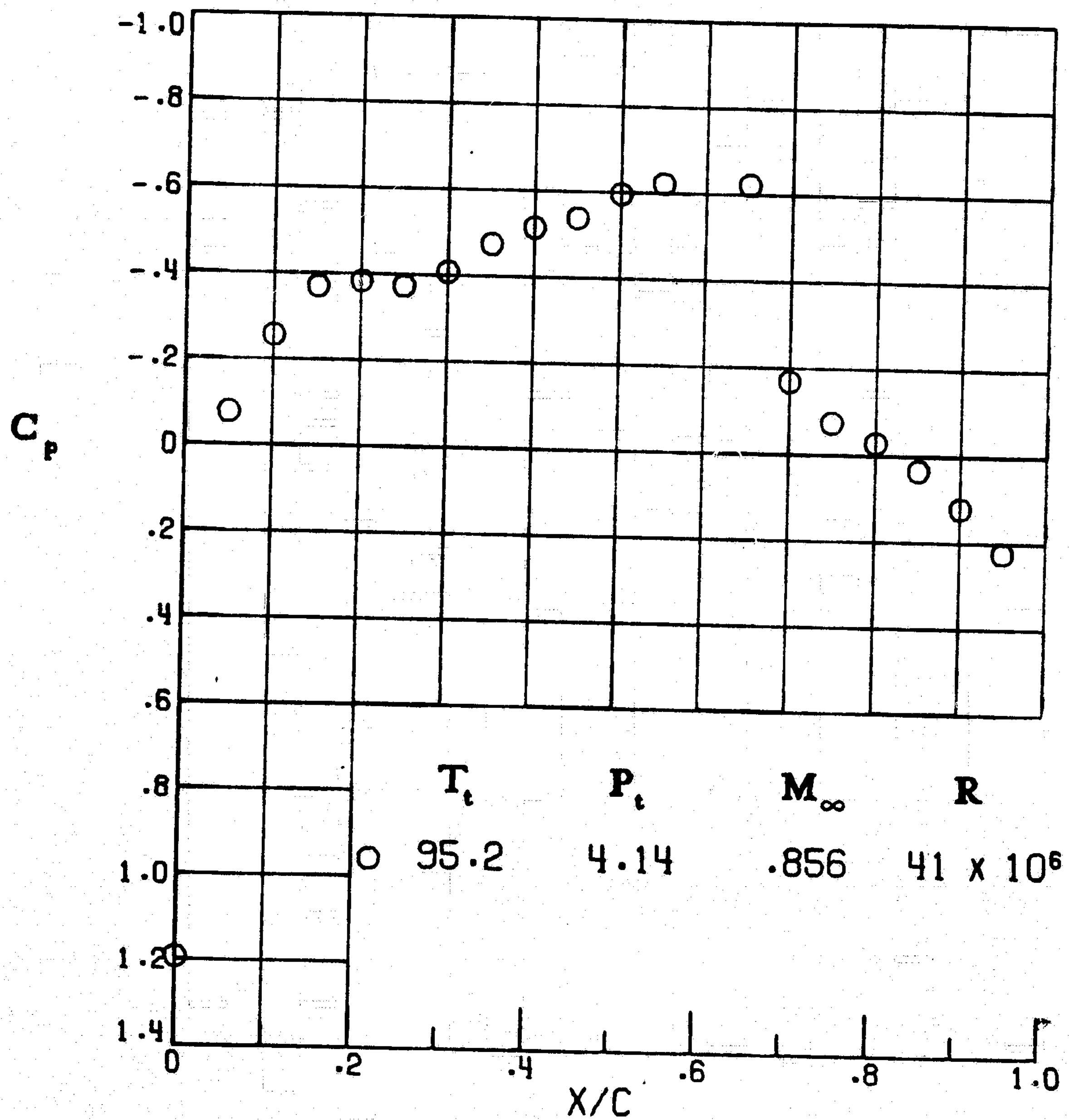

Figure A63.- Path 5, below free-stream saturation.

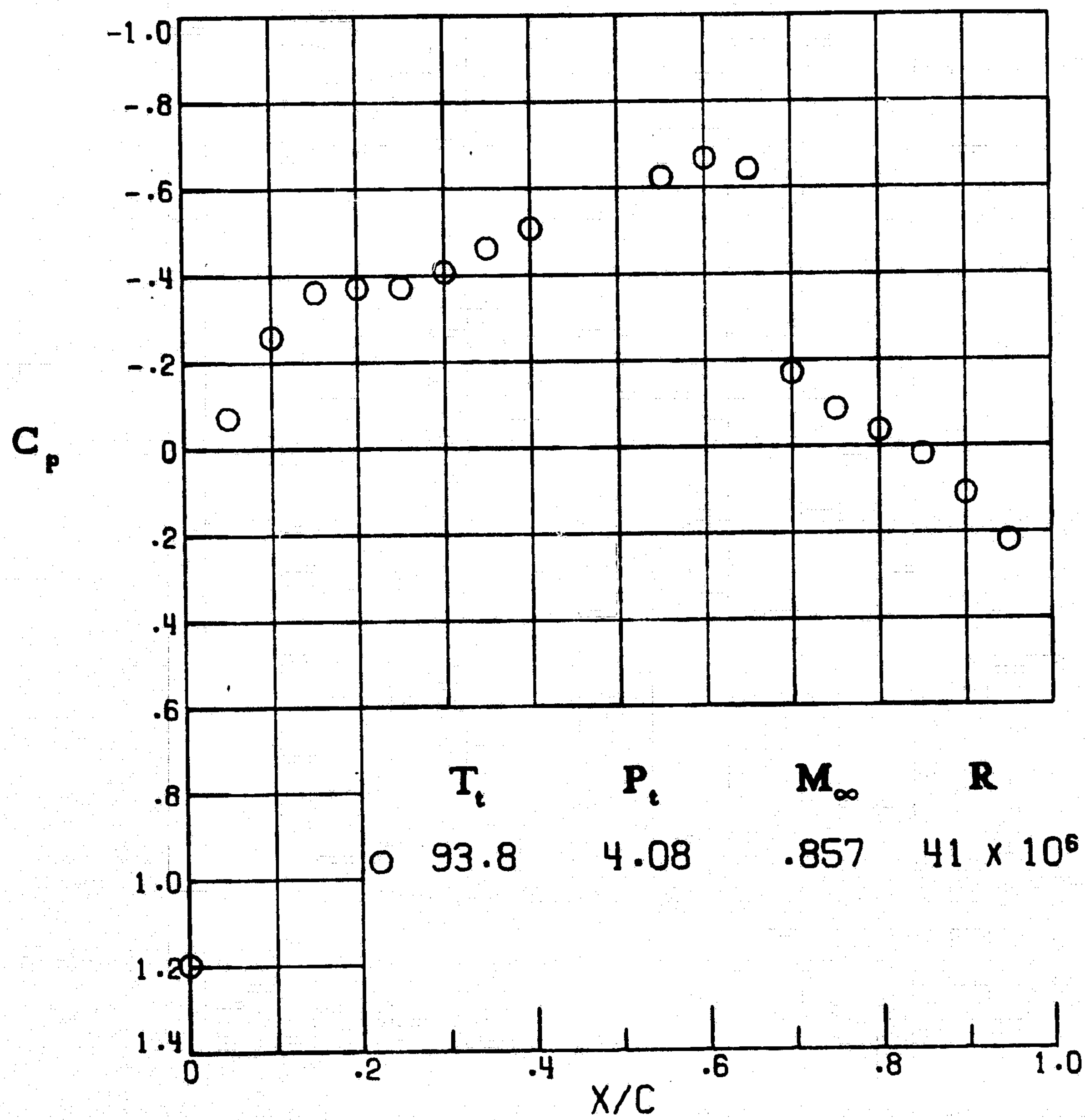

Figure A64.- Path 5, below free-stream saturation.

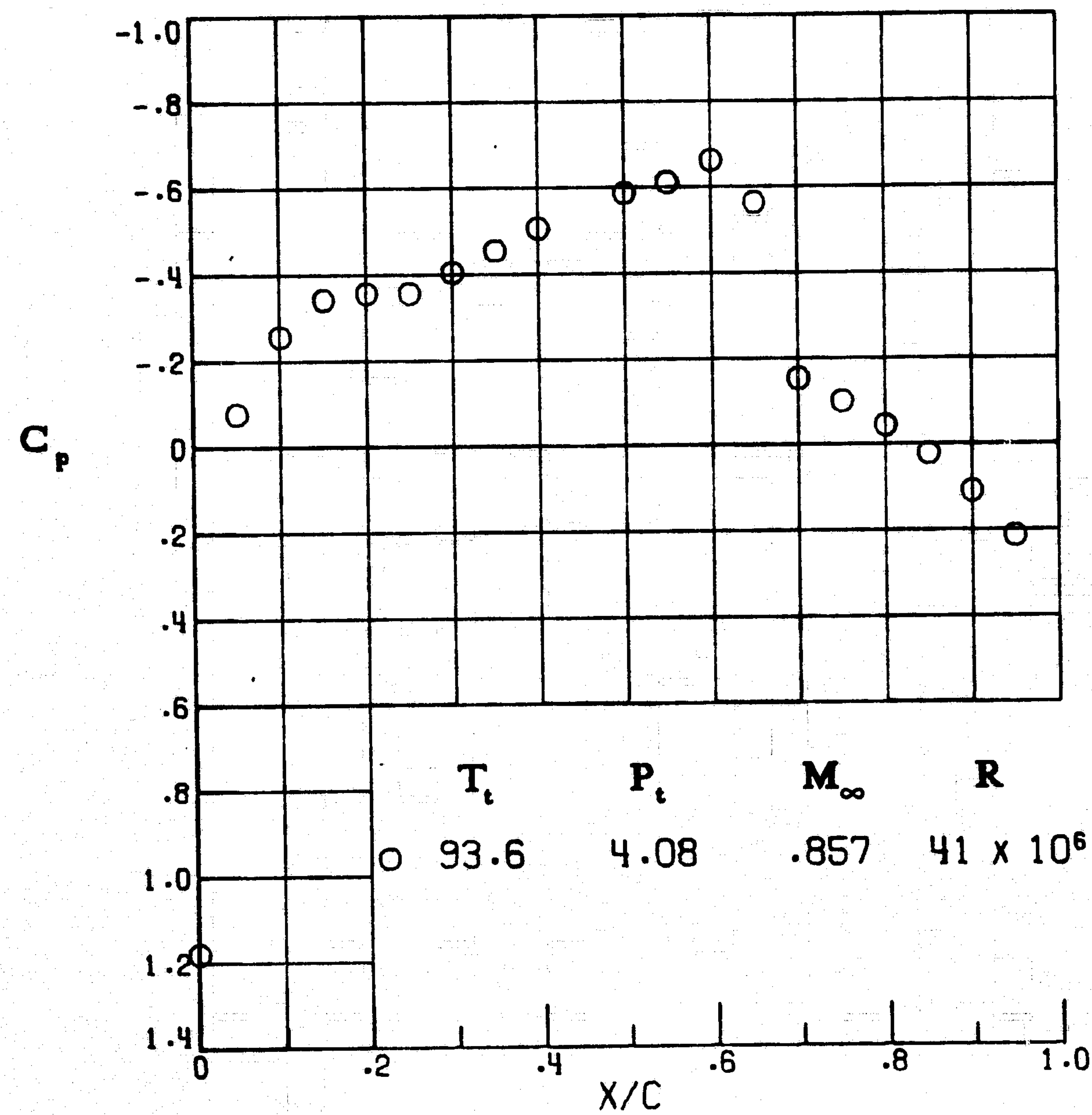

Figure A65.- Path 5, below free-stream saturation.

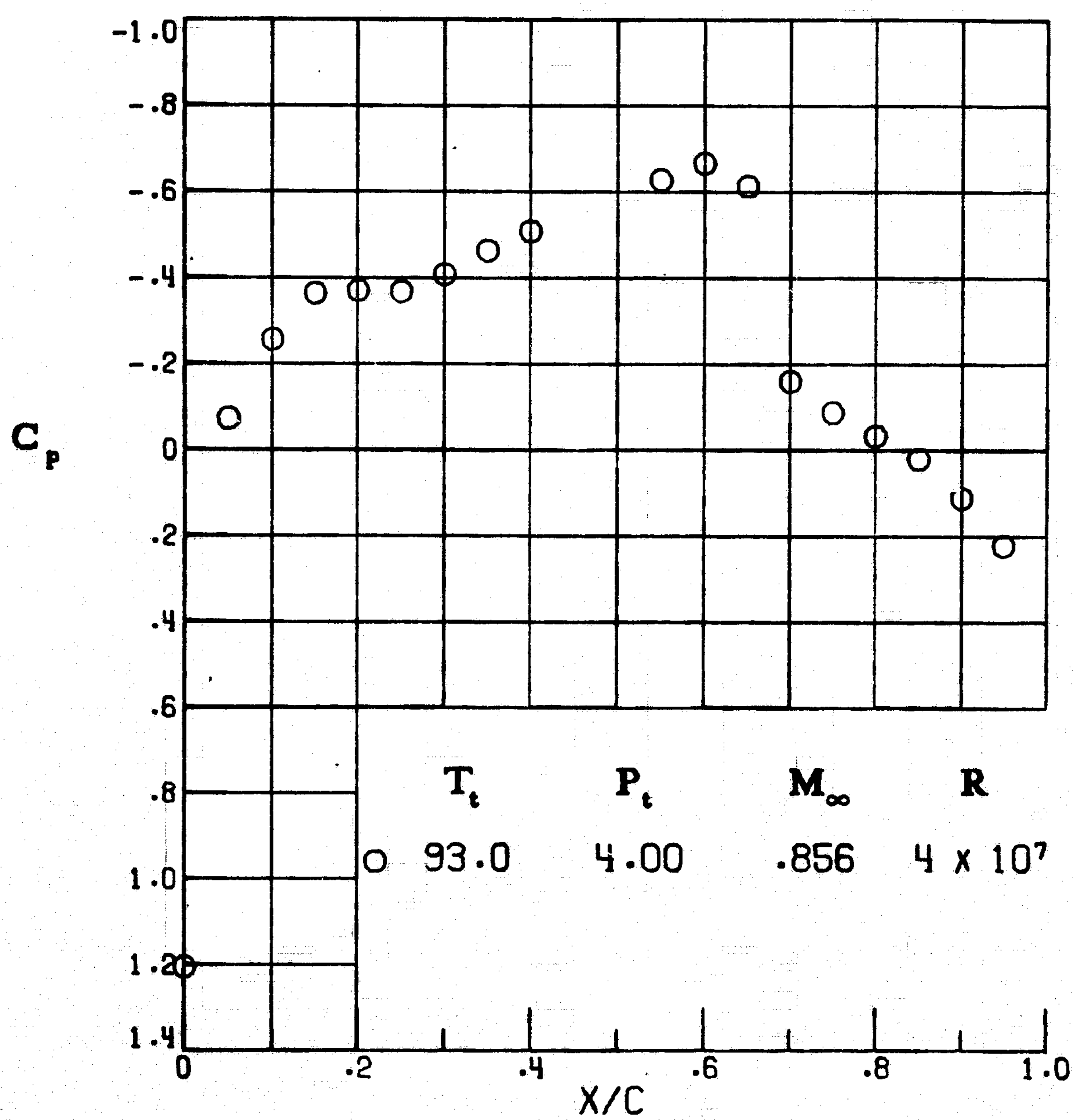

Figure A66.- Path 5, below free-stream saturation.

B L A N K

Figure A67. - Path 6, reference, lost because of a data acquisition problem.

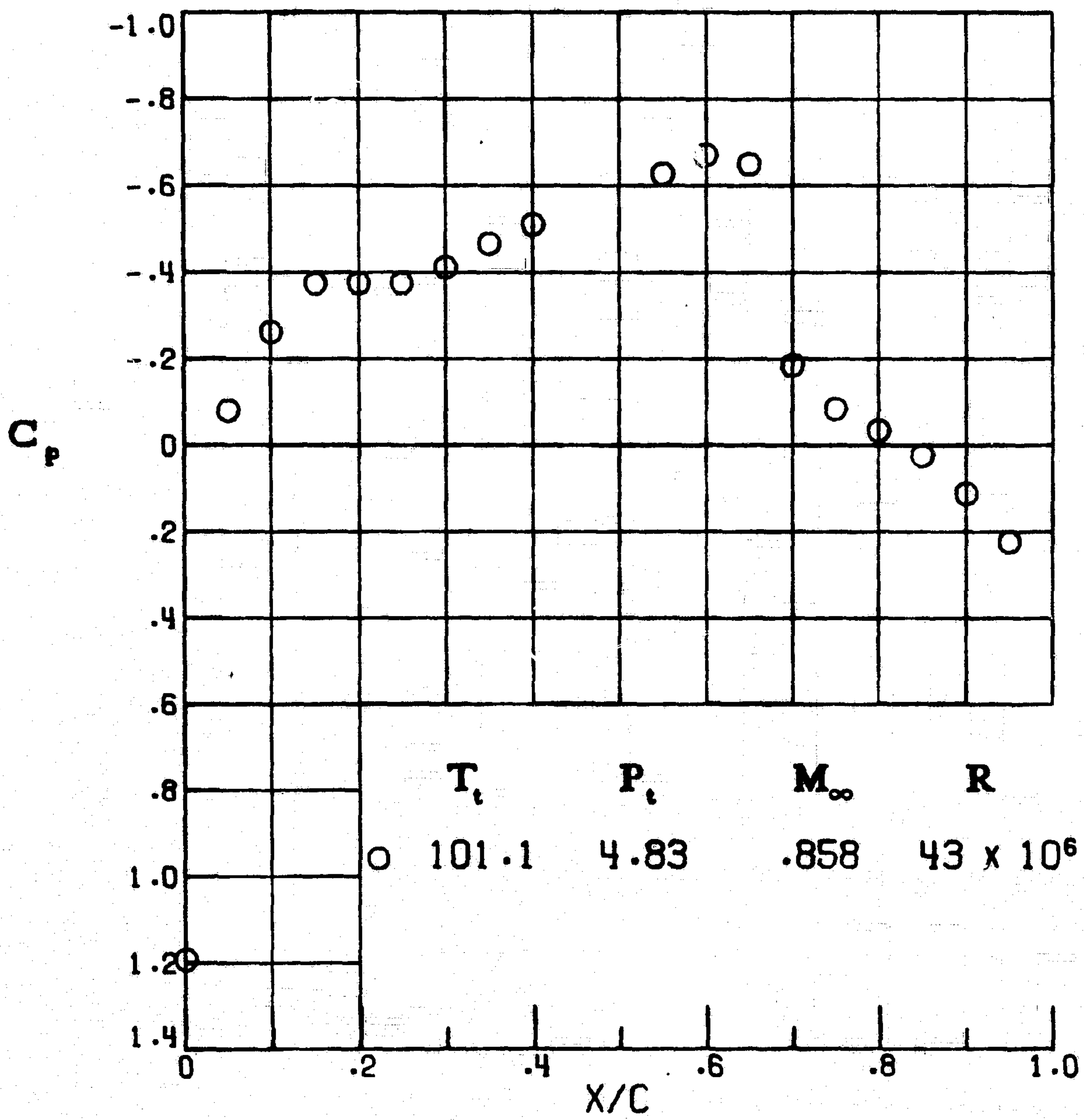

Figure A68. - Path 6, reference, below local saturation.

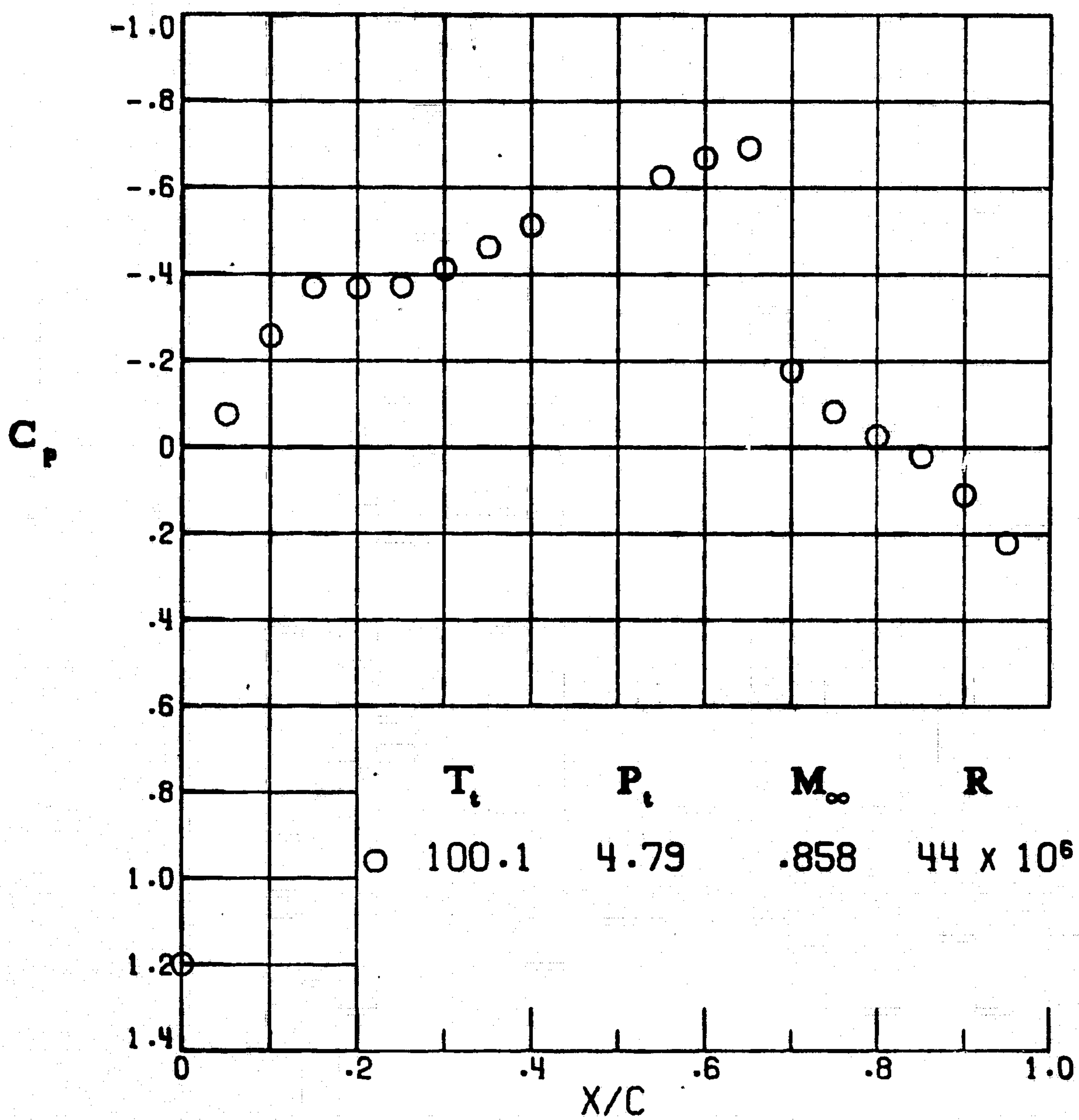

Figure A69.- Path 6, below local saturation.

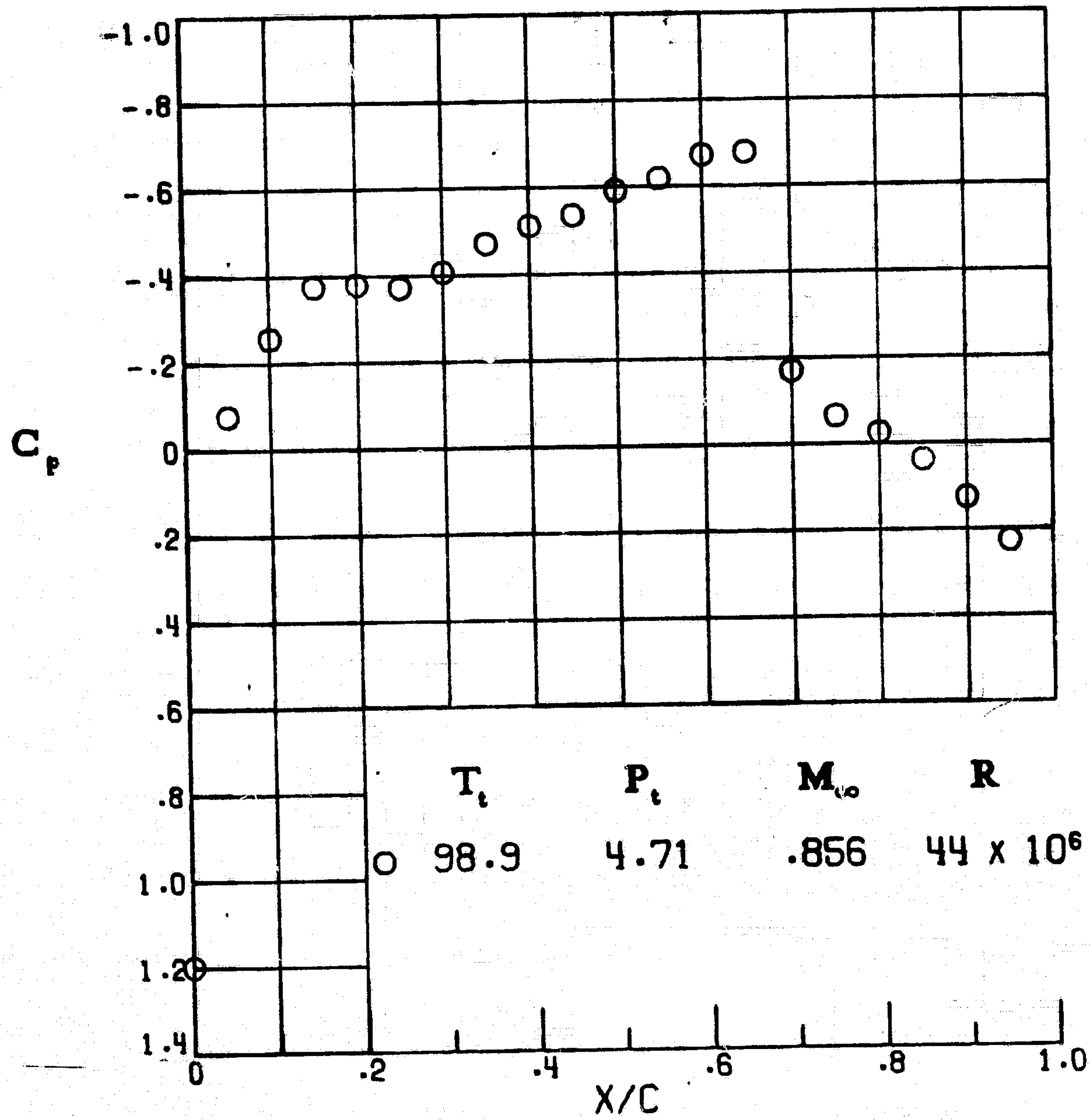

Figure A70.- Path 6, below free-stream saturation.

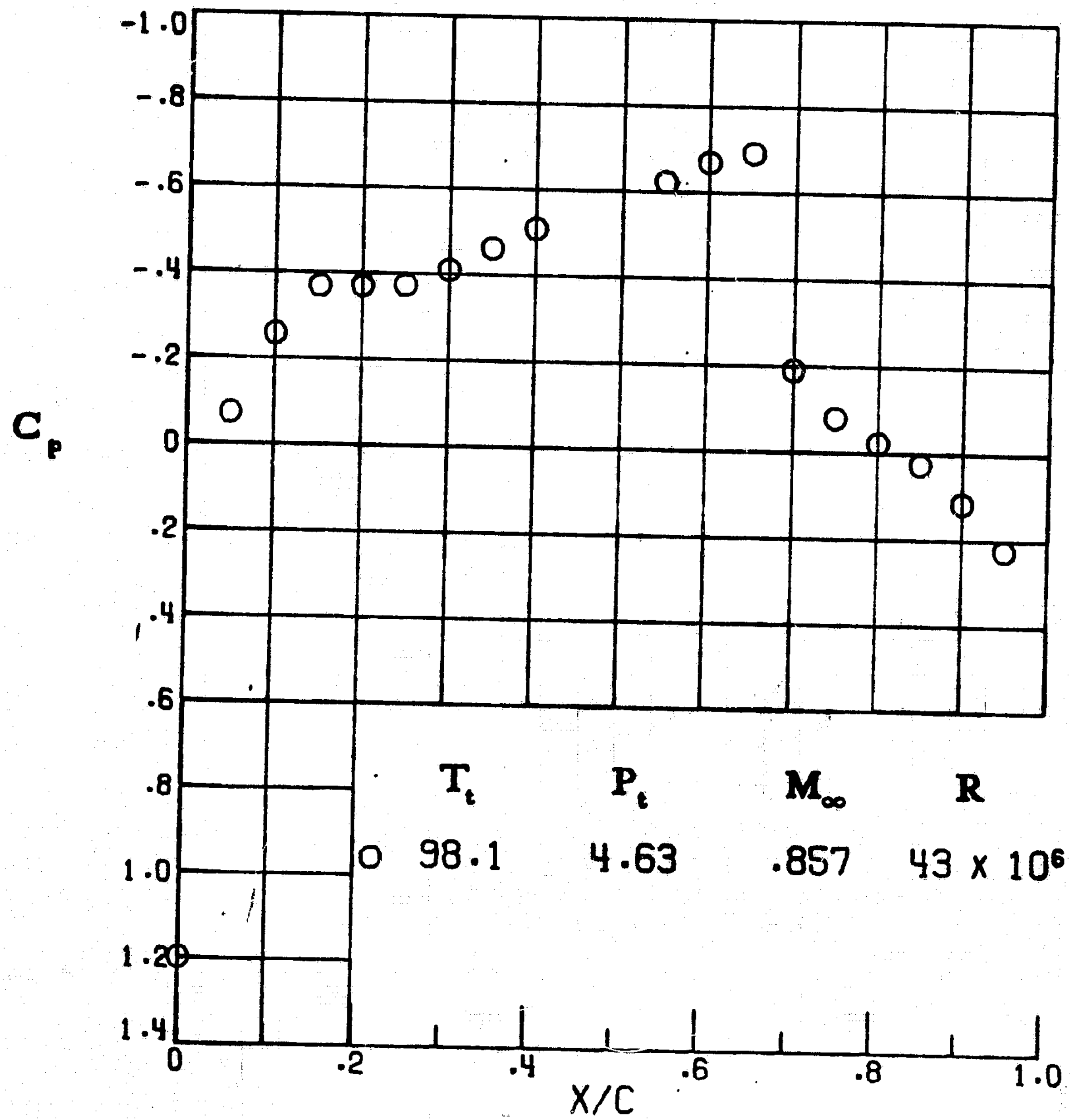

Figure A71.- Path 6, below free-stream saturation.

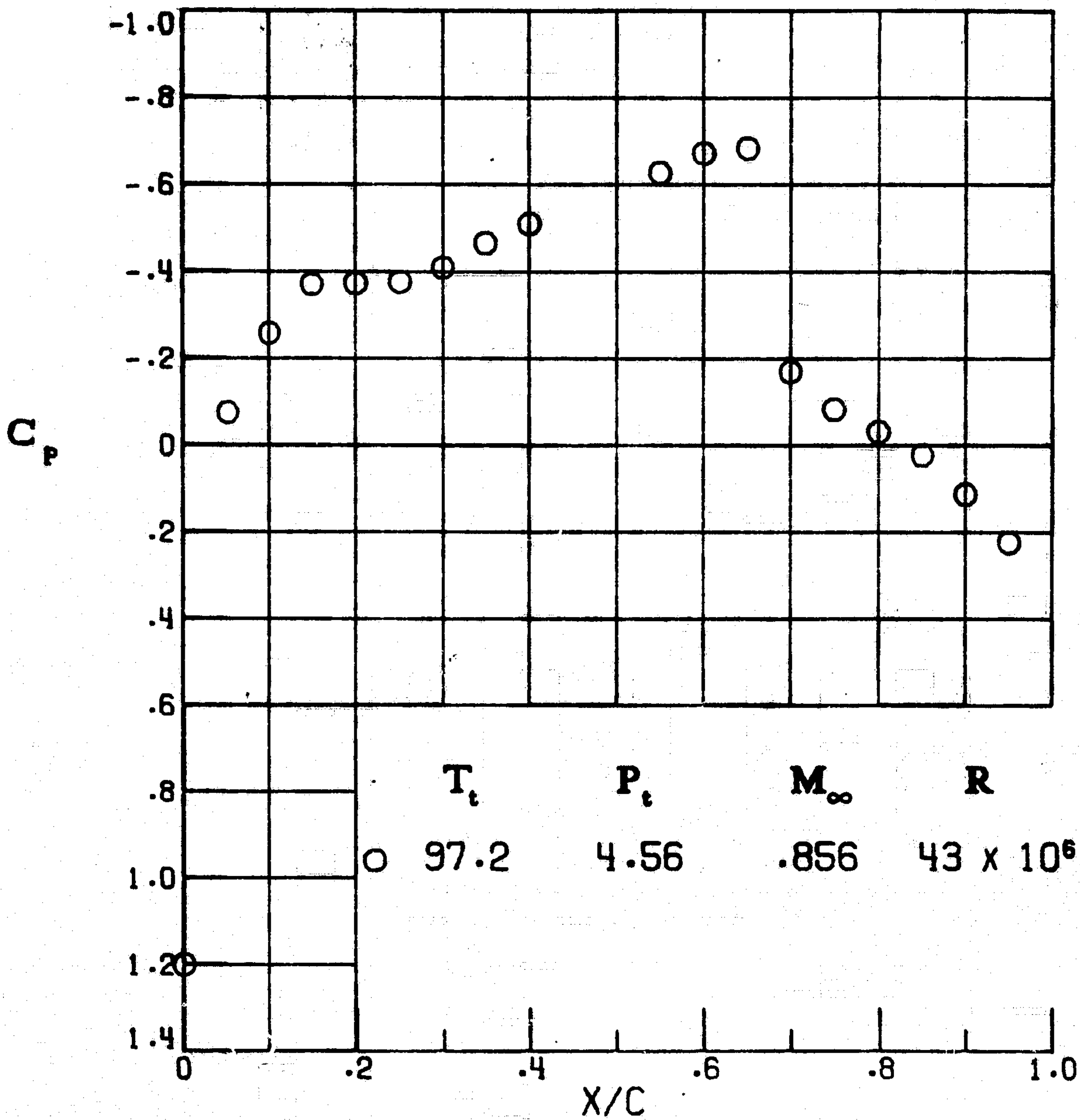

Figure A72.- Path 6, below free-stream saturation.

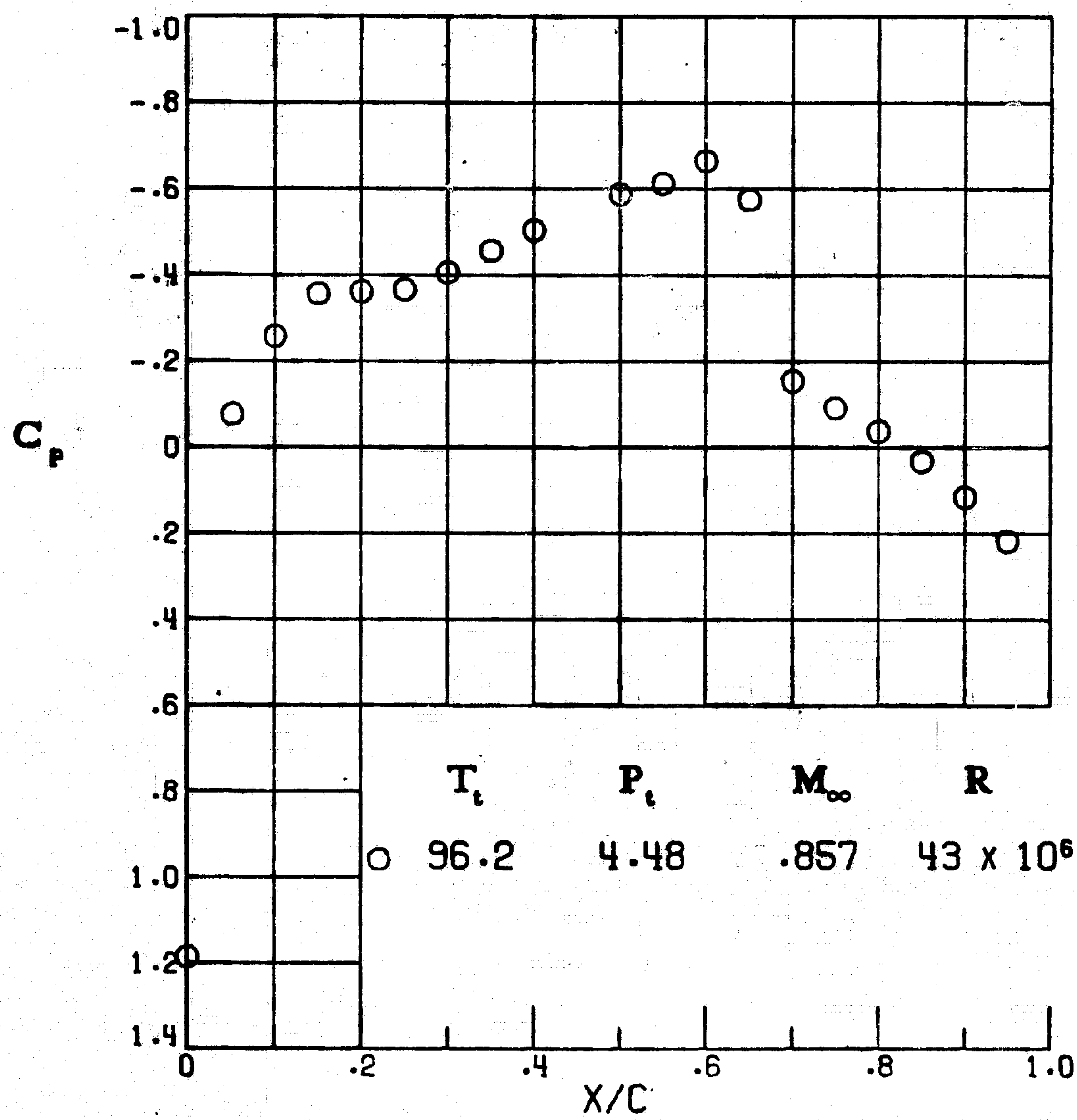

Figure A73.- Path 6, below free-stream saturation.

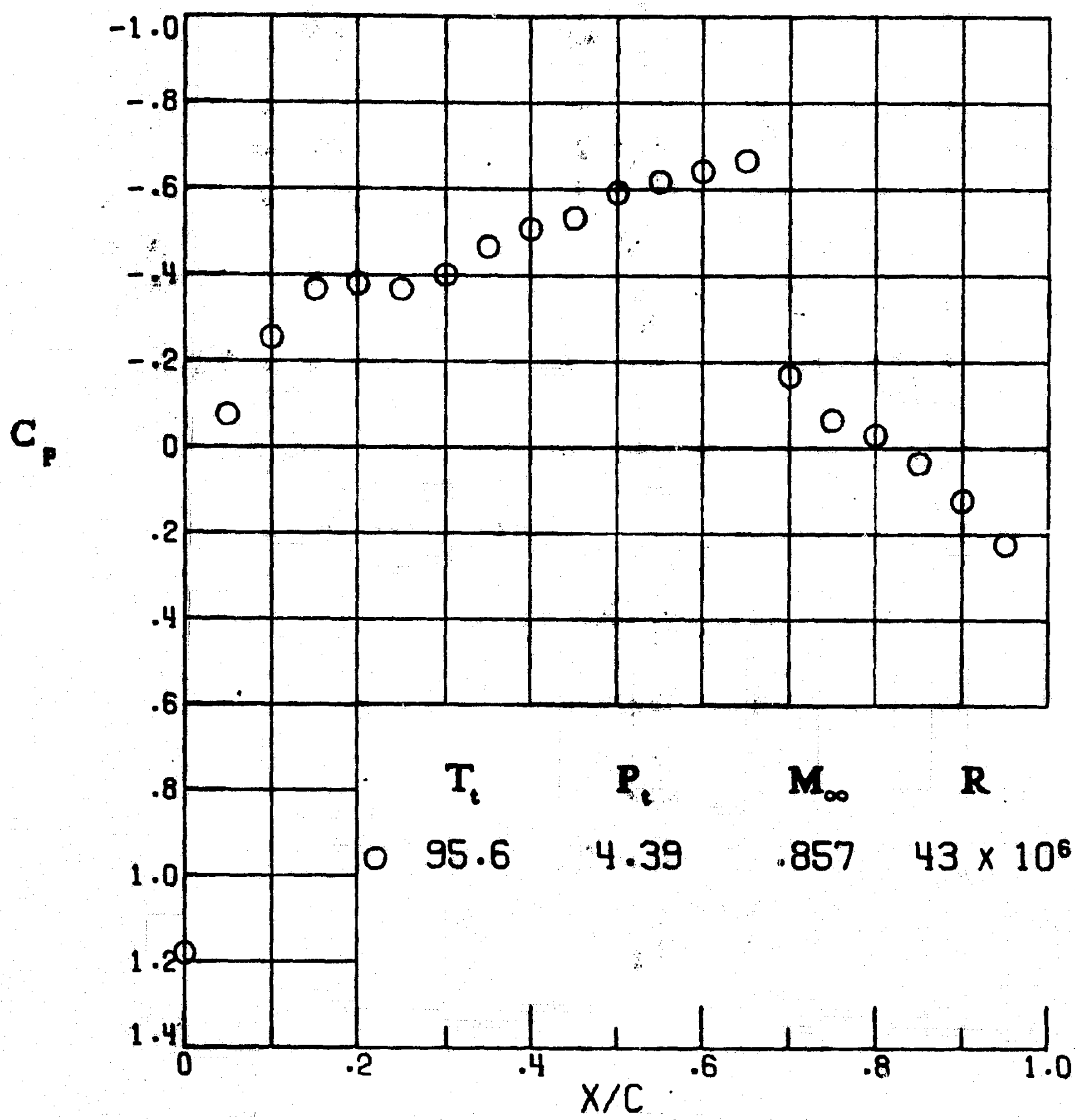

Figure A74.- Path 6, below free-stream saturation.

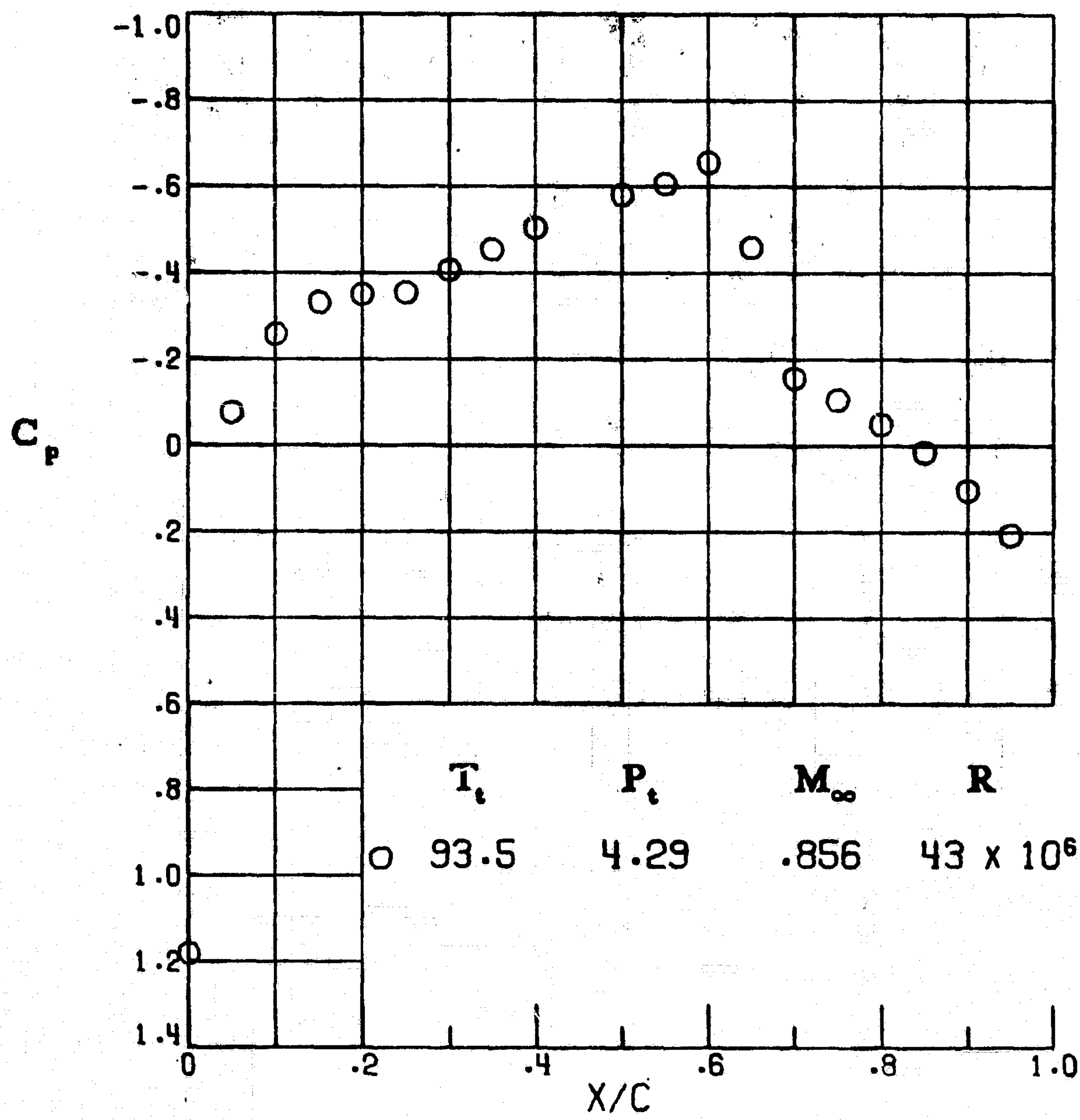

Figure A75.- Path 6, below free-stream saturation.